AD_____

(Leave blank)

Award Number:
W81XWH-11-1-0031

TITLE:
Molecular Mechanism of BCAR3-p130Cas in Breast Cancer

PRINCIPAL INVESTIGATOR:
Peter D. Mace

CONTRACTING ORGANIZATION:
Sanford-Burnham Medical Research Institute
La Jolla, CA 92037

REPORT DATE:

May 2013

TYPE OF REPORT:

Annual Summary

PREPARED FOR: U.S. Army Medical Research and Materiel Command
Fort Detrick, Maryland 21702-5012

DISTRIBUTION STATEMENT: (Check one)

☑ Approved for public release; distribution unlimited

☐ Distribution limited to U.S. Government agencies only; report contains proprietary information

REPORT DOCUMENTATION PAGE

Form Approved
OMB No. 0704-0188

1. REPORT DATE *(DD-MM-YYYY)*	2. REPORT TYPE	3. DATES COVERED *(From - To)*
May 2013	Annual Summary	01 December 2010—10 May 2013

4. TITLE AND SUBTITLE
Molecular Mechanism of BCAR3-p130Cas in Breast Cancer

5a. CONTRACT NUMBER
W81XWH-11-1-0031

5b. GRANT NUMBER
W81XWH-11-1-0031

5c. PROGRAM ELEMENT NUMBER

6. AUTHOR(S)
Peter D. Mace

5d. PROJECT NUMBER

5e. TASK NUMBER

5f. WORK UNIT NUMBER

7. PERFORMING ORGANIZATION NAME(S) AND ADDRESS(ES)
Sanford-Burnham Medical Research Institute
La Jolla, CA 92037

8. PERFORMING ORGANIZATION REPORT NUMBER

9. SPONSORING / MONITORING AGENCY NAME(S) AND ADDRESS(ES)
U.S. Army Medical Research and Material Command
Fort Detrick, Maryland
21702-5012

10. SPONSOR/MONITOR'S ACRONYM(S)

11. SPONSOR/MONITOR'S REPORT NUMBER(S)

12. DISTRIBUTION / AVAILABILITY STATEMENT

Approved for public release; distribution unlimited

13. SUPPLEMENTARY NOTES

14. ABSTRACT
Anti-estrogen drugs such as tamoxifen have become widely used to treat patients with estrogen-receptor positive tumors. Although effective in many cases, significant proportions of estrogen-receptor positive tumors are intrinsically unresponsive to anti-estrogens or have acquired resistance over time. Two proteins that have emerged as key players in this resistance are aptly named Breast Cancer Anti-estrogen Resistance 3 (BCAR3) and BCAR1 (also known as p130Cas). Not only can BCAR3 and p130Cas confer anti-estrogen resistance individually, but the two have subsequently been found to directly interact with each other. We have solved the crystal structures of the p130Cas interaction domain of BCAR3, and the complex of the close BCAR3 homolog, NSP3, bound to the C-terminal domain of p130Cas. Unbound breast cancer antiestrogen resistance 3 (BCAR3/NSP2) adopts the Cdc25-homology fold characteristic of Ras GTPase exchange factors, but in a unique "closed" conformation incapable of enzymatic activity. The structure of the BCAR3 relative, NSP3, in complex with p130Cas further reveals that the closed conformation is instrumental for interaction with a focal adhesion-targeting (FAT)-like region in Cas proteins. This novel enzyme-to-adaptor conversion enables high affinity interactions between BCAR3 (or NSP3) and Cas family proteins to link their signaling networks.

15. SUBJECT TERMS
p130Cas, BCAR3, BCAR1, anti-estrogen resistance, GTPase exchange factor, GEF, Cdc25-homology domain

16. SECURITY CLASSIFICATION OF:			17. LIMITATION OF ABSTRACT	18. NUMBER OF PAGES	19a. NAME OF RESPONSIBLE PERSON
a. REPORT	b. ABSTRACT	c. THIS PAGE			USAMRMC
U	U	U	UU	48	19b. TELEPHONE NUMBER *(include area code)*

Table of Contents

Page

Introduction…….....……..…….…….…..…..5
Body…….……..……..6
Key Research Accomplishments…….....……..…..……..15
Reportable Outcomes……..……...……15
Conclusion……..…….……17
References…….……..….17
Appendices……..…….……..18

Introduction

Anti-estrogen drugs such as tamoxifen have become widely used to treat patients with estrogen-receptor positive tumors. Although effective in many cases, significant proportions of estrogen-receptor positive tumors are intrinsically unresponsive to anti-estrogens or have acquired resistance over time. Two proteins that have emerged as key players in this resistance are aptly named Breast Cancer Anti-estrogen Resistance 3 (BCAR3) and BCAR1 (also known as p130Cas). Not only can BCAR3 and p130Cas confer anti-estrogen resistance individually, but the two have subsequently been found to directly interact with each other. There is also evidence that the two co-operatively activate the Src kinase, which is implicated in metastasis and invasion by cancer cells. This implicates the BCAR3–p130Cas complex as a central regulatory switch influencing treatment of mammary carcinomas. The C-termini of both BCAR3 and p130Cas are responsible for their interaction, and the C-termini of BCAR3 has also been proposed as a GTP exchange factor (GEF) for Ras family GTPases. However little is know the molecular details of this interaction, and how this relates to the putative exchange factor activity of BCAR3. The proposed project aims to structurally characterize BCAR3 and p130Cas (BCAR1), and to investigate the role of their association in breast cancer. Further structural studies will investigate the influence of BCAR3 and p130Cas in the context of their wider signaling pathways and downstream effectors.

Body

This final report summarizes progress made over the entire period of the fellowship, which will be terminated effective May 10, 2013. I have been awarded a prestigious Rutherford Discovery Fellowship by the Royal Society of New Zealand, and will be moving to New Zealand to start my own research group investigating molecular signaling mechanisms of cancer development. At this time I wish to convey my sincere appreciation of the support granted to me by the Department of Defense Breast Cancer Research Program, which has been instrumental in helping me progress my career as an independent researcher.

This report pertains to the entire research period, and description of research, key research accomplishments and reportable outcomes that are most relevant to the period since the year 2 report are indicated by bold text.

Task 1. Crystallization and structure determination of the complex between BCAR3 and p130Cas, and BCAR3 alone (months 1-12):

1a. Crystallization trials with existing constructs (months 1-3).
1b. Modification of expression constructs and further crystallization (months 3-6).
1c. Diffraction data collection and structure determination (months 6-12).
1d. Model building and analysis (months 6-12).

There was excellent progress towards all aspects of Task 1. Expression constructs of BCAR3 were tested and expressed large amounts of soluble proteins. However, these constructs required further optimization, particularly mutagenesis to prevent non-specific initiation leading to impurities during recombinant expression in *E. coli*. This construct yielded highly pure protein that eluted as a single peak upon size exclusion and formed a 1:1 complex with the p130Cas C-terminal domain.

The modified expression construct allowed expression and purification of large quantities of BCAR3 suitable for crystallization trials. These crystallization trials yielded an initial hit that was optimized by several rounds of grid screening, additive screening and crystal 'seeding'. Final optimal conditions grew crystals that diffracted X-rays to a resolution of 2.4 Å. The structure of the BCAR3 C-terminal domain was solved by molecular replacement using the homologous structure of NSP3 (solved below) as a search model. Model building and refinement led to a final model with excellent stereochemical properties and R_{factor}/R_{free} of 0.17/0.24.

Many crystallization trials were established for the complex between the C-terminal domains of BCAR3 and p130Cas. No crystals were forthcoming for the BCAR3-p130Cas complex. However, crystals of the BCAR3 homolog, NSP3, bound to p130Cas were optimized to a stage where experimental phasing could be performed. NSP3 (also known as Shep1) is the closest sequence homolog of BCAR3. The structure of NSP3 bound to p130Cas was solved to a resolution of 2.5 Å. It showed that NSP3 and BCAR3 are extremely structurally similar (See reference 1) and thus the complex of p130Cas bound to NSP3 serves as an excellent model for

BCAR3-p130Cas binding.

These structures show that BCAR3 and NSP3 share a novel adaptation of the Cdc25-homology domain fold (1), which renders them in "closed" conformation (Figures 1 & 2 in reference 1). This makes them very unlikely to function as bona fide GTPase exchange factors. These structural findings are in line with biochemical and biophysical experiments (Task 2), and mass spectrometric analysis initiated in (Task 3). Most strikingly, the NSP3-p130Cas structure showed that p130Cas binds at a new interface created by the closed conformation of the Cdc25-homology domain (Figure 2 in reference 1). Overall our results suggest that the NSP family of proteins, of which BCAR3 and NSP3 are both members, possess a C-terminal domain that has evolved from a catalytic function to an adaptor facilitating protein-protein interactions.

The structure of NSP3 bound to p130Cas also represents the first atomic level detail of the C-terminal domain of p130Cas, a protein widely implicated in cancer progression and metastasis. This region adopts a four-helical bundle extremely similar to that seen in the focal-adhesion targeting (FAT) domain of focal adhesion kinase (Figure 3 in reference 1).

Methodological details, as well as detailed structural analysis and discussion is included in the attached manuscript "NSP-Cas protein structures reveal a promiscuous interaction module in cell signaling. Mace PD, Wallez Y, Dobaczewska MK, Lee JJ, Robinson H, Pasquale EB, Riedl SJ. (2011) Nature Structural and Molecular Biology".

Task 2. Analysis of candidate GTPases (months 1–6):

2a. Cloning and expression of designated Ras-family GTPases (month 1).
2b. Binding studies using isothermal titration calorimetry (months 2–6).
2c. GTP exchange assays (months 2–6).
2d. Assays and binding studies with potential GTPases identified in task 3 (months 12–15).

Cloning and expression of putative Ras-family GTPases proposed for BCAR3 proceeded smoothly, and optimized expression procedures for large quantities of Rap1A, Rap2, RalA, RalB and r-Ras have been established. Isothermal titration calorimetry was used extensively to test for binding of BCAR3 to target GTPases. However, in line with our structural findings no binding could be detected (1).

GTPase exchange assays were also carried out with candidate GTPases loaded with the fluorescent GDP analog, "mant-GDP". In addition to BCAR3, a suitable control GTPase exchange factor (GEF) for target GTPases had to be cloned, expressed and purified. After considering and testing several putative GEFs for Rap1a (data not shown), C3G was successfully purified and exhibited expected nucleotide exchange factor activity (1). The results of these assays also supported the finding that BCAR3 is unlikely to perform as a bona fide nucleotide exchange factor, with no GDP-exchange factor activity observed for BCAR3 (or NSP3/Shep1) in the presence or absence of p130Cas (See Figures 1f and 2c in reference 1).

The findings from these biophysical and biochemical experiments are very much in line with the structural details revealed by our newly solved crystal structures (Task 1). The essence being that rather than performing an enzymatic function, the C-terminal domains of BCAR3 and NSP3 are protein:protein interaction domains. This suggested greater emphasis should be placed on the signaling crosstalk brought about by the interaction between BCAR3 and p130Cas, potentially other Cas family members, and downstream kinase effectors.

Task 3. Identification of GTPases bound by BCAR3 using mass spectrometry (months 3–12):

As described in previous reports, excellent progress was made to address the goals of Tasks 1–3, in line with the scheduled timeline. This included the solution of the structure of the C-terminal GEF-like domain of BCAR3, and the structure of the complex between p130Cas and NSP3 (a close homolog of BCAR3) (1). Consequently, the focus of later work progressed to tackle the biological implications of our structural findings; namely that the C-terminal domain of BCAR3 does not appear to be a competent GTP exchange factor, but rather a highly-evolved protein-protein interaction domain that specifically facilitates crosstalk between the BCAR3 and p130Cas signaling pathways. This finding emphasizes the importance of Tasks 4 and 5, which focus on wider signaling interactions rather than GTP exchange functions of BCAR3.

Task 4. Disruption of BCAR-p130Cas function by mutagenesis (months 12–24):

4a. Planning and synthesis of mutants for *E. coli* expression (month 12).
4b. Testing of *E.coli* expressed mutants for folding, binding (months 13–15).
4c. Synthesis of mutant constructs for expression in breast cancer cell lines (months 15–16).
4d. Analysis of transfected cell lines for anti-estrogen resistance and invasiveness (months 17–24).

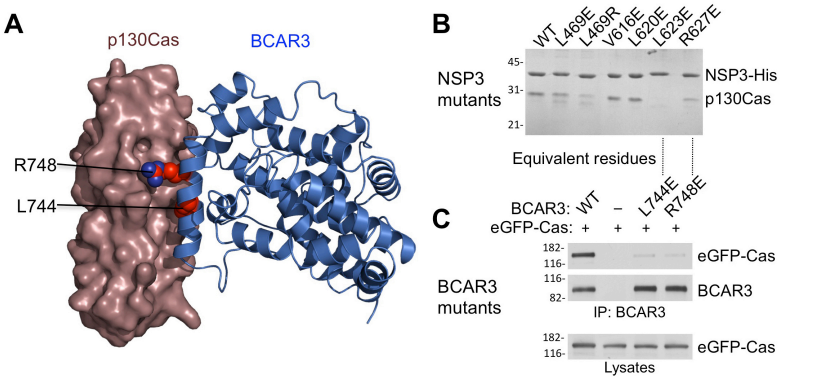

Figure 1 – Position and efficacy of BCAR3–p130Cas interface mutants relevant to Task 4. (A) Structural model of the complex between the C-terminal domains of BCAR3 and p130Cas. The positions of Arg748 and Leu744 are indicated. (B) Affinity purification assay of recombinantly expressed His_6-tagged mutants of NSP3 (the closest homolog of BCAR3) to test binding to p130Cas. Leu623 (the equivalent of BCAR3 Leu744) is the most effective mutant, followed by Arg627 (equivalent to BCAR3 Arg748). (C) Co immunoprecipitations assay of effective BCAR3 interface mutants with p130Cas. (based on Ref (1)).

Mutants of NSP3 (the closest homolog of BCAR3) were created based on the structure of NSP3 bound to p130Cas. These interface mutants were screened for expression and soluble behavior using *E. coli*, which is an excellent indicator for proper protein folding. Using these constructs we were able to establish a panel of NSP3 and p130Cas mutants that disrupted binding between the two molecules (Figure 1). The most effective binding mutants of NSP3 were conserved in BCAR3, as expected from their conserved fold and similar functions, and also disrupted BCAR3 binding to p130Cas (Figure 1). The combination of precise structural information and extensive

mutagenesis allowed us to address several pivotal questions about the function of BCAR3.

A report published during 2011 proposed that anti-estrogen resistance and migration induced by BCAR3 can occur independent of its ability to bind to p130Cas (2). However, this observation was based on a single arginine point mutant of BCAR3. Our mutant screen showed that mutating the equivalent arginine in human NSP3, or BCAR3, reduces but does not completely abrogate binding to p130Cas in *in vitro* and *in vivo* binding assays respectively (Figure 1 and data not shown). This finding is in accordance with the structural model of BCAR3 binding to p130Cas shown in Figure 1A. Arg748 is certainly directly involved in the BCAR3–p130Cas interaction, but is also partially solvent exposed. We thus decided to combine a mutation of Arg748, with another very effective binding mutant, Leu744, with the expectation that the combination of these two binding mutants would more effectively disrupt binding between BCAR3 and p130Cas.

In order to assess the effectiveness of this double-mutant we measured it's ability to stabilize and promote phosphorylation of p130Cas, given that p130Cas phosphorylation is a crucial factor in the assembly of a p130Cas–CRK signaling complex that drives invasion through Rac1 ((3) and Figure 6A below). Here we observed that the single mutant R748E indeed was still able to promote stabilization of p130Cas and promote tyrosine phosphorylation. However, the L744/R748 double mutant completely lost the ability to stabilize and promote phosphorylation of p130Cas, which had similar phosphorylation levels to that observed in the vector control. These results suggest that phosphorylation of p130Cas is a more sensitive readout for p130Cas and BCAR3 association than simple co-immunoprecipitation. This is likely because the affinity between the two proteins is extremely tight (K_D~30 nM as previously shown in Year 1 report and reference 1), and the single mutant reduces the binding affinity somewhat but is unable to stop transient BCAR3–p130Cas interactions that promote Cas phosphorylation.

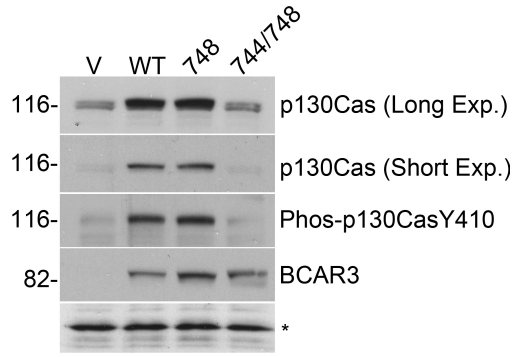

Figure 2 - BCAR3 stabilizes p130Cas in an interaction-dependent manner. MCF-7 cells were stably transduced with empty lentiviral vector (V), BCAR3-WT (WT), BCAR3-R748E (748), BCAR3-L744E/R748E (744/748) and assessed for p130Cas expression and phosphorylation by Western blotting using indicated antibodies. A non-specific band, indicated by an asterisk, verifies equal protein loading.

Having shown that a double interface mutant in BCAR3 effectively prevents p130Cas phosphorylation, we next sought to test the downstream consequences for migration and invasion of cells bearing mutant BCAR3. To this end we measured the ability of BCAR3 to induce

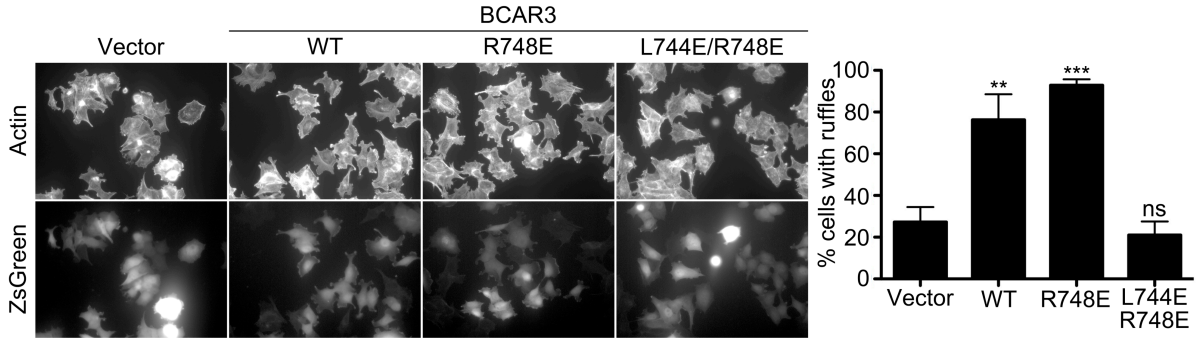

Figure 3 - BCAR3-induced lamellipodia formation and p130Cas recruitment to ruffles is dependent upon complex formation. MCF-7 cells were stably transduced with empty lentiviral vector (V), BCAR3-WT (WT), BCAR3-R748E (748), BCAR3-L744E/R748E (744/748). The cells were plated on fibronectin-coated coverslips and then stained with phalloidin to label filamentous actin (red, upper panels). The graph shows the percentage of ZsGreen-expressing (middle panels) transfected cells that contain ruffles. **Pb0.01 and ***Pb0.001 for the comparison with vector control transfected cells by one way-ANOVA followed by Dunnett's multiple comparison posthoc test.

lamellipodia formation and BCAR1 recruitment to membrane ruffles in MCF-7 breast cancer cells (Figure 3). Cells were stably transduced with lentiviral vectors for wild-type, single and double point mutants of BCAR3, and an empty vector control. The cells were plated on fibronectin-coated coverslips and then stained with phalloidin to label filamentous actin to indicate cellular migration. Again, it was clear that the L744/R748 mutant of BCAR3 is incapable of promoting lamellipodia formation, whereas the wild-type and R748E forms of BCAR3 were able to promote both phenotypes.

Given that our double BCAR3 mutant does not induce p130Cas phosphorylation or cell migration, relative to wild-type or a single point mutant, we have tested whether this most effective BCAR3–p130Cas disruption mutant is also able to abrogate anti-estrogen resistance induced by BCAR3. For this experiment, stably tranduced MCF-7 cells grown in media with or without the estrogen receptor antagonist ICI182780, a high affinity estrogen receptor antagonist devoid of any partial agonism. Cells growth was determined over a period of 33 days by counting manually with a hemocytometer. As seen in Figure 4, cells expressing wild-type BCAR3 or BCAR3 R748E become resistant to

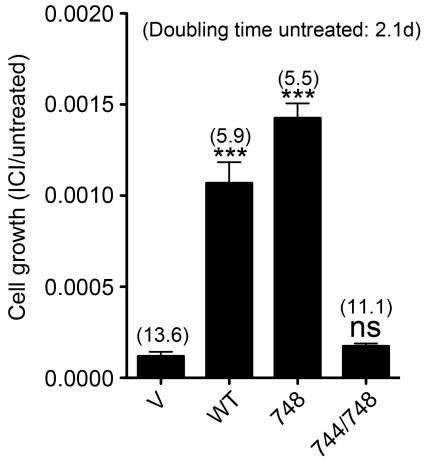

Figure 4 - BCAR3-mediated anti-estrogen resistance requires complex formation with p130Cas.
MCF-7 cells stably transduced with empty lentiviral vector (V), BCAR3-WT (WT), BCAR3-R748E (748), BCAR3-L744E/R748E (744/748) were plated in triplicate and grown in media with or without ERa antagonist ICI 182,780 at 100 μM. Cells growth was determined over a period of 33 days by counting manually with a hemocytometer. Relative cell growth (number of cells treated with ICI/number of cells untreated) and standard error are shown. The doubling time of the different cell cultures was calculated by the algorithm provided by http://www.doubling-time.com. ***P<0.001 for the comparison with vector control infected cells by one way-ANOVA.

antiestrogen treatment, and have a doubling time of approximately 5 days. However, cells expressing the completely binding-deficient BCAR3 double mutant are as sensitive to antiestrogen treatment as the vector only control, and have a doubling time approximately twice that of cells expressing wild-type BCAR3.

Task 5. Characterization of BCAR3-p130Cas interactions with other binding partners (months 6–30):

5a. Further analysis of p130Cas binding to Src kinase in relation to BCAR3 (month 6–24).
5b. Binding studies with proteins identified by mass spectrometry (months 6–24).
5c. Crystallization trials with other putative binding partners (months 12–30).

We progressed to testing interactions between p130Cas and Src kinase *in vitro*, in order to assess the effect of BCAR3 on this interaction and Src activity. As shown in Figure 5, preliminary results did not show a stable interaction between the Src binding region of p130Cas and Src kinase, either in the presence or absence of the BCAR3 C-terminal domain (Figure 5). A likely explanation for this is that p130Cas requires phosphorylation on Tyr664/666, in order for Src kinase to effectively dock its SH2 domain to this site. Tests with and without ATP demonstrate that Src is not able to carry out this phosphorylation, at least in the context of these p130Cas and Src kinase constructs. Tyr664/666 phosphorylation has been proposed to be carried out *in vivo* by focal-adhesion kinase (FAK) (4). Strategies were investigated

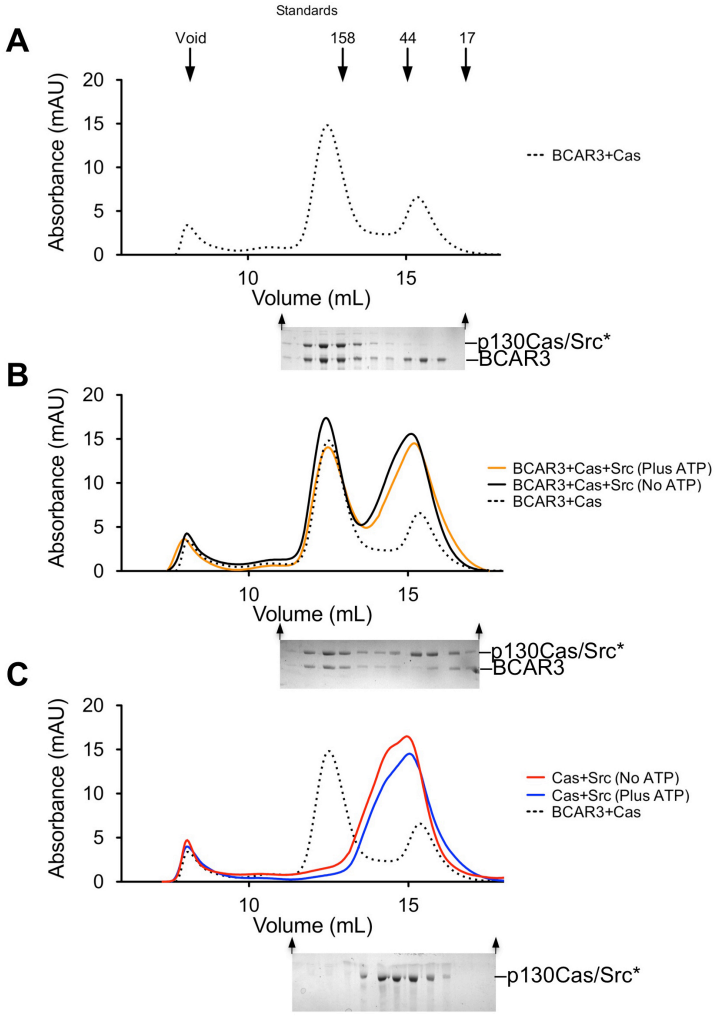

Figure 5 - Recombinant proteins currently at hand do not form a stable heterocomplex between p130Cas, BCAR3 and Src kinase. (A) Size-exclusion chromatography showing that p130Cas (residues 454–870) and BCAR3 (502–825) form a stable complex (SDS-PAGE below shows stoichiometric BCAR3–p130Cas complex and some excess BCAR3). No higher order oligomers form when either (BCAR3, p130Cas and Src are incubated together **(B)**, of p130Cas and Src are incubated together **(C)**. In both **(B)** and **(C)** and ATP incubation step was trialed to promote phosphorylation of Tyr 664/666 by Src kinase and enhance affinity, however this did not cause a significant change in the elution profile. *It should be noted that p130Cas (residues 454–870) and Src kinase are very close in size and cannot be distinguished on SDS-PAGE

to prepare FAK on a suitable scale to purify preparative quantities of p130Cas phospho-Tyr664/666. However, at the time of reporting this procedure was not well established.

Another line of research that was explored over this time period is the signaling kinase ERK2, which lies downstream of Src-kinase (which is activated by p130Cas) (Figure 6). This signaling axis represents another avenue stemming from p130Cas that could promote cell survival and poor prognosis in breast cancer, separate from the effects of p130Cas/BCAR3 on invasiveness demonstrated in Figure 4. ERK2 kinase activation leads to cellular transformation, and inappropriate ERK stimulation occurs in a large proportion of human cancers. We sought to understand the structural basis for ERK2 suppression by PEA-15, given that PEA-15 is correlated with hormone receptor status (thus response to anti-estrogen therapy), and growth inhibition in breast cancer cells (5). Despite it's central signaling role in a broad range of cancers, as well as breast cancer, there is currently no published structure of a folded protein in complex with ERK2.

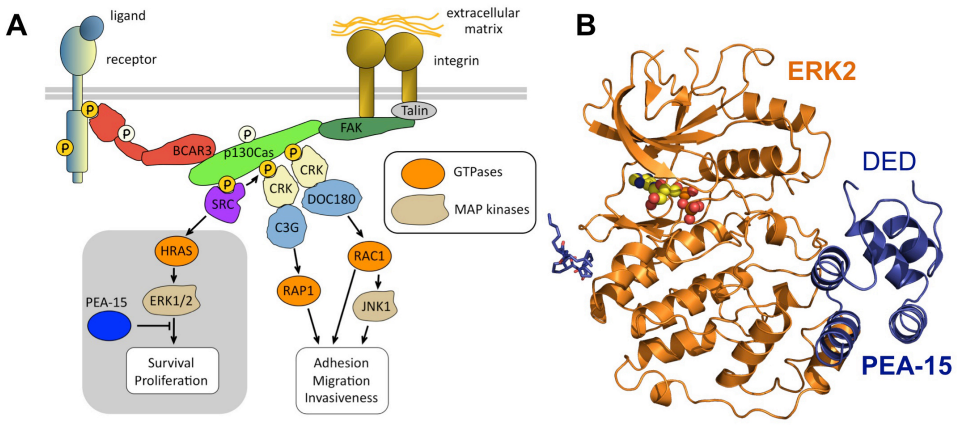

Figure 6 – Suppression of the proliferation branch of signaling downstream of p130Cas–BCAR3. (A) Schematic illustrating signaling pathways stemming from p130Cas–BCAR3. The ERK pathway is highlighted with a grey box. (B) Structure of the complex between ERK2 (orange) and PEA-15 (blue).

The scaffolding protein PEA-15 is a death effector domain protein that directly interacts with ERK1/2 and affects ERK1/2 subcellular localization and phosphorylation. To understand this regulation of ERK1/2 signaling, we solved the crystal structures of PEA-15 bound to three different ERK2 phospho-conformers. The structures reveal that PEA-15 uses a bipartite binding mode, occupying two key docking sites of ERK2 (Figure 6). Remarkably, PEA-15 concomitantly binds the ERK activation loop in the critical Thr-X-Tyr region across different phosphorylation states. PEA-15 binding triggers an extended allosteric conduit in ERK2 that disarms the dually phosphorylated kinase. These mechanisms show how PEA-15 has the potential to block both transformation and proliferation that is triggered by ERK2 downstream of the p130Cas–BCAR3 signaling pathway.

In the months since the Year 2 report, a manuscript describing the ERK2–PEA-15 complex was prepared and underwent peer review (reference 6), followed by significant revision and development of the overall message that is depicted in Figure 7. In this work we showed that a major capability of PEA-15 is to decouple the phosphorylation status of ERK2 (which is widely regarded as a measure of proliferative signaling in cancer cells), from its actual activity. By binding to the phosphorylated form of ERK2, PEA-15 wild-type but not ERK binding mutants, cause an accumulation of phospho-ERK2 (Figure 7a). The

fact that PEA-15 preserved ERK2 phosphorylation when upstream signaling was blocked using MEK inhibitors (Figure 7b) strongly suggested that this was through preventing phosphatases from dephosphorylating ERK2. The overall model depicted in Figure 7c shows how this behaviour means that PEA-15 can be both a suppressor of cancer signaling, but also promote tumor growth by increasing levels of phosphorylated ERK2.

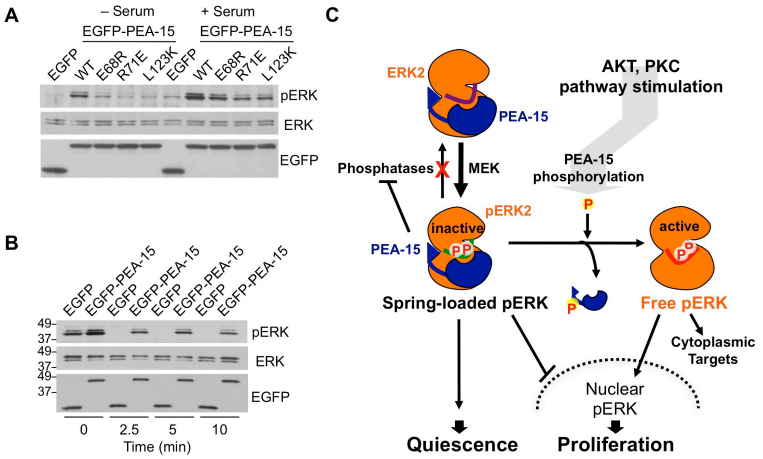

Figure 7 – PEA-15 can propogate a phosphorylated, "spring loaded" form of ERK2 by protecting it from dephosphorylation (A) ERK2 phosphorylation status was monitored following transfection with indicated PEA-15 constructs and serum stimulation (B) HEK293 cells were stimulated with serum then treated with U0126 to inhibit MEK1, the upstream kinase of ERK2. Cells expressing PEA-15 are markedly protected from dephosphorylation. (C) Schematic showing the possible consequences of high PEA-15 levels in a cellular setting.

Methodological details, as well as detailed structural analysis and discussion is included in the attached manuscript "Structure of ERK2 bound to PEA-15 reveals a mechanism for rapid release of activated MAPK. Mace PD, Walez Y, Egger MF, Dobaczewska MK, Robinson H, Pasquale EB, Riedl SJ (2013)".

Task 6. Concluding Tasks (months 24–36)

6a. Development of assays for high-throughput screening (24–36)
6b. Manuscript preparation (28–36)

The manuscript describing the structures and investigation of the ERK2–PEA-15 complex was initially submitted for publication at the time of Year 2 reporting, and in the interim was revised and additional experiments added. A manuscript describing further investigations of the interplay between NSP3, BCAR3 and p130Cas is currently in

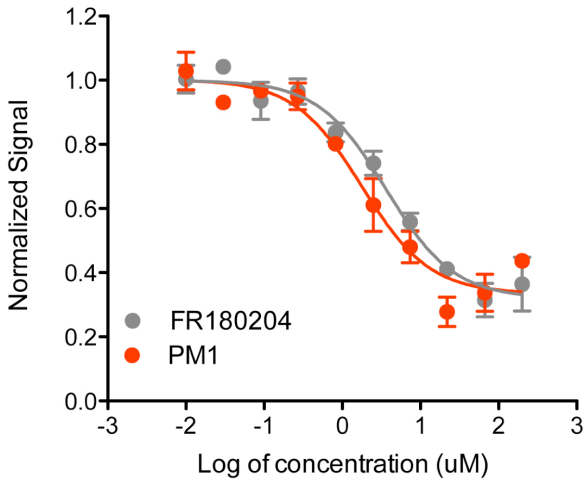

Figure 8 – PM1 has improved activity over FR180204. ADP-glo assay measuring ERK2 activity in the presence of an exisiting ERK2 inhibitor (FR180204), or the compound developed in this work (PM1). The IC_{50} value for PM1 (1.8 µM) is approximately half that of FR180204 (3.6 µM) calculated in this experiment.

preparation and will be submitted at a later date.

The unexpectedly extensive interaction of BCAR3 and p130Cas makes developing screens for compounds to disrupt this protein-protein interaction conceptually difficult. Instead, advances have been made developing a novel class of compound to target the downstream signaling target of p130Cas, ERK2. This compound (PM1) combines features of a moderate ERK2 targeted compound (FR180204), with features observed in the ERK2–PEA-15 complex, in an effort to enhance the selectivity and potency of the existing ERK2 compound. Preliminary testing of PM1 showed an approximately two-fold improved efficacy (Figure 8). Although this improvement is modest at this stage, modifications have been planned to improve this compound further, and will be an ongoing focus in the Riedl and Pasquale Laboratories.

Key Research Accomplishments

- Crystal growth and structure solution of the BCAR3 C-terminal domain
- Comparison of the BCAR3 C-terminal domain with the closely related protein NSP3 (Shep1) bound to p130Cas shows that no large structural rearrangement occurs upon p130Cas binding.
- Structural analysis revealing that BCAR3 and NSP3 share the core commonly found in Cdc25-homology domain GTPase-exchange factors, but have rearrangements in catalytic regions leading to a closed arrangement.
- Thorough biochemical and biophysical analysis of potential GTPase exchange factor activity of BCAR3, showing canonical GTPase activity is unlikely.
- Discovery that the C-terminal domain of p130Cas forms a four-helical bundle extremely similar to that seen in the focal-adhesion targeting (FAT) domain of focal adhesion kinase
- Extensive mutagenesis of the NSP3–p130Cas interface showing that targeted disruption of the NSP3–p130Cas interface impairs migration towards chemotactic stimuli. Corresponding mutants of BCAR3 also disrupt p130Cas binding.
- Establishment of expression constructs for c-Src, several p130Cas truncation constructs and many other interacting partners. These will serve as useful rearrangements for investigations of downstream signaling interactions and events.
- Establishment of *bona fide* mutants that disrupt association between BCAR3 and p130Cas despite the tight nature of the complex. A double mutant based on these experiments has proven a very effective tool for cell-based experiments
- Clear evidence that direct association is required for p130Cas tyrosine-phosphorylation that is promoted by BCAR3.
- Evidence that physical linkage between p130Cas and BCAR3 is needed for both invasion, and antiestrogen resistance induced by BCAR3.
- Completion of three crystal structures of the ERK2–PEA-15 complex, which have been submitted to the Protein Data Bank upon acceptance of the manuscript described above.
- **Development of experiments showing that PEA-15 can propagate a pool of phosphorylated ERK2 by directly binding to the ERK2 activation loop, preventing dephosphorylation**
- **Preliminary experiments developing a specific ERK2 inhibitor based on features present in the ERK2–PEA-15 structure.**

Reportable Outcomes

- Submission of two X-ray crystal structures to the Protein Data Bank. The structures of BCAR3, and the complex between NSP3 and p130Cas have been submitted to the protein databank with accession codes 3T6A and 3T6G respectively.

- Accepted publication in Nature Structural and Molecular Biology. The manuscript "NSP-Cas protein structures reveal a promiscuous interaction module in cell signaling. Mace PD, Wallez Y, Dobaczewska MK, Lee JJ, Robinson H, Pasquale EB, Riedl SJ. (2011) Nature Structural & Molecular Biology. 18, 1381-7" (Included in Appendix).
- Poster Presentation, Gordon Conference on Mechanisms of Cell Signaling, ME, USA (2011) "Conformational adaptation enables NSP-Cas network signaling"
- Oral Presentation, Pacific Coast Protease Meeting, CA, USA (2011) "Exclusive Promiscuity – Structural Studies of NSP–Cas Signaling Modules"
- Recipient of the Eric Dudl Award (2011). This scholarship is awarded annually to one Postdoctoral Fellow at Sanford-Burnham Medical Research Institute to recognize significant contributions to cancer research.
- Accepted publication in *Genes and Cancer*. The manuscript "NSP-CAS Protein Complexes: Emerging Signaling Modules in Cancer. Wallez Y, Mace PD, Pasquale EB, Riedl SJ. (2012) Genes & Cancer. 3, 382–93." (Included in Appendix).
- Oral Presentation, Post-Translational Regulation of Cell Signaling Meeting, Salk Institute for Biological Studies, La Jolla, CA, USA (2012)
- Oral Presentation, Pacific Coast Protease Meeting, CA, USA (2012)
- Oral Presentation, Sanford Burnham Medical Research Institute Cancer Center Open House, La Jolla CA, USA (2012)
- **Awarded a Rutherford Discovery Fellowship by the Royal Society of New Zealand. (2012), to be initiated in mid-2013**
- **Submission of three X-ray crystal structures of the ERK2–PEA-15 complex to the Protein Data Bank, with accession codes 4IZ5, 4IZ7 and 4IZA.**
- **Participation in the Torrey Pines Mesa Training Consortium Academic Leadership Symposium (2013).**
- **Attendance at the American Association of Cancer Research General Meeting, Washington DC (2013)**
- **Accepted publication in Nature Communications. The manuscript "Structure of ERK2 bound to PEA-15 reveals a mechanism for rapid release of activated MAPK. Mace PD, Walez Y, Egger MF, Dobaczewska MK, Robinson H, Pasquale EB, Riedl SJ (2013) Nature Communications. 4, 1681." has been published (Included in Appendix).**

Conclusion

The crystal structures of the p130Cas interaction domain of NSP family proteins, BCAR3 and NSP3, in their unbound form and in complex with the C-terminal domain of p130Cas allowed us to design mutants that selectively target BCAR3–p130Cas signaling. Experiments based on these structurally-informed mutants reveal that the ability of BCAR3 to induce Cas-phosphorylation, invasion, and anti-estrogen resistance is highly dependent on its ability to form a stable complex with p130Cas. This work provides a precise structural understanding for future work exploring the role of BCAR3 and p130Cas in breast cancer, and has facilitated clear experiments showing the role of this signaling node in anti-estrogen resistance. Our experiments suggest that the physical linkage between BCAR3 and p130Cas, rather than a previously proposed enzymatic function is key to their co-operative pathology in breast cancer, which is a fundamental change in how these proteins should be investigated and could potentially be targeted for disease therapy.

We also further investigated interactions of these proteins with signaling partners such as Src kinase, and downstream signaling partners. With regard to the latter we have solved structures of PEA-15 (a suppressor of proliferative signaling) with ERK kinase, a central proliferative kinase that lies downstream of p130Cas-based signaling pathways. This structure has wide implications for the regulation of ERK2 signaling, and in the future will be used to develop novel compounds to inhibit ERK signaling.

References

1. Mace PD, Wallez Y, Dobaczewska MK, Lee JJ, Robinson H, Pasquale EB, Riedl SJ. NSP-Cas protein structures reveal a promiscuous interaction module in cell signaling. Nat Struct Mol Biol. 2011 Dec;18(12):1381–7.

2. Vanden Borre P, Near RI, Makkinje A, Mostoslavsky G, Lerner A. BCAR3/AND-34 can signal independent of complex formation with CAS family members or the presence of p130Cas. Cell Signal. 2011 Jun;23(6):1030–40.

3. Cabodi S, del Pilar Camacho-Leal M, Di Stefano P, Defilippi P. Integrin signalling adaptors: not only figurants in the cancer story. Nat Rev Cancer. 2010 Dec 1;10(12):858–70.

4. Ruest PJ, Shin NY, Polte TR, Zhang X, Hanks SK. Mechanisms of CAS substrate domain tyrosine phosphorylation by FAK and Src. Mol Cell Biol. 2001 Nov;21(22):7641–52.

5. Bartholomeusz C, Gonzalez-Angulo AM, Kazansky A, Krishnamurthy S, Liu P, Yuan LXH, et al. PEA-15 inhibits tumorigenesis in an MDA-MB-468 triple-negative breast cancer xenograft model through increased cytoplasmic localization of activated extracellular signal-regulated kinase. Clin Cancer Res. 2010 Mar 15;16(6):1802–11.

6. Mace PD, Wallez Y, Egger MF, Dobaczewska MK, Robinson H, Pasquale EB, Riedl SJ. Structure of ERK2 bound to PEA-15 reveals a mechanism for rapid release of activated MAPK. Nature Communications. 4, 1681.

Appendices

The following published manuscripts are included in this appendix

Mace PD, Walez Y, Egger MF, Dobaczewska MK, Robinson H, Pasquale EB, Riedl SJ (2013) Structure of ERK2 bound to PEA-15 reveals a mechanism for rapid release of activated MAPK. *Nature Communications*. 4, 1681.

Walez Y, **Mace PD**, Pasquale EB, Riedl SJ (2012) NSP-CAS Protein Complexes: Emerging Signaling Modules in Cancer. *Genes & Cancer*. 3, 382–93.

Mace PD, Walez Y, Dobaczewska MK, Lee JJ, Robinson H, Pasquale EB, Riedl SJ (2011) NSP-Cas protein structures reveal a promiscuous interaction module in cell signaling. *Nature Structural & Molecular Biology*. 18, 1381-7.

nature COMMUNICATIONS

ARTICLE

Received 16 Oct 2012 | Accepted 28 Feb 2013 | Published 9 Apr 2013

DOI: 10.1038/ncomms2687

Structure of ERK2 bound to PEA-15 reveals a mechanism for rapid release of activated MAPK

Peter D. Mace[1], Yann Wallez[2], Michael F. Egger[1], Małgorzata K. Dobaczewska[1], Howard Robinson[3], Elena B. Pasquale[2,4] & Stefan J. Riedl[1]

ERK1/2 kinases are the principal effectors of a central signalling cascade that converts extracellular stimuli into cell proliferation and migration responses and, when deregulated, can promote cell oncogenic transformation. The scaffolding protein PEA-15 is a death effector domain protein that directly interacts with ERK1/2 and affects ERK1/2 subcellular localization and phosphorylation. Here, to understand this ERK1/2 signalling complex, we have solved the crystal structures of PEA-15 bound to three different ERK2 phospho-conformers. The structures reveal that PEA-15 uses a bipartite binding mode, occupying two key docking sites of ERK2. Remarkably, PEA-15 can efficiently bind the ERK2 activation loop in the critical Thr-X-Tyr region in different phosphorylation states. PEA-15 binding triggers an extended allosteric conduit in dually phosphorylated ERK2, disrupting key features of active ERK2. At the same time PEA-15 binding protects ERK2 from dephosphorylation, thus setting the stage for immediate ERK activity upon its release from the PEA-15 inhibitory complex.

[1] Program in Apoptosis and Cell Death Research, Cancer Center, Sanford-Burnham Medical Research Institute, 10901 North Torrey Pines Road, La Jolla, California 92037, USA. [2] Program in Signal Transduction, Cancer Center, Sanford-Burnham Medical Research Institute, 10901 North Torrey Pines Road, La Jolla, California 92037, USA. [3] Department of Biology, Brookhaven National Laboratory, Upton, New York 11973, USA. [4] Department of Pathology, University of California San Diego, 9500 Gilman Drive, La Jolla, California 92093, USA. Correspondence and requests for materials should be addressed to S.J.R. (email: sriedl@sanfordburnham.org).

The RAS–RAF–MEK–ERK signalling axis represents a core regulatory cascade governing the fundamental cellular processes of cell proliferation, migration and invasion[1–3]. Components of this pathway, particularly the RAS small GTPase and the RAF serine/threonine kinase, are among the most frequently mutated genes in human cancer and also represent key targets for cancer therapy[4]. Binding of GTP-loaded RAS family GTPases[5] activates RAF, which phosphorylates and activates the dual specificity mitogen-activated protein (MAP) kinase kinase, MEK1. In turn, MEK1 activates ERK (extracellular signal-regulated kinase)1/2 through dual phosphorylation of a critical Thr-X-Tyr motif in the ERK activation loop. This cascade is further controlled by scaffolding proteins such as Kinase Suppressor of Ras (KSR), which recruits multiple components of the pathway to facilitate efficient signal transduction culminating in ERK1/2 activation[2,6]. Activated ERK1/2 phosphorylate cytosolic substrates but also translocate to the nucleus, where they phosphorylate an array of critical targets to promote proliferation and differentiation[7,8]. While the RAS–RAF–MEK cascade represents the main ERK1/2 upstream regulatory cascade, control of ERK1/2 function can also occur at the level of the kinase itself[2].

PEA-15 (15 kDa phosphoprotein enriched in astrocytes) is a widely expressed protein that efficiently regulates ERK1/2 despite consisting of only a death effector domain (DED) and a short carboxy-terminal tail. By directly binding ERK1/2, PEA-15 is capable of inhibiting ERK1/2 activity and preventing their translocation to the nucleus, therefore, regulating the two most pivotal aspects of ERK signalling [9–12]. The designation of PEA-15 as an ERK inhibitor is based on multiple studies showing that PEA-15 inhibits the classical outcomes of ERK signalling. For example, in neuroblastomas, PEA-15 impairs cell migration[13], and in astrocytic tumours inversely correlates with tumour malignancy[14]. Binding of PEA-15 to ERK has also been reported to impair tumour cell invasion and to contribute to Ras induced cell senescence[15,16]. Additionally, PEA-15 can directly inhibit ERK-mediated phosphorylation of the classical ERK1/2 substrates ELK-1 and ETS-1 in *in vitro* assays[17].

However, recent studies reporting oncogenic functions of PEA-15 hint at a regulatory role rather than a solely inhibitory impact on ERK1/2 signalling. These oncogenic functions of PEA-15 include potentiating H-Ras-mediated epithelial cell transformation and protecting glioblastoma cells from glucose deprivation-induced cell death[18,19]. Thus, PEA-15 appears to efficiently suppress ERK1/2 function, but in certain settings can also function to promote tumour growth.

Here we present three structures of PEA-15 bound to different phosphorylated states of ERK2, which provide the first structural insight into an ERK2 regulator complex. Our study reveals how PEA-15 has evolved to act as an ERK1/2 repressor that, in its inhibitory complex with the kinase, induces an accumulation of phosphorylated ERK and thus sets the stage for ERK pathway activation. PEA-15 targets the two main ERK-docking sites, using a 'minimal' D-peptide-docking site interaction and a 'regulatory' DEF-docking site interaction. The structures also show that as part of the regulatory DEF-docking site interaction, PEA-15 directly binds the ERK activation loop, which is accompanied by an extended network of allosteric changes. Altogether, the molecular mechanism of the ERK–PEA-15 interaction transforms the view of PEA-15 from a mere ERK1/2 inhibitor to a sophisticated ERK1/2 regulator and reveals a plethora of ERK2 regulatory elements.

Results

Structure of the PEA-15–ERK2 complex. To obtain insight into the mechanism underlying ERK1/2 regulation by PEA-15, we sought to obtain the crystal structure of the PEA-15-ERK complex by using several combinations of full-length PEA-15 with different activation states and phosphomimetic mutants of ERK2 in crystallization trials. After testing these in a broad array of crystallization screens, we succeeded in crystallizing an activation loop phosphomimetic (T185E) mutant of ERK2 (residues 8–360) in complex with full-length PEA-15 and solved the structure of the complex at a resolution of 3.2 Å (Fig. 1a, Table 1). In the structure, the crystallographic asymmetric unit shows a subarrangement of two ERK2 molecules bound to two molecules of PEA-15 (Supplementary Fig. S1a). In the most completely defined subarrangement, electron density was observed for PEA-15 residues 1–30 and 37–86 (defining the DED), and residues 122–127 (defining the PEA-15 C-terminal interaction segment). Residues 31–36 of the DED and the linker region (87–121) connecting the C-terminal interaction segment with the PEA-15 DED lacked electron density and were not included in the model. ERK2 electron density was observed for residues 9–357, with an adenosine diphosphate (ADP) nucleotide occupying the nucleotide-binding site of the kinase. To identify the biologically relevant assembly, we examined the complex in solution using analytical ultracentrifugation and size-exclusion chromatography (Supplementary Fig. S1b,c). This revealed an assembly consistent with one ERK2 molecule bound to one PEA-15 molecule in solution. Thus, we inferred that an arrangement consisting of an ERK2 molecule in complex with the PEA-15 DED and C-terminal segment as depicted in Fig. 1a constitutes the PEA-15–ERK2 complex.

PEA-15 occupies key ERK2-docking sites in a bipartite manner. The complex structure reveals that PEA-15 employs a bipartite binding mode involving both its DED and the segment within its C-terminus to interact with ERK2 (Fig. 1b), which is in line with earlier biochemical analysis of the ERK2–PEA-15 interaction[11,17]. Generally, bipartite binding enhances the affinity of individually weaker interactions and allows for greater binding specificity. Beyond the advantages inherent to bipartite binding, PEA-15 applies this mode of binding to occupy two key docking sites on ERK2, namely the D-peptide-binding site and the DEF interaction site (Fig. 1b) (ref. 20).

The ERK2 D-peptide-binding site is targeted by proteins that contain a distinctive D-motif (also termed DEJL/docking site for ERK and JNK, LXL or KIM/kinase interaction motif)[20]. These proteins include substrates, but also upstream kinases, scaffolding proteins and phosphatases[21]. The D-peptide-binding site is the only binding site on ERK2 that has been structurally characterized at high resolution before this study, with five structures now available of peptide fragments from ERK2 partners bound to the ERK2 D-peptide-binding site[22–25].

The other site on ERK1/2 that is targeted by PEA-15 is known as the DEF-docking site (docking site for ERK, FxF), due to its characteristic ability to bind proteins that contain a consensus motif with two phenylalanine residues separated by one amino acid (FxF)[26]. This docking site is key to ERK1/2's interaction with substrates and scaffold proteins, as well as components of the nuclear transport machinery that are crucial for ERK1/2 nuclear translocation. Thus, utilizing a bipartite binding mode that engages both sites (Fig. 1b) enables PEA-15 to inhibit ERK1/2 function and explains its general capacity to inhibit ERK enzymatic activity (Supplementary Fig. S2a)[17], as well as its tumour suppressor role[13–16].

PEA-15 uses a minimal inverted D-peptide binding mode. Closer examination of the interaction between the C-terminal segment of PEA-15 (residues 122–127) and the

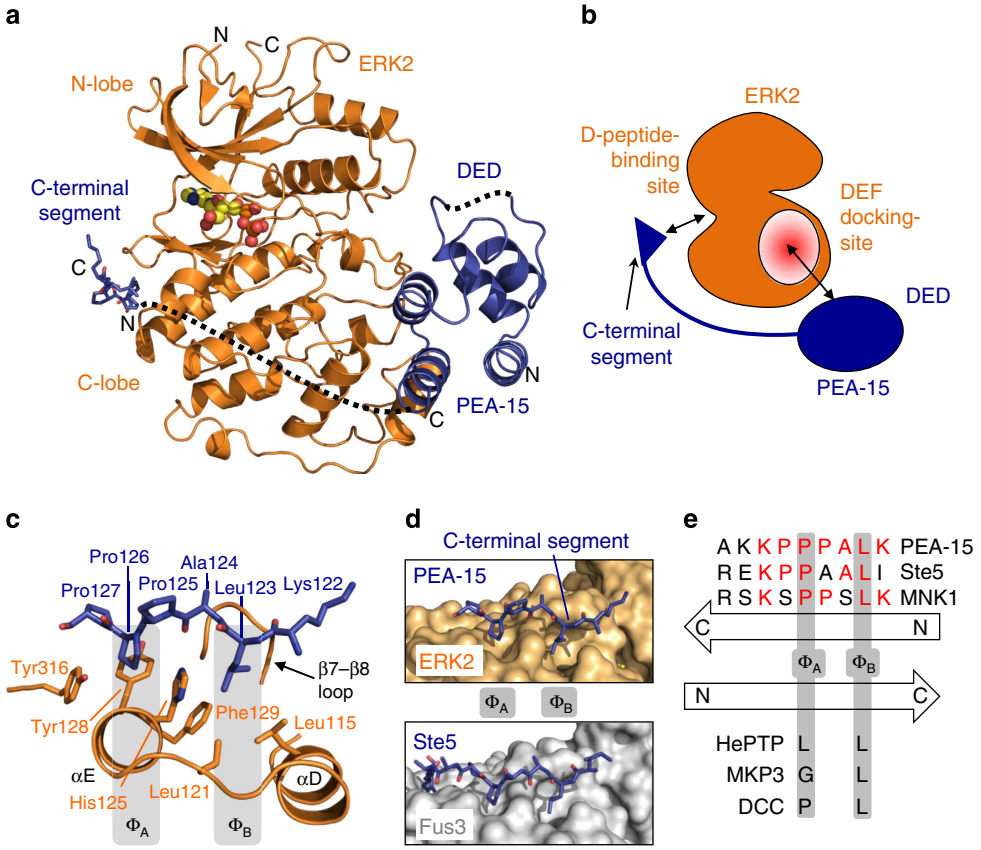

Figure 1 | PEA-15 interacts with ERK2 using a bipartite binding mode. (**a**) Structure of the PEA-15–ERK2 complex. Shown is the structure of ERK2 (orange) with bound ADP (yellow) and the DED and C-terminal segment of PEA-15 in blue (regions not defined by electron density are schematically indicated by dotted lines; N and C termini of the DED and C-terminal segment are indicated). (**b**) Cartoon illustration of the PEA-15–ERK2 complex. PEA-15 utilizes a bipartite binding mode to occupy the two main regulatory sites of ERK2. The DED of PEA-15 (blue) occupies the ERK2 DEF-docking region (red), while the C-terminal segment of PEA-15 occupies the D-peptide-binding site. (**c**) Detailed view of the PEA-15 C-terminal segment (residues 122–127; blue sticks) binding to the D-peptide-binding site on ERK2 (orange). Interface sidechains and secondary structural elements are labelled. (**d**) The PEA-15 C-terminal segment binds ERK2 (top) in a manner similar to the binding of the scaffold protein Ste5 to the yeast MAP kinase Fus3 (bottom; residues 306–314, PDB: 2f49). (**e**) Conservation between PEA-15, Ste5 and MNK1. Schematic illustration of binding modes (see also Supplementary Figs S2 and S3). Displayed are the respective D-peptide sequences with residues occupying the Φ_A and Φ_B sites annotated. Relative directionality and key interaction residues are depicted in comparison with the canonical D-peptide binding mode.

D-peptide-binding site of ERK2 (Fig. 1c, Supplementary Fig. S2b,c) shows that this segment of PEA-15 adopts an extended conformation, occupying the groove between helices αD and αE and the β7-β8 turn on the C-terminal lobe of ERK2. Comparison with the crystal structures of peptides from deleted in colorectal cancer (DCC), MAP kinase phosphatase and hematopoietic tyrosine phosphatase bound to ERK2 shows that PEA-15 occupies this site in a non-canonical manner (Supplementary Fig. S3). Intriguingly, PEA-15 utilizes a minimal D-peptide interaction consensus motif (see also below) that binds in the opposite direction to that observed in the above structures[17,21]. In detail, the Φ_A pocket on the ERK2 D-peptide-binding site is occupied by Pro126 of PEA-15, with Pro127 extending the hydrophobic interaction by packing against Tyr128 and Tyr316 at the edge of the pocket. The Φ_B pocket created by ERK2 residues Leu115, Leu121 and Phe129 is filled by Leu123 of PEA-15 (Fig. 1c). Analysis over a wider array of MAP kinase–D-peptide complexes shows that the PEA-15 C-terminal segment is almost identical to the binding-motif used by the yeast scaffold protein Ste5 to regulate its target kinase Fus3 (Fig. 1d,e)[27]. Very recently, the structures of MNK1 and RSK1 D-peptides have been solved in complex with ERK2 and also exhibit a reverse D-peptide binding mode[25] (Fig. 1e; Supplementary Fig. S2d). Intriguingly, the MNK1 D-peptide shows remarkable similarity in the backbone conformation of residues 435–439 when compared with the PEA-15 C-terminal segment. However, the MNK1 peptide interaction also includes an extended helical-binding element (MNK1 residues 439–450), (Supplementary Fig. S2d), which buries an additional 380 Å^2 of interaction surface, resulting in a tight interaction with a dissociation constant of 700 nM (ref. 25). In contrast, the much smaller PEA-15 ERK D-peptide-binding interaction is rather weak, with a dissociation constant of 18 μM (Supplementary Fig. S2e). Thus, PEA-15 utilizes a minimal inverse D-peptide that blocks the hydrophobic portion of the D-peptide-binding site with moderate affinity, consistent with regulatory rather than constitutive inhibition of ERK2. In line with this, mutation of L123K in the C-terminal segment of PEA-15 substantially weakens the binding to ERK2 (Fig. 2d), and results in the failure of the PEA-15 L123K mutant to prevent ERK nuclear translocation (Fig. 2e). Taken together, the minimal reverse D-peptide binding of PEA-15 demonstrates the structural adaptability of the D-peptide-docking site and raises the possibility that other ERK1/2-binding partners employ this mode of binding, which may be a hallmark of moderate affinity regulatory interactions with this site.

Table 1 | Data collection and refinement statistics.

	ERK2(T185E)-PEA-15 FL	ERK2-PEA-15 (1-96)	Phospho-ERK2-PEA-15 (1-96)
Data collection			
Space group	$P2_1$	P 2_1 2_1 2	P 2_1 2_1 2
Cell dimensions			
a, *b*, *c* (Å)	80.80, 149.13, 98.87	73.48, 205.33, 57.75	73.76, 204.02, 61.13
α, β, γ (°)	90.00, 90.41, 90.00	90, 90, 90	90, 90, 90
Wavelength	1.075	1.075	1.075
Resolution (Å)	29.8–3.19	29.7–1.8	29.72–1.93
R_{merge}	0.079 (0.345)	0.08 (0.772)	0.082 (0.421)
$I/\sigma I$	21.4 (5.3)	24.8 (3.8)	21.4 (4.8)
Completeness (%)	98.6 (91.7)	99.1 (96.5)	99.8 (98.8)
Redundancy	6.0 (5.7)	14.4 (14.4)	12.6 (9.3)
Refinement			
Resolution (Å)	29.8–3.19	29.7–1.8	29.72–1.93
No. of reflections	36,572	77,047	66,545
R_{work}/R_{free}	0.243/0.292	0.187/0.222	0.199/0.243
No. of atoms			
Protein	14,061	6,276	6,280
Ligand/ion	188	1	-
Water	-	649	633
B-factors			
Protein	41.9	22.92	25.63
Ligand/ion	63.4	27.2	-
Water	-	33.67	32.01
Root mean squared deviations			
Bond lengths (Å)	0.068	0.096	0.015
Bond angles (°)	1.0724	1.362	1.319

The DED of PEA-15 occupies the ERK2 DEF-docking site. PEA-15 utilizes its DED to bind the ERK2 DEF-docking site[26,28], and our structure provides the first high-resolution structural insight into an ERK2–DEF site interaction (Fig. 2a). It is also the first structural view of the interaction of a death domain protein with a kinase. The PEA-15–ERK2 structure shows that the DED of PEA-15 utilizes helices α5 and α6 and the linker between the two helices to bind ERK2 residues residing in helices αG and αEF (Fig. 2a). This interaction network is supported by ERK2 residues from the first helix of the MAP kinase insert, which is characteristic of MAP kinases (Fig. 2a). In detail, the DEF-docking site interaction surface utilized by PEA-15 is generated by ERK2 Tyr233 and Leu234 and the DEF-docking site region proper, as well as the stem of Lys259, Ala260 and Tyr263 from the MAP kinase insert, which together form a hydrophobic surface to accommodate Pro73, Leu76 and Val80 of PEA-15. This patch is completed by polar interactions between residues Asp19, Glu68 and particularly Arg71 (see also Fig. 3) from PEA-15 and Arg191, Tyr205, Asn257 and Lys259 from ERK2 (Fig. 2b). The DEF docking interaction is crucial for PEA-15 function, including its ability to sequester ERK1/2 and prevent its translocation to the nucleus[29–31]. Accordingly, the mutation of PEA-15 Arg71 at the centre of the interface abrogates cytoplasmic retention of ERK2 by PEA-15 (Fig. 2d,e)[10,11].

PEA-15 DED RXDL motif serves to position binding residues. The PEA-15–ERK2 structure also shows that the DEF-docking site interaction does not directly involve residues Arg72, Asp74 or Leu75, which constitute the so called RXDL motif of the PEA-15 DED. Generally, the RXDL motif is a hallmark of DED proteins and is conserved among members of this family. The function of this motif has remained unclear, although it has been proposed to have a role in the interaction with binding partners[32]. Surprisingly, PEA-15 residues Glu68, Arg71 and Leu76, which are key for the interaction with ERK2, are not part of the RXDL motif but reside directly beside the residues constituting the motif (Fig. 2c). Instead, Arg72, Pro73, Asp74, Leu75 (RXDL) partake in interactions within the DED of PEA-15, thus reinforcing the local structure of the domain. Hence, the role of the RXDL motif lies not in binding but in stabilization of the α5-loop-α6 region, thus properly positioning the critical binding residues of PEA-15 (Fig. 2c).

The PEA-15 DED directly binds the ERK2 activation loop. An unexpected aspect of PEA-15 interaction with the ERK2–DEF site is that the ERK2 activation loop directly participates in the binding interface. This is surprising, given that kinase activation loops are commonly characterized by a large degree of plasticity[33–35], which could potentially make them a destabilizing factor in binding interactions. However, the structure reveals that in the PEA-15–ERK2 complex the region around the Glu185 of the activation loop is 'captured' by a binding pocket created by residues from both PEA-15 and ERK2 (Fig. 3a). As outlined above, Glu185 was used as phosphomimetic for pThr185 of the ERK2 Thr-X-Tyr motif. The PEA-15–ERK2 composite pocket captures the Glu185 phosphomimetic utilizing an arginine stretch that includes ERK2 residues Arg191, Arg194 and particularly Arg71 from PEA-15, which is the most central residue of this interaction (Fig. 3a). As a consequence of this capture, the activation loop adopts a helical conformation and is fully defined in the PEA-15–ERK2 complex (Fig. 3a). This mechanism explains how PEA-15 is able to engage a threonine-phosphorylated ERK2 activation loop. Yet, PEA-15 exhibits similar binding affinities for all phosphorylation states of ERK2 (Supplementary Fig. S4), raising the question of how PEA-15 interacts with the unphosphorylated and dually phosphosphorylated ERK2 kinase.

PEA-15 captures the activation loop in two distinct modes. To answer this question we solved the structures of the PEA-15 DED (residues 1–96) bound to unphosphorylated and dually phosphorylated ERK2 at resolutions of 1.8 and 1.9 Å, respectively (Supplementary Figs S5a,b and S6). These structures show a similar overall interaction by the PEA-15 DED (Supplementary Fig. S5c,d), but importantly reveal how PEA-15 is able to avidly bind ERK2 regardless of its phosphorylation status by using two distinct binding modes to capture the activation loop.

The structure of PEA-15 in complex with the unphosphorylated ERK2 shows that the composite pocket formed by PEA-15 and the DEF-docking site of ERK2 is able to also bind the unphosphorylated activation loop, but by interacting with Tyr187 from the Thr-X-Tyr motif (Fig. 3b). The binding of Tyr187 is accompanied by a register shift of two amino acids within the activation loop, compared with the binding of the phosphomimetic Glu185. As a consequence, the activation loop following Thr185 adopts an extended rather than helical conformation in this binding mode (mode 1) and the N-terminal portion of the activation loop (residues 179–184) is partially disordered. Furthermore, Arg71 of PEA-15 now undergoes a stacking interaction with the aromatic side chain of Tyr187 to anchor the activation loop (Fig. 3b, right panel).

The structure of dually phosphorylated ERK2 in complex with PEA-15 demonstrates mode 2 of activation loop binding, which is highly similar to that observed in the structure of PEA-15 in complex with the phosphomimetic Glu185 mutant. The

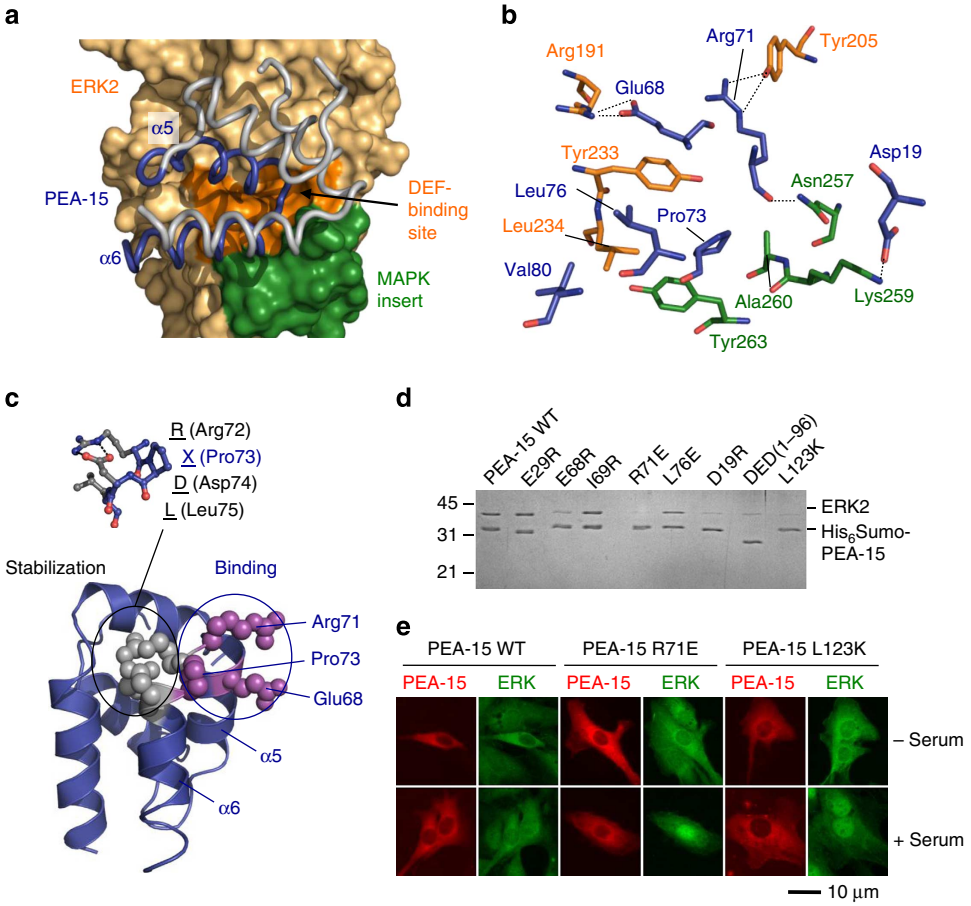

Figure 2 | The PEA-15 DED interacts with the ERK2 DEF-docking site. (**a**) PEA-15 DED (worm representation) binding to ERK2 (surface). The PEA-15 DED is rendered in grey with interacting helices α5-α6 coloured blue, while binding residues of ERK2 residing in the DEF-binding region and the MAP kinase insert are coloured orange and green, respectively. (**b**) Detailed view of the PEA-15–DEF-binding-site interaction (PEA-15 residues are depicted in blue, ERK2 DEF-binding site and MAP kinase insert residues are rendered orange and green, respectively). (**c**) The DED RXDL motif is not involved in binding. The PEA-15 DED (blue ribbon) is depicted with Arg72, Asp74 and Leu75 of the RXDL motif displayed as grey spheres (detailed view shown in stick representation above). The RXDL residues do not participate in the interaction with ERK2 but function to stabilize the neighbouring residues Glu68, Arg71 and Pro73 (magenta), which do interact with ERK2. (**d**) Mutational analysis of PEA-15 residues involved in ERK2 binding. Recombinantly expressed and purified His_6-tagged PEA-15 proteins were incubated with untagged ERK2 and captured on Ni-NTA resin, which after wash steps was subjected to SDS-PAGE. Protein bands were visualized with Coomassie blue. (**e**) Effect of PEA-15 WT and mutants deficient in ERK2 binding on nuclear translocation of ERK2. NIH3T3 cells expressing WT and mutant EGFP-PEA-15 (pseudocoloured in red) were immunolabelled for ERK1/2 (pseudocoloured in green). A representative scale bar of 10 μm is displayed below. PEA-15 is always located in the cytosol. In serum-starved cells, ERK2 is retained in the cytosol in the presence of PEA-15 WT and to a lesser extent in the presence of the mutant PEA-15. In serum-stimulated cells, strong nuclear translocation of ERK2 can be observed in the presence of the R71E and L123K PEA-15 mutants compared with PEA-15 WT.

activation loop adopts the same helical conformation, with the phosphate moiety of pThr185 binding to the composite pocket formed by ERK2 and PEA-15 (Fig. 3c).

PEA-15 binding reveals extended allosteric conduit in ERK2. Comparison of dually phosphorylated ERK2 in its unbound- and PEA-15-bound forms[33] also reveals that the binding of the PEA-15 DED triggers a network of allosteric changes in ERK2. Firstly, PEA-15 counteracts the interaction of the two phosphate groups of pThr185 and pTyr187 with their binding pockets in ERK2 (Fig. 4a), which leads to the rearrangement of the activation loop described above. This modification in turn leads to an extended network of short- and long-range allosteric rearrangements in the kinase (Fig. 4a, Supplementary Movie). In detail, Glu68 of PEA-15 displaces Tyr233 towards the αEF helix and dislodges pTyr187 from its pocket on ERK2. In parallel, Arg71 of PEA-15 directly sequesters pThr185, as well as Tyr205, which flips away from its previous location lining the pThr185 pocket in ERK2 (Fig. 4a, Supplementary Fig. S7).

The activation loop rearrangement is accompanied by several conformational adjustments of key functional elements of the kinase, such as the Glycine-rich loop and C-helix (see Supplementary Movie 1). In parallel, a large exposed hydrophobic patch distal from the catalytic center of the kinase (formed by residues Phe183, Phe331 and Leu335) becomes buried upon PEA-15 binding (Fig. 4). These rearrangements reveal an interconnected conformational conduit that is linked to the PEA-15–ERK2 DEF-binding site interaction and may also be utilized by other binding partners for ERK regulation. The conduit spans from the nucleotide-binding region of ERK2 through the central groove to the outlined hydrophobic patch, which has been speculated to mediate ERK2 dimerization events and other protein interactions[36–38].

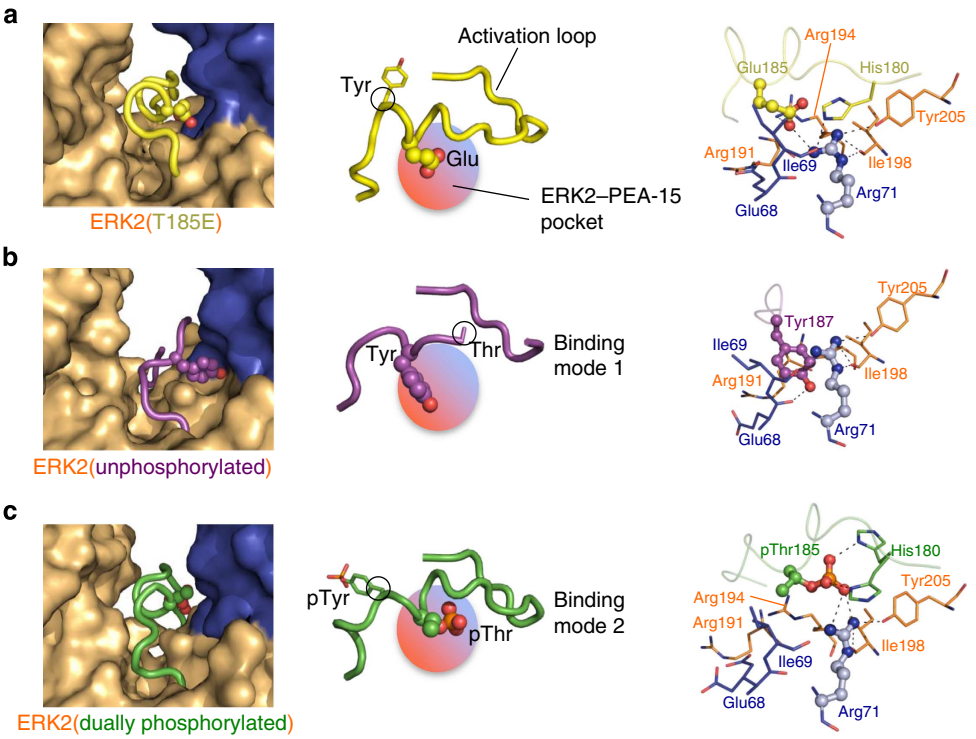

Figure 3 | PEA-15 binds the ERK2 activation loop in two distinct modes. (**a**) PEA-15 binding to ERK2(T185E). Left: Close-up of the PEA-15–ERK2 composite surface pocket (orange/blue) accepting Glu185 and the activation loop in a helical conformation (yellow). Middle: Schematic of the activation loop showing Tyr187 and Glu185 and the activation loop conformation in relation to the composite pocket. Right: Detailed view of interactions surrounding Glu185 (ERK2 residues coloured orange and PEA-15 residues blue, and activation loop residues rendered in yellow). (**b**,**c**) Analogous representations of the PEA-15–ERK2 pocket accommodating (**b**) unphosphorylated ERK2 activation loop and (**c**) the dually phosphorylated activation loop (activation loop residues are coloured purple and green, respectively).

PEA-15 binding defines a regulatory ERK DEF site interaction. The allosteric conduit triggered by PEA-15 in combination with the activation loop engagement revealed by our ERK2–PEA-15 complex structures suggests a new view of ERK DEF-binding site interactions that distinguishes between 'substrate like' and 'regulatory' type interactions. Firstly, PEA-15 binding causes the activation loop in ERK2 to adopt an inactive conformation despite being dually phosphorylated. This becomes evident when a putative substrate, derived from the structure of substrate-bound cyclic adenosine monophosphate-dependent protein kinase[39], is overlaid onto dually phosphorylated ERK2 unbound or bound to PEA-15 (ref. 33) (Fig. 4b). The overlay shows that in PEA-15-bound ERK2 the pThr and pTyr, together with the helical conformation of the activation loop, completely occlude the substrate-binding region normally available in phospho-ERK2.

Secondly, as outlined above, the term DEF-docking site was initially based on its ability to interact with substrates containing a FxF motif downstream of the substrate Ser/Thr residue. While no structure of an FxF-type substrate-bound to ERK is available, various groups have predicted features of this interaction[26,28,40]. The surface pockets highlighted in Fig. 4b and Supplementary Fig. S8 are based on a model by Turk and colleagues[28] and illustrate the two key binding regions in ERK2 that are predicted to accommodate the Phe moieties of FxF substrate motifs. However, PEA-15 does not contain a FxF motif and the binding of the PEA-15 DED occurs only in the general area of these pockets. In fact, only Leu234 and Tyr263 from the predicted FxF-binding pockets make a direct hydrophobic contact with PEA-15 (Fig. 2b), while Tyr 231 and pTyr 185 reorient as part of the allosteric PEA-15 interaction mechanism (Supplementary Fig. S8). Thus, PEA-15 binding partially dismantles the binding pocket for the first Phe of the motif, in addition to relocating the activation loop.

These features suggest the existence of two types of DEF interactions. One represents a classic FxF-type DEF interaction, in which substrates bind to the defined FxF pockets of dually phosphorylated ERK1/2 in a catalytically competent conformation. The second type of DEF-site interaction mediates the regulatory binding of ERK effectors. In this case, the binding partners utilize an interaction pattern that differs from the FxF substrate-type binding. Instead, these factors use the DEF-docking site to alter the ERK1/2 activation loop, which may also facilitate its phosphorylation or dephosphorylation.

PEA-15 protects phospho-ERK1/2 from dephosphorylation. We next sought to investigate the physiological consequences of the ability of PEA-15 to capture the Thr-X-Tyr activation loop of ERK in its different phosphorylation states. First, we examined the effect of PEA-15 binding on ERK2 activation by its upstream kinase MEK1 (Fig. 5a, Supplementary Fig. S9a–c). Our *in vitro* kinase assays show that PEA-15 reduces the rate of MEK1-dependent ERK2 phosphorylation, but it nevertheless allows accumulation of fully phosphorylated ERK2. In fact we find that at a concentration of 17 μM, which may reflect MEK–KSR–ERK activation platforms, MEK1 is able to displace PEA-15 (Supplementary Fig. S9d). Taken together, these results are consistent with earlier *in vitro* studies that define PEA-15 as an inhibitor of ERK1/2 phosphorylation[10], but suggest that PEA-15 is a permissive regulator rather than inhibitor of ERK2 phosphorylation.

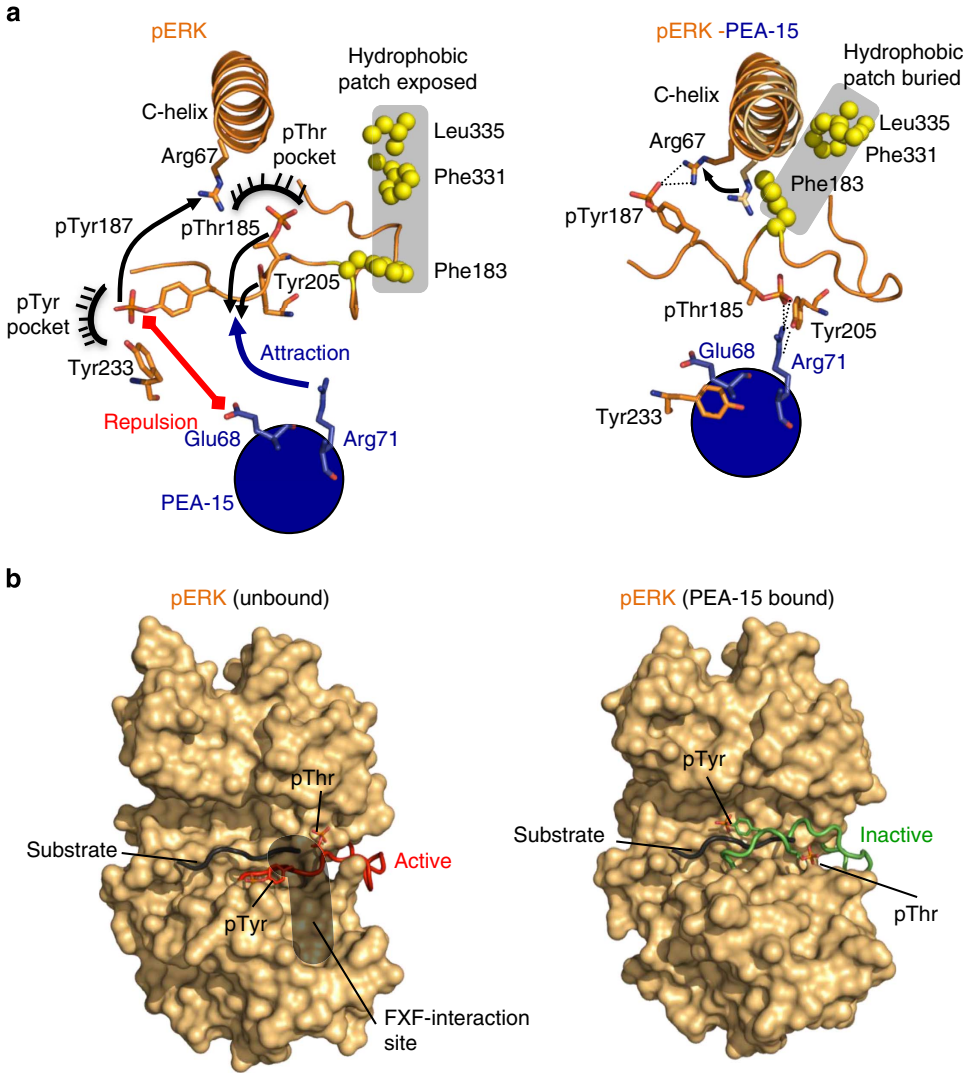

Figure 4 | PEA-15-ERK2 regulatory interaction. (**a**) PEA-15 binding triggers concerted allosteric changes in phospho-ERK2. Left: Unbound ERK2 before PEA-15 binding. Phospho-Thr185 and phospho-Tyr187 are anchored into defined pockets in phosphorylated ERK2 (PDBid:2erk). Upon binding, PEA-15 Glu68 repels phospho-Tyr187 and Tyr233, while Arg71 of PEA-15 attracts phospho-Thr185 and Tyr205 (indicated by red and blue arrows). Right: Conformations observed in the PEA-15–phosphor-ERK2 complex. In the complex, PEA-15 Arg71 forms a direct salt bridge with pThr185 and coordinates Tyr205, while pTyr187 interacts with Arg67 located in the αC-helix. As a consequence, the activation loop adopts a helical conformation that is accompanied by long-range allosteric changes (see also Supplementary Movie 1) in catalytic elements such as the αC-helix, as well as the burial of a distal hydrophobic patch (residues displayed in yellow spheres). (**b**) PEA-15 'regulatory' DEF interaction differs from- and precludes substrate-like binding. Comparison of the activation loop conformations of unbound dually phosphorylated ERK2 (left panel, red; PDB: 2erk) and PEA-15-bound phospho-ERK2 (right panel, green). The position of a putative peptide substrate (black; depicting residues P−3 to P+3 of a substrate from a cAMP-dependent protein kinase substrate complex/PDB:1L3R) is also depicted. Additionally the putative FxF-binding region on ERK2 is indicated for unbound phospho-ERK2 (grey area; see also Supplementary Fig. S8). This region has been shown to capture a characteristic FxF sequence motif downstream of the phosphorylation site in key ERK substrates.

Additionally, we found that PEA-15 overexpression leads to an accumulation of phosphorylated ERK1/2 in transiently transfected cells (Fig. 5b), in agreement with previous studies[18,41]. We also observed this accumulation in the absence of growth factor stimulation while PEA-15 interface mutants fail to propagate this effect (Fig. 5b). This observation suggests that PEA-15 protects phospho-ERK1/2 from dephosphorylation. To investigate this function of PEA-15, we examined its effect on the progressive decline of phospho-ERK1/2 following block of MEK activity. We measured phospho-ERK1/2 levels in the presence or absence of overexpressed PEA-15 in cells treated with the MEK inhibitor U0126 for various periods of time (Fig. 5c). The results show that, indeed, PEA-15 provides prolonged protection of phospho-ERK1/2 from dephosphorylation in serum-stimulated HEK293 cells treated with U0126 as compared with control cells where ERK1/2 phosphorylation is rapidly lost.

Discussion

The physiological outcome of the multifaceted binding mechanism applied by PEA-15 is an accumulation of a 'spring-loaded' phospho-ERK2 in complex with PEA-15. This accumulation occurs not only when upstream components of the ERK pathway are activated, but also under unstimulated conditions. However, even though ERK bound to PEA-15 is phosphorylated, its activation loop is held in an inactive conformation (Fig. 4b) and

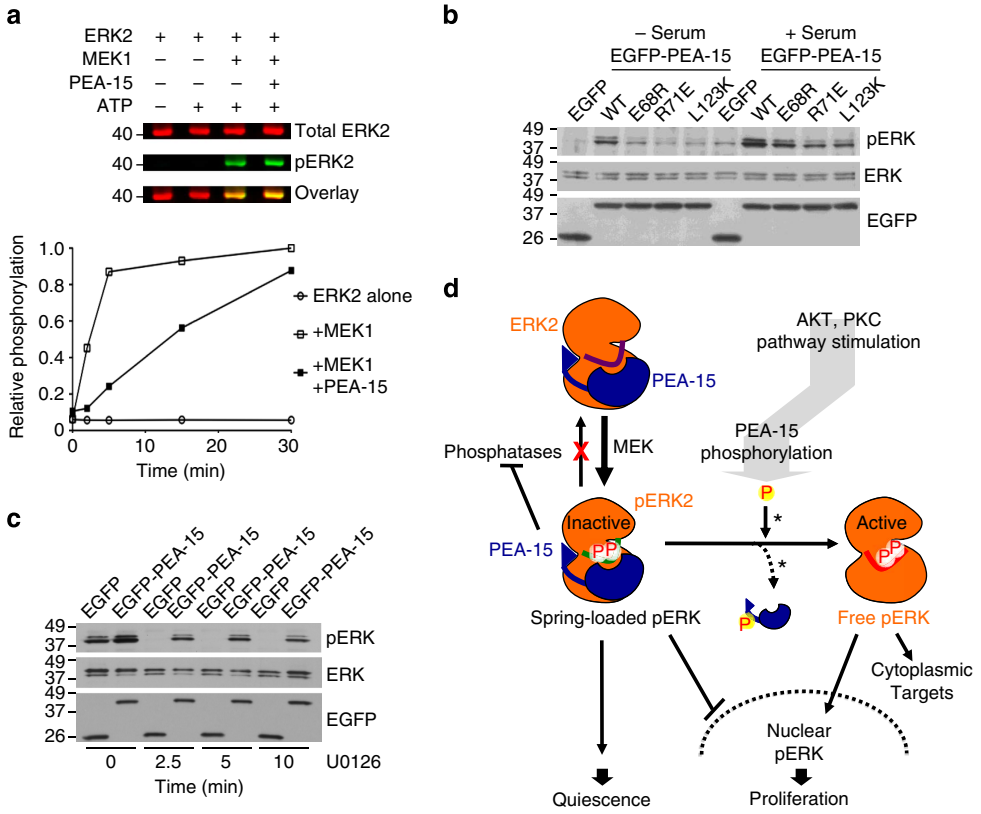

Figure 5 | PEA-15 leads to the stabilization of spring-loaded ERK1/2. (**a**) PEA-15-bound ERK2 is permissive to phosphorylation by MEK1. An *in vitro* phosphorylation assay of ERK2 shows a decreased rate of ERK phosphorylation but still allows for accumulation of phospho-ERK2. Time course of ERK2 phosphorylation by constitutive active MEK1 (quantified, bottom) and 30 min end points of the assay (LICOR visualization, top). (**b**) Wild-type PEA-15, but not binding interface mutants, leads to enrichment of dually phosphorylated ERK1/2 in both unstimulated and serum-stimulated cells. Extracts from cells expressing wild-type PEA-15, or ERK1/2-binding interface mutants of PEA-15, were probed for dually phosphorylated ERK2. (**c**) PEA-15 protects phospho ERK from dephosphorylation. HEK293 cells expressing EGFP-PEA-15 or control vector were stimulated with serum and subsequently treated with 10 μM U0126 to inhibit MEK1 for the indicated times. Extracts were analysed at the indicated time points by western blotting with the indicated antibodies. (**d**) Accumulation of halted, 'spring-loaded' phospho-ERK1/2 highlights the dual nature of PEA-15. Schematic illustrating the cellular consequences of the PEA-15-ERK regulatory mechanism, which allows for integration of diverse pathways and signalling outcomes (asterisks next to the arrows describing the release of phosphorylated PEA-15 from ERK1/2 indicate that the mechanism of this release is not known and may involve displacement through an additional unknown protein)[17].

its nuclear transport is blocked. Consequently, in this scenario PEA-15 inhibits the activity of ERK1/2, proliferative signals are suppressed, and PEA-15 acts as tumour suppressor (Fig. 5d). However, the regulatory character of the PEA-15 ERK interaction allows PEA-15 to be released from ERK2. This release is reported to involve phosphorylation of PEA-15 Ser104/Ser116 (refs 42,43), yet occurs by an unknown mechanism because phosphorylation of PEA-15 has no direct effect on ERK binding[17]. Regardless of the mechanism of PEA-15 release, its consequence is that 'spring-loaded' phospho-ERK1/2 can now promptly adopt its default active conformation without further need for phosphorylation by upstream kinases (Fig. 5d). The released phospho-ERK1/2 will then phosphorylate their cytosolic substrates and translocate to the nucleus to phosphorylate nuclear substrates, inducing transcription and ultimately proliferation.

Among the kinases that have been reported to phosphorylate PEA-15 on Ser104/Ser116 are protein kinase C, CaMKII and AKT (refs 42,43). Thus PEA-15 can link different pathways to ERK1/2 and, as in the case of AKT or protein kinase C, enhance their oncogenic effect. Importantly, the mechanism applied by PEA-15 also explains how ERK1/2 phosphorylation can be uncoupled from its signalling outcome[44]. While ERK1/2 phosphorylation is frequently used as marker for malignancy, the mechanism utilized by PEA-15 suggests that clinical testing strategies considering PEA-15 levels and phosphorylation, as well as a readout of ERK1/2 activity, can provide a more powerful prognostic tool than simply ERK1/2 phosphorylation levels[42].

In summary, the structural information from the PEA-15-ERK complex demonstrates that PEA-15 acts as an efficient mechanism-based regulator that employs known, as well as novel MAP kinase regulatory features. PEA-15 uses a bipartite binding mode and captures different activation states of ERK2 to suppress and direct the ultimate outcome of the ERK-signalling pathway. The structural features of this regulation provide remarkable insight into the inner workings of ERK1/2 kinase function, which involve a previously unidentified allosteric network. They also provide mechanistic insight into how a tumour suppressor can lead to an enrichment of phospho-ERK1/2, potentially priming the cell for a rapid activation of ERK1/2 by signalling pathways that target PEA-15.

Methods

Protein expression and purification. For crystallization Human ERK2 (Uniprot: P28482) residues 8–360 was cloned into a modified pET-LIC vector (kindly gifted by the Netherlands Cancer Insitute (NKI) Protein Facility with funding from grant no. 175.010.2007.012) incorporating an N-terminal His_6 tag and 3C protease

cleavage site. To prepare dually phosphorylated ERK2 this construct was coexpressed with constitutively active MEK1 from pETDuet-ACYC in *Escherichia coli*, while unphosphorylated kinase was prepared by coexpression of YopH tyrosine phosphatase to minimize ERK2 autophosphorylation[45]. Full-length human PEA-15 (Uniprot: Q15121 residues 1–130) for crystallization was expressed from pET28b. All biophysical and biochemical experiments were performed using full-length ERK2 and PEA-15 expressed from a modified pET vector incorporating an N-terminal His_6-tag and SUMO1 fusion protein. Treatment of these proteins with SENP1 protease yielded species with no residually amino acids for ERK2 (1–360) and a single additional glycine residue for PEA-15 in order to facilitate protease cleavage. The DED construct of PEA-15 for crystallization (residues 1–96) was also produced as a SUMO-fusion protein. All mutagenesis was performed using QuikChange site-directed mutagenesis. All proteins were initially purified by Ni^{2+} affinity chromatography, and purified to homogeneity after cleavage with respective proteases using anion-exchange (Source Q 10/10) and size-exclusion (Superdex-200) chromatographies. Isolated proteins and complexes were flash frozen for storage in 10 mM HEPES (7.6), 100 mM NaCl and 0.5 mM tris-(2-carboxyethyl)phosphine.

Crystallization. For crystallization ERK2 T185E (8–360) and full-length PEA-15 were combined at high concentration and the complex was purified by size-exclusion chromatography at a protein concentration of $\sim$20 mg ml^{-1}. Initial crystals of ERK2 T185E bound to full-length PEA-15 were grown by sitting drop vapour diffusion using a precipitant condition containing 0.1 M Bis-Tris (pH 5.5) and 2.0 M ammonium sulphate. These crystals diffracted anisotropically to 4 Å in the best dimension, and were improved by cycles of additive screening and soaking with nucleotides. Final crystals were grown from a condition containing 0.1 M Bis-Tris (pH 5.5), 1.8 M ammonium sulphate and 3% sucrose, soaked with 2 mM ADP for $\sim$15 min in mother liquor, and cryoprotected by transferring to mother liquor containing 20% glycerol before freezing in a nitrogen cryostream.

Purified unphosphorylated, and dually phosphorylated, ERK2 (8–360) were each mixed with PEA-15 (1–96) at equimolar ratios, concentrated to $\sim$15 mg ml^{-1} and directly subjected to crystallization screening. Diffraction quality crystals of unphosphorylated ERK2–PEA-15 DED grew from a condition containing 0.2 M sodium malonate and 20% PEG 3350 (measured pH 5.5). Crystals of the dually phosphorylated ERK2 complex grew from 0.2 M potassium phosphate monobasic and 20% w/v Polyethylene glycol 3,350 (measured pH 5.0). Both crystal types were transferred to mother liquor containing 15% glycerol for cryoprotection before freezing.

Structure determination. Final diffraction data for all crystals was collected at National Synchrotron Light Source beamline X29 and processed using XDS[46] and SCALA[47]. The structure of the ERK2 T185E–PEA-15 complex was solved by molecular replacement in Phaser[48] using the structure of dually phosphorylated ERK2 (PDBid: 2erk) with the activation loop deleted as a search model. PEA-15 was successfully located using an edited poly-alanine model of the DED from MC159 (PDBid: 2bbr) as a search model. The overall structure was iteratively built and refined using Refmac5 (ref. 49) and COOT[50]. Structures of the complex between un- or dually phosphorylated ERK2 with the PEA-15 DED were solved by independent searches for the individually chains from the above structure, with the activation loop of ERK2 deleted from search models. In each crystal the asymmetric unit contained one molecule of PEA-15 bound to ERK2, and a second ERK2 polypeptide not bound to PEA-15.

Isothermal titration calorimetry and analytical ultracentrifugation. Isothermal titration calorimetry (ITC) was carried out using a MicroCal iTC200 calorimeter. PEA-15 full-length or fragments thereof (200–500 μM) were injected into ERK2 variants (20–50 μM) in a matched buffer containing 10 mM HEPES (7.6), 100 mM NaCl and 0.5 mM Tris-(2-carboxyethyl)phosphine. AMP-PNP (2 mM) was incorporated into the buffer of the diluent kinase to mimic the physiological presence of nucleotide. Analytical ultracentrifugation sedimentation equilibrium experiments were performed in a ProteomeLab XL-I (BeckmanCoulter) analytical ultracentrifuge with protein in the same buffer used for ITC. Analysis was done using HeteroAnalysis software (by J.L. Cole and J.W. Lary, University of Connecticut; http://www.biotech.uconn.edu/auf/).

ERK2 activation assays. Activation of ERK2 by MEK1 *in vitro* was performed using purified MEK1-R4F[51] purified with a C-terminal His_6-tag. Combinations of ERK2 (5 μM), MEK1 (0.5 μM) and PEA-15 (10 μM) were incubated in a buffer containing 25 mM HEPES (pH 7.5), 100 mM NaCl, 20 mM $MgCl_2$, 2 mM dithiothreitol, and 0.5 mM EGTA, with adenosine triphosphate (5 mM) added to initiate reactions. At indicated time points samples were removed, combined with SDS–polyacrylamide gel electrophoresis (PAGE) sample buffer and boiled to terminate the reaction. Following electrophoreses and western blotting, transferred proteins were probed with mouse derived α-ERK2 and rabbit α-phospho-ERK2 antibodies (both from Cell Signaling Technology). Detection was performed using LICOR IRDye α-mouse and α-rabbit secondary antibodies.

PEA-15 inhibition assay of ERK2 activity. ADP-glo assays (Promega) were performed to measure kinase activity of activated ERK2 in the presence and absence of PEA-15. Reactions were carried out in an identical buffer to the ERK2 activation assays described above. ERK2 (0.4 μM) was incubated with MBP (50 μM) and adenosine triphosphate (50 μM) with/without PEA-15 (5 μM) at room temperature for 30 min. Amounts of generated ADP were measured through luminescence according to the manufacturers' instructions in 384-well plates.

***In vitro* binding assays between PEA-15 and ERK2**. Untagged full-length ERK2 was isolated as described above in the protein expression and purification section; namely expressed as a His-Sumo-fusion protein, cleaved from the His-Sumo tag and finally purified using anion-exchange chromatography. Wild-type His-Sumo-PEA-15, or mutants thereof, were expressed as described above and purified via Ni-affinity chromatography. After elution His-Sumo-PEA-15 proteins were incubated with an excess ($\sim$2:1) of the untagged ERK2 wt protein for 25 min at room temperature and then applied to Ni-NTA beads. After wash steps using a 10 mM Tris (pH 8.0), 100 mM NaCl, 10% glycerol, 10% sucrose and 2 mM dithiothreitol containing 30 mM imidazole, the Ni-NTA beads were mixed with SDS–PAGE sample buffer and subjected to SDS–PAGE. Protein bands were visualized using Coomassie staining.

Characterization of ERK2–PEA-15 regulation in cells. For immunoblotting, HEK 293 cells were cultured in DMEM supplemented with 10% fetal bovine serum (FBS) and penicillin/streptomycin and transiently transfected with EGFP or EGFP-tagged PEA-15 plasmids using Lipofectamine 2000 (Invitrogen). Twenty-four hours after transfection, the cells were starved in DMEM with 0.2% FBS for 18 h. The cells were then stimulated for 45 min with 20% FBS or maintained in 0.2% FBS and then lysed in modified RIPA buffer (150 mM NaCl, 50 mM Tris, pH 7.5 with 1% Triton X-100, 0.5% Na deoxycholate, 0.1% SDS, 2 mM EDTA, 1 mM sodium orthovanadate, 1 mM sodium fluoride, aprotinin, leupeptin, pepstatin 1 μg ml^{-1} each and 1 mM phenylmethylsulphonyl fluoride) and centrifuged at 16,000 *g* for 15 min at 4 °C. Total extracts were resolved by SDS–PAGE and transferred to PVDF membranes (Millipore) and then probed by immunoblotting with anti-phospho-ERK1/2 (Thr202/Tyr204) and anti-ERK1/2 antibodies (Cell Signaling; 1:50 dilution). Expression of transfected EGFP-PEA-15 was assessed by immunoblotting with an anti-GFP antibody (GeneTex; 1:2,500 dilution). After primary antibody incubation, membranes were incubated with an horseradish-conjugated anti-rabbit antibody (Millipore; 1:5,000 dilution) and a chemiluminescence system (GE Healthcare Life Sciences) was used for detection.

To assess ERK dephosphorylation in the presence of PEA-15, HEK 293 cells transfected with either EGFP or PEA-15 WT were starved overnight. The cells were then stimulated with 20% FBS for 30 min to increase pERK levels, treated with 10 μM of the MEK inhibitor U0126 for different time periods, and lysed in modified RIPA buffer.

For immunocytochemistry, NIH3T3 cells were cultured in DMEM (Cellgro, Mediatech) supplemented with 10% FBS and penicillin/streptomycin, and were transiently transfected with EGFP or EGFP-PEA-15 plasmids using Lipofectamine 2000 (Invitrogen). Fifteen hours after transfection, the cells were trypsinyzed and plated on glass coverslips coated with fibronectin (10 μg ml^{-1}; Millipore). Twenty-four hours after transfection, the cells were starved in DMEM with 0.2% FBS for 18 h. The cells were then stimulated for 3 h with 20% FBS or maintained in 0.2% FBS and then fixed with 4% formaldehyde and permeabilized in 0.5% Triton X-100 in PBS. After a 30 min incubation with 10% normal goat serum in PBS at room temperature, the cells were incubated overnight at 4 °C with anti-ERK1/2 antibody (Cell Signaling; 1:50 dilution) in 10% normal goat serum in PBS. After PBS washes, the cells were incubated for 1 h at room temperature with the secondary anti-rabbit antibody conjugated with Alexa Fluor 568 (Invitrogen; 1:200 dilution). Nuclei were counterstained with 4′,6-diamidino-2-phenylindole (Sigma; 1:5,000) and the cells were mounted in ProLong Gold antifade reagent (Invitrogen).

References

1. Chang, L. & Karin, M. Mammalian MAP kinase signalling cascades. *Nature* **410,** 37–40 (2001).
2. Kolch, W. Coordinating ERK/MAPK signalling through scaffolds and inhibitors. *Nat .Rev. Mol. Cell. Biol.* **6,** 827–837 (2005).
3. Johnson, G. L. & Lapadat, R. Mitogen-activated protein kinase pathways mediated by ERK, JNK, and p38 protein kinases. *Science* **298,** 1911–1912 (2002).
4. Santarpia, L., Lippman, S. M. & El-Naggar, A. K. Targeting the MAPK-RAS-RAF signaling pathway in cancer therapy. *Exp. Opin. Ther. Targets* **16,** 103–119 (2012).
5. Nassar, N. *et al.* The 2.2 A crystal structure of the Ras-binding domain of the serine/threonine kinase c-Raf1 in complex with Rap1A and a GTP analogue. *Nature* **375,** 554–560 (1995).
6. Brennan, D. F. *et al.* A Raf-induced allosteric transition of KSR stimulates phosphorylation of MEK. *Nature* **472,** 366–369 (2011).
7. Carlson, S. M. *et al.* Large-scale discovery of ERK2 substrates identifies ERK-mediated transcriptional regulation by ETV3. *Sci. Signal* **4,** rs11 (2011).

8. Chen, R. H., Sarnecki, C. & Blenis, J. Nuclear localization and regulation of erk- and rsk-encoded protein kinases. *Mol. Cell. Biol.* **12,** 915–927 (1992).
9. Formstecher, E. *et al.* PEA-15 mediates cytoplasmic sequestration of ERK MAP kinase. *Dev. Cell* **1,** 239–250 (2001).
10. Whitehurst, A. W., Robinson, F. L., Moore, M. S. & Cobb, M. H. The death effector domain protein PEA-15 prevents nuclear entry of ERK2 by inhibiting required interactions. *J. Biol. Chem.* **279,** 12840–12847 (2004).
11. Hill, J. M., Vaidyanathan, H., Ramos, J. W., Ginsberg, M. H. & Werner, M. H. Recognition of ERK MAP kinase by PEA-15 reveals a common docking site within the death domain and death effector domain. *EMBO J.* **21,** 6494–6504 (2002).
12. Chou, F.-L. *et al.* PEA-15 binding to ERK1/2 MAPKs is required for its modulation of integrin activation. *J. Biol. Chem.* **278,** 52587–52597 (2003).
13. Gawecka, J. E. *et al.* PEA15 impairs cell migration and correlates with clinical features predicting good prognosis in neuroblastoma. *Int. J. Cancer* **131,** 1556–1568 (2012).
14. Watanabe, Y. *et al.* Expression of phosphoprotein enriched in astrocytes 15 kDa (PEA-15) in astrocytic tumors: a novel approach of correlating malignancy grade and prognosis. *J. Neurooncol.* **100,** 449–457 (2010).
15. Glading, A., Koziol, J. A., Krueger, J. & Ginsberg, M. H. PEA-15 inhibits tumor cell invasion by binding to extracellular signal-regulated kinase 1/2. *Cancer Res.* **67,** 1536–1544 (2007).
16. Gaumont-Leclerc, M.-F., Mukhopadhyay, U. K., Goumard, S. & Ferbeyre, G. PEA-15 is inhibited by adenovirus E1A and plays a role in ERK nuclear export and Ras-induced senescence. *J. Biol. Chem.* **279,** 46802–46809 (2004).
17. Callaway, K., Abramczyk, O., Martin, L. & Dalby, K. N. The anti-apoptotic protein PEA-15 is a tight binding inhibitor of ERK1 and ERK2, which blocks docking interactions at the D-recruitment site. *Biochemistry* **46,** 9187–9198 (2007).
18. Eckert, A. *et al.* The PEA-15/PED protein protects glioblastoma cells from glucose deprivation-induced apoptosis via the ERK/MAP kinase pathway. *Oncogene* **27,** 1155–1166 (2008).
19. Sulzmaier, F. J. *et al.* PEA-15 potentiates H-Ras-mediated epithelial cell transformation through phospholipase D. *Oncogene* **31,** 3547–3560 (2012).
20. Akella, R., Moon, T. M. & Goldsmith, E. J. Unique MAP Kinase binding sites. *Biochim. Biophys. Acta.* **1784,** 48–55 (2008).
21. Goldsmith, E. J. Three-dimensional docking in the MAPK p38α. *Sci. Signal.* **4,** pe47 (2011).
22. Ma, W. *et al.* Phosphorylation of DCC by ERK2 Is facilitated by direct docking of the receptor P1 domain to the kinase. *Structure* **18,** 1502–1511 (2010).
23. Zhou, T., Sun, L., Humphreys, J. & Goldsmith, E. J. Docking interactions induce exposure of activation loop in the MAP kinase ERK2. *Structure* **14,** 1011–1019 (2006).
24. Liu, S., Sun, J.-P., Zhou, B. & Zhang, Z.-Y. Structural basis of docking interactions between ERK2 and MAP kinase phosphatase 3. *Proc. Natl Acad. Sci. USA* **103,** 5326–5331 (2006).
25. Garai, A. *et al.* Specificity of linear motifs that bind to a common mitogen-activated protein kinase docking groove. *Sci. Signal.* **5,** ra74 (2012).
26. Lee, T. *et al.* Docking motif interactions in MAP kinases revealed by hydrogen exchange mass spectrometry. *Mol. Cell.* **14,** 43–55 (2004).
27. Bhattacharyya, R. P. *et al.* The Ste5 scaffold allosterically modulates signaling output of the yeast mating pathway. *Science* **311,** 822–826 (2006).
28. Sheridan, D. L., Kong, Y., Parker, S. A., Dalby, K. N. & Turk, B. E. Substrate discrimination among mitogen-activated protein kinases through distinct docking sequence motifs. *J. Biol. Chem.* **283,** 19511–19520 (2008).
29. Matsubayashi, Y., Fukuda, M. & Nishida, E. Evidence for existence of a nuclear pore complex-mediated, cytosol-independent pathway of nuclear translocation of ERK MAP kinase in permeabilized cells. *J. Biol. Chem.* **276,** 41755–41760 (2001).
30. Whitehurst, A. W. *et al.* ERK2 enters the nucleus by a carrier-independent mechanism. *Proc. Natl Acad. Sci. USA* **99,** 7496–7501 (2002).
31. Kosako, H. *et al.* Phosphoproteomics reveals new ERK MAP kinase targets and links ERK to nucleoporin-mediated nuclear transport. *Nat. Struct. Mol. Biol.* **16,** 1026–1035 (2009).
32. Muppidi, J. R. *et al.* Homotypic FADD interactions through a conserved RXDLL motif are required for death receptor-induced apoptosis. *Cell Death Differ.* **13,** 1641–1650 (2006).
33. Canagarajah, B. J., Khokhlatchev, A., Cobb, M. H. & Goldsmith, E. J. Activation mechanism of the MAP kinase ERK2 by dual phosphorylation. *Cell* **90,** 859–869 (1997).
34. Zhang, F., Strand, A., Robbins, D., Cobb, M. H. & Goldsmith, E. J. Atomic structure of the MAP kinase ERK2 at 2.3 A resolution. *Nature* **367,** 704–711 (1994).
35. Huse, M. & Kuriyan, J. The conformational plasticity of protein kinases. *Cell* **109,** 275–282 (2002).
36. Khokhlatchev, A. V. *et al.* Phosphorylation of the MAP kinase ERK2 promotes its homodimerization and nuclear translocation. *Cell* **93,** 605–615 (1998).
37. Casar, B., Pinto, A. & Crespo, P. Essential role of ERK dimers in the activation of cytoplasmic but not nuclear substrates by ERK-scaffold complexes. *Mol. Cell.* **31,** 708–721 (2008).
38. Casar, B., Pinto, A. & Crespo, P. ERK dimers and scaffold proteins: unexpected partners for a forgotten (cytoplasmic) task. *Cell Cycle* **8,** 1007–1013 (2009).
39. Madhusudan, Akamine, P., Xuong, N.-H. & Taylor, S. S. Crystal structure of a transition state mimic of the catalytic subunit of cAMP-dependent protein kinase. *Nat. Struct. Biol.* **9,** 273–277 (2002).
40. Lee, S. *et al.* Examining docking interactions on ERK2 with modular peptide substrates. *Biochemistry* **50,** 9500–9510 (2011).
41. Bartholomeusz, C. *et al.* PEA-15 inhibits tumorigenesis in an MDA-MB-468 triple-negative breast cancer xenograft model through increased cytoplasmic localization of activated extracellular signal-regulated kinase. *Clin. Cancer Res.* **16,** 1802–1811 (2010).
42. Sulzmaier, F., Opoku-Ansah, J. & Ramos, J. Phosphorylation is the switch that turns PEA-15 from tumor suppressor to tumor promoter. *Small GTPases* **3,** 173–177 (2012).
43. Kriegsheim, von, A. *et al.* Cell fate decisions are specified by the dynamic ERK interactome. *Nat. Cell Biol.* **11,** 1458–1464 (2009).
44. Houben, R. *et al.* Phospho-ERK staining is a poor indicator of the mutational status of BRAF and NRAS in human melanoma. *J. Invest. Dermatol.* **128,** 2003–2012 (2008).
45. Seeliger, M. A. *et al.* High yield bacterial expression of active c-Abl and c-Src tyrosine kinases. *Protein Sci.* **14,** 3135–3139 (2005).
46. Kabsch, W. XDS. *Acta. Crystallogr. D Biol. Crystallogr.* **66,** 125–132 (2010).
47. Collaborative Computational Project, Number 4, The CCP4 suite: programs for protein crystallography. *Acta. Crystallogr. D Biol. Crystallogr.* **50,** 760–763 (1994).
48. Storoni, L., McCoy, A. & Read, R. Likelihood-enhanced fast rotation functions. *Acta. Crystallogr. D Biol. Crystallogr.* **60,** 432–438 (2004).
49. Murshudov, G. N. *et al.* REFMAC5 for the refinement of macromolecular crystal structures. *Acta. Crystallogr. D Biol. Crystallogr.* **67,** 355–367 (2011).
50. Emsley, P. & Cowtan, K. Coot: model-building tools for molecular graphics. *Acta. Crystallogr. D Biol. Crystallogr.* **60,** 2126–2132 (2004).
51. Khokhlatchev, A. *et al.* Reconstitution of mitogen-activated protein kinase phosphorylation cascades in bacteria. Efficient synthesis of active protein kinases. *J. Biol. Chem.* **272,** 11057–11062 (1997).

Acknowledgements

We thank Dr Andrey Bobkov for analytical ultracentrifugation and ITC and Dr Guy Salvesen for critical discussion of the manuscript. We also thank the Hope for a Cure Foundation (www.hopeforacurefoundation.org) for donation of equipment and Dr John Badger (DeltaG technologies, http://deltagtech.com) for assistance in model building and evaluation. This work was supported by NIH grants R01AA017238 to SJR, 1R01CA160457 to SJR and EBP, and DOD-BCRP Fellowship BC100466 to P.D.M. P.D.M. is the recipient of the Eric Dudl Memorial Scholarship. Data collection at beamline X29 of the National Synchrotron Light Source was also supported by Biological and Environmental Research Department of Energy and the NIH National Center for Research Resources.

Author contributions

P.D.M. grew crystals, solved the crystal structures, designed and carried out *in vitro* experiments and wrote the manuscript. Y.W. designed, carried out and analysed *in vivo* experiments, M.F.E grew crystals and M.K.D purified proteins. H.R. carried out crystallographic data collection. S.J.R. and E.B.P. designed experiments, analysed data and wrote the manuscript.

Additional information

Accession codes: Atomic coordinates and structure factors have been deposited in the Protein Data Bank under accession codes 4IZ5 ((ERK2 T185E)–PEA-15), 4IZ7 (Non-phosphorylated ERK2–PEA-15(1–96)) and 4IZA (Dually phosphorylated ERK2–PEA-15(1–96)).

Supplementary Information accompanies this paper at http://www.nature.com/naturecommunications

Competing financial interests: The authors declare no competing financial interests.

Reprints and permission information is available online at http://npg.nature.com/reprintsandpermissions/

How to cite this article: Mace, P.D. *et al.* Structure of ERK2 bound to PEA-15 reveals a mechanism for rapid release of activated MAPK. *Nat. Commun.* 4:1681 doi: 10.1038/ncomms2687 (2013).

Genes & Cancer
3(5-6) 382–393

DOI: 10.1177/1947601912460050
http://ganc.sagepub.com
SAGE

NSP-CAS Protein Complexes: Emerging Signaling Modules in Cancer

Yann Wallez[1], Peter D. Mace[1], Elena B. Pasquale[1,2], and Stefan J. Riedl[1]

Abstract

The CAS (CRK-associated substrate) family of adaptor proteins comprises 4 members, which share a conserved modular domain structure that enables multiple protein-protein interactions, leading to the assembly of intracellular signaling platforms. Besides their physiological role in signal transduction downstream of a variety of cell surface receptors, CAS proteins are also critical for oncogenic transformation and cancer cell malignancy through associations with a variety of regulatory proteins and downstream effectors. Among the regulatory partners, the 3 recently identified adaptor proteins constituting the NSP (novel SH2-containing protein) family avidly bind to the conserved carboxy-terminal focal adhesion–targeting (FAT) domain of CAS proteins. NSP proteins use an anomalous nucleotide exchange factor domain that lacks catalytic activity to form NSP-CAS signaling modules. Additionally, the NSP SH2 domain can link NSP-CAS signaling assemblies to tyrosine-phosphorylated cell surface receptors. NSP proteins can potentiate CAS function by affecting key CAS attributes such as expression levels, phosphorylation state, and subcellular localization, leading to effects on cell adhesion, migration, and invasion as well as cell growth. The consequences of these activities are well exemplified by the role that members of both families play in promoting breast cancer cell invasiveness and resistance to antiestrogens. In this review, we discuss the intriguing interplay between the NSP and CAS families, with a particular focus on cancer signaling networks.

Keywords: migration, invasion, antiestrogen resistance, tyrosine phosphorylation, serine phosphorylation, SRC kinase

Introduction

Transmembrane receptors localized on the cell surface, such as integrin receptors for extracellular matrix proteins, growth factor receptor tyrosine kinases, and cytokine receptors, convey extracellular stimuli into a cascade of intracellular signaling events that lead to cell proliferation and survival, cytoskeletal reorganization, and cell migration. Signaling pathways emanating from cell surface receptors rely on networks of adaptor proteins (which contain multiple protein interaction domains) and scaffold proteins (which bring together multiple components of a signaling pathway).[1,2] Although adaptor and scaffold proteins lack enzymatic activity, they represent both crucial links to downstream effector molecules and nodes that interconnect different signaling pathways. By regulating the flow of information in signaling networks, adaptor and scaffold proteins are critical for normal cellular physiology and homeostasis. Consequently, their dysregulation can lead to a spectrum of diseases and particularly cancer development and progression. The members of the CAS (CRK-associated substrate) and NSP (novel SH2-containing protein) families (Table 1) are multidomain proteins that combine both adaptor and scaffold functions to form unique signaling modules in complex signaling networks (Figs. 1 and 2). They achieve this by interacting with each other through their conserved carboxy-terminal domains. In this review, we provide an overview of both families and their shared involvement in cell signaling and cancer malignancy.

The CAS Family

Domain organization and general signaling mechanisms. The CAS protein family consists of 4 members, BCAR1, NEDD9, EFS, and CASS4 (see Table 1 for alternative names), which share a conserved multidomain organization (Fig. 1). The amino-terminal SH3 domain of CAS proteins binds polyproline motifs of interacting partners, the most studied of which is the focal adhesion kinase FAK[3] (Fig. 2). This is followed by the substrate domain (Fig. 1), which can be "stretched" to expose its many YxxP motifs for phosphorylation, thus functioning as a sensor of cell mechanical stress.[4,5] Once phosphorylated by kinases such as SRC, these motifs provide binding sites for the SH2 domains of adaptor proteins, with CRK and CRKL being the most important.[6-8] The subsequent serine-rich region can recruit regulatory 14-3-3 proteins through serine-phosphorylated motifs.[9] Structurally, this region folds into a 4–helix bundle domain that is reminiscent of the focal adhesion–targeting (FAT) domains found in focal adhesion proteins.[10] This is followed by the SRC-binding region, which includes a polyproline motif that can bind

[1]Sanford-Burnham Medical Research Institute, La Jolla, CA, USA
[2]University of California, San Diego, La Jolla, CA, USA

Corresponding Authors:
Elena Pasquale, Sanford-Burnham Medical Research Institute, 10901 N. Torrey Pines Rd., La Jolla CA 92037. (E-mail: elenap@sanfordburnham.org).
Stefan J. Riedl, Sanford-Burnham Medical Research Institute, 10901 North Torrey Pines Road, La Jolla, CA 92037 (Email: sriedl@sanfordburnham.org).

Table 1. CAS and NSP Family Members

Official gene name	Other names
CAS family	
BCAR1, breast cancer antiestrogen resistance protein 1	**p130CAS**/**CAS**, CRK-associated substrate **HEF1**, human enhancer of filamentation 1
NEDD9, neural precursor cell expressed developmentally downregulated protein 9	**CAS-L**/**CASL**, CAS-related protein lymphocyte type
EFS, embryonal FYN-associated substrate	**SIN**, SRC-interacting or signal-integrating protein
CASS4, CAS scaffolding protein family member 4	**HEPL**, HEF1-EFS-p130CAS–like protein
NSP family	
SH2D3A, SH2 domain–containing 3A	**NSP1**, novel SH2-containing protein 1
BCAR3, breast cancer antiestrogen resistance protein 3	**NSP2**, novel SH2-containing protein 2 **AND-34**, identified from AND TCR transgenic mice clone 34.1
SH2D3C, SH2 domain–containing 3C	**NSP3**, novel SH2-containing protein 3 **SHEP1**, SH2 domain–containing EPH receptor–binding protein 1 **CHAT**, CAS/HEF1-associated signal transducer **CHAT-H**, hematopoietic cell–specific CHAT

Note: Included are the most common names according to UniProtKB/Swiss-Prot (uniprot.org).

the SRC SH3 domain and/or a tyrosine-containing motif that, when phosphorylated by FAK, can bind the SRC SH2 domain.[11,12] Notably, features of the SRC-binding region vary among the family members, with CASS4 lacking both SRC-binding motifs. A stretch of approximately 70 amino acids with an unknown structure and function precedes the carboxy-terminal domain, which was only recently revealed to adopt a FAT-type 4–helix bundle fold.[13] This domain is responsible for the interaction with NSP proteins as well as several ubiquitin ligases.[14,15] Furthermore, in at least some family members, the CAS carboxy-terminal domain can be released by caspases and function independently to promote apoptosis.[11,12,16]

The detailed signaling mechanisms of CAS proteins have been extensively discussed in several excellent recent reviews.[8,11,12,16,17] Therefore, here, we highlight only the main general features of their signaling pathways (Fig. 2). Cell adhesion mediated by integrin receptors is the best characterized event linked to CAS signaling since it leads to the activation of FAK.[11,12] FAK can directly recruit SRC family kinases and at the same time phosphorylate the SRC-binding region in CAS proteins, thus generating the binding site for the SRC SH2 domain.[11,12] Binding of the SRC SH2/SH3 domains to the FAK-CAS complex relieves their intramolecular inhibition on the kinase domain, leading to SRC activation.[18-21] In addition, it positions the activated SRC for phosphorylation of the multiple tyrosines in the CAS substrate domain.[22,23] This hyperphosphorylation is a hallmark of the active signaling form of CAS proteins and generates binding sites for CRK adaptors, which then recruit the nucleotide exchange factors DOCK180 and C3G.[24-27] DOCK180 is a key activator of the RHO family GTPase RAC1, which in turn controls activation of the JNK MAP kinase and actin cytoskeleton remodeling, while C3G activates the RAS family GTPase RAP1, leading to increased integrin activity.[25,28-33] Together, these 2 pathways promote cell substrate adhesion, migration, and invasiveness as well as proliferation.[6,8,27,28,31,34-37] Moreover, RAC1 activation by CAS proteins can also occur through PI3 kinase–dependent activation of guanine nucleotide exchange factors, while the PI3 kinase–AKT axis additionally supports cell survival downstream of CAS[27,37-39] (Fig. 2).

In addition to FAK, SRC, and the CRK-DOCK180-RAC1, CRK-C3G-RAP1, and PI3 kinase axes, many other signaling molecules have been described as CAS regulators and effectors, accounting for the diverse biological functions of the family.[11,12] Among these are the NSP family proteins, which are featured in this review. Although less investigated, the 3 proteins forming the NSP family seem to be among the most avid CAS-binding partners. They are also capable of interacting with receptor tyrosine kinases, thus directly linking CAS proteins to receptor tyrosine kinase–initiated signaling. Before delving into the details of NSP-CAS signaling, we provide an overview of each of the 4 CAS proteins and the distinctive properties that account for their different roles in various malignancies.

BCAR1 (p130CAS). BCAR1 is the founding member of the CAS family and is ubiquitously expressed in adult human tissues and cancer cell lines[11,17] (broadinstitute.org/ccle). It was originally discovered in v-CRK– and v-SRC–transformed cells as p130CAS (Table 1), an abundant and highly phosphorylated 130-kDa protein that interacts with the transforming oncogenes.[40-42] Later studies revealed that BCAR1 plays an essential role in cell transformation by SRC and several other oncogenes.[37,43-48] The human gene was identified in a genome-wide screen for proteins whose overexpression in estrogen-dependent breast cancer cells confers resistance to antiestrogens (hence, the name breast cancer antiestrogen resistance protein 1, abbreviated to BCAR1) (Table 1).[49-51] BCAR1 has also been implicated in resistance to the chemotherapeutic drug doxorubicin.[52] Furthermore, high levels of the BCAR1 protein in breast cancer specimens have been correlated with high ERBB2 receptor expression, enhanced proliferation, increased risk for resistance to tamoxifen therapy, and poor clinical outcome.[37,53,54] The ability of BCAR1 to support

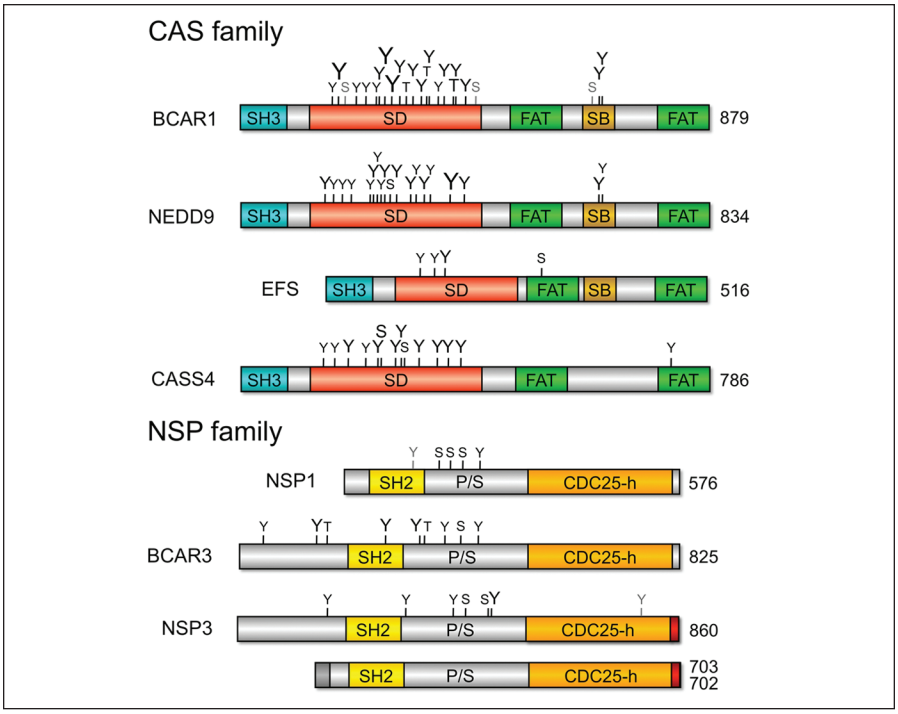

Figure 1. Domain structure and phosphorylation sites of CAS and NSP family proteins. Shown are the main isoforms for the various family members and their amino acid lengths. Isoforms of different lengths are shown only for NSP3; the 2 NSP3 shorter isoforms of 702 and 703 amino acids differ from each other in their most amino-terminal segment (indicated in dark gray). CDC25-h = CDC25 homology domain; FAT = focal adhesion–targeting domain (the central serine-rich region of the CAS proteins has the structure of a FAT domain, although it is not commonly designated as such); P/S = proline/serine-rich region; SB = SRC-binding region (containing binding sites for both SRC SH2 and SH3 domains in BCAR1 and EFS and only for the SRC SH2 domain in NEDD9); SH2 = SH2 domain; SH3 = SH3 domain. Phosphorylation sites (Y = tyrosine; S = serine; T = threonine) were obtained from phosphosite.org; the smallest font indicates sites identified by mass spectrometry in >5 samples, the intermediate-sized font indicates sites identified in >50 samples, and the largest font indicates sites identified in >500 samples. It should be noted that identification of phosphorylation sites by mass spectrometry is not necessarily comprehensive. Indicated in gray are the 3 serine phosphorylation sites in the substrate domain of BCAR1 that depend on BCAR3 expression in MDA-MB-231 breast cancer cells[94] (the first of which was also detected in >5 other samples), the tyrosine phosphorylated downstream of the EGF receptor in the SH2 domain of NSP1,[81] and the tyrosine phosphorylated downstream of the overexpressed EPHB2 receptor in the CDC25 homology domain of NSP3.[90]

long-term proliferation in the presence of antiestrogens, which appears to be unique among the CAS family proteins, has been linked to tyrosine phosphorylation of its substrate domain.[55,56] BCAR1 signaling has also been associated with cell proliferation, survival, and migration/invasion in many tumor types besides breast cancer, including ovarian and prostate cancer, glioblastoma, melanoma, and hematopoietic malignancies.[11,12,17,27,57-63] Accordingly, a great abundance of BCAR1 tyrosine- and serine/threonine-phosphorylated peptides have been detected in a wide variety of cancers (phosphosite.org) (Fig. 1).

NEDD9. This member of the CAS family is widely expressed in tissues, and interestingly, its levels are low in the G1 phase of the cell cycle but increase dramatically during mitosis.[12,16] NEDD9 is also expressed in most cancer cell lines, with highest levels detected in melanoma and medulloblastoma cell lines[12,64] (broadinstitute.org/ccle). Furthermore, many tyrosine-phosphorylated peptides from the NEDD9 substrate domain have been detected by mass spectrometry in a large number and a wide variety of cancer cell lines and tumor samples (phosphosite.org) (Fig. 1), consistent with the reported importance of NEDD9 signaling in most cancers including hematopoietic tumors.[12,16,17,65] Interestingly, a distinctive role of NEDD9 in driving invasiveness and metastasis has been extensively documented in melanoma, breast cancer, and other cancers.[16,17,64,66-73] In addition, analysis of NEDD9 knockout mice has implicated this CAS family member in tumor initiation in the MMTV–Polyoma middle T mouse mammary tumor model through activation of FAK, SRC, AKT, and ERK.[74] However, besides reducing tumor development, over time, the lack of NEDD9 expression can also promote cancer cell aggressiveness by causing genetic instability.[75] Consistent with a complex role in tumorigenesis, NEDD9 overexpression may also negatively affect cancer development by causing defects in cytokinesis through its multiple effects on the mitotic machinery as well as by promoting apoptosis through caspase-dependent release of its carboxy-terminal domain.[12,16]

EFS and CASS4. EFS and CASS4 are the least characterized members of the CAS family, and their roles in cancer have not yet been extensively explored. EFS mRNA is expressed in the adult brain, lung, and thymus as well as in sarcoma cell lines and a subset of cell lines from other cancers, including lung cancer[76,77] (broadinstitute.org/ccle). Only a few tyrosine-phosphorylated peptides from the EFS substrate domain have been identified in a variety of tumors and cancer cell lines, including breast cancers and pheochromocytomas (phosphosite.org) (Fig. 1). Therefore, the available evidence suggests that EFS has a more limited role in cancer than the other members of the CAS family.

The most recently identified family member, CASS4, has a restricted tissue distribution and is predominantly found in the lung and spleen.[76] In cancer cell

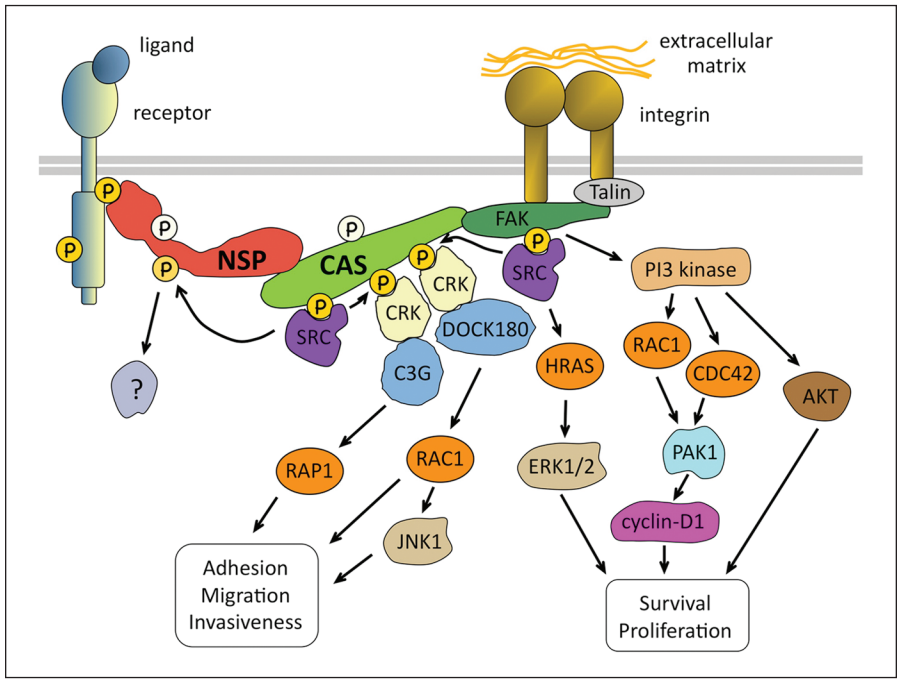

Figure 2. NSP-CAS signaling networks. The schematic diagram illustrates pathways discussed in the text, depicting how NSP proteins integrate CAS signaling downstream of integrins with signaling pathways downstream of other cell surface receptors. Signaling pathways downstream of cell surface receptors as well as many other known regulators and effectors of CAS family proteins are not shown. Overexpression of several NSP and CAS proteins has been implicated in cancer malignancy and resistance to chemotherapy, which may be due at least in part to perturbation of the signaling interactions shown in the figure.

lines, CASS4 mRNA expression is highest in leukemia cell lines (broadinstitute.org/ccle). Despite lacking the SRC-binding region, CASS4 is phosphorylated on tyrosines in the substrate domain, likely through FAK-associated SRC.[23,76] Multiple tyrosine-phosphorylated peptides derived from the substrate domain of CASS4 have been detected by mass spectrometry in cancers, with the great majority from chronic myelogenous leukemias and a smaller number from lung cancer samples (phosphosite.org) (Fig. 1). Even though CASS4 seems to have similar activities as the other CAS proteins, its carboxy-terminal domain has the most divergent sequence of the 4 family members, and it is not yet known whether it can support a tight interaction with NSP family members.[13]

The NSP Family

Domain organization and general signaling mechanisms. The NSP family consists of 3 members, NSP1, BCAR3, and NSP3 (see Table 1 for alternative names), which share a similar domain organization (Fig. 1). The amino-terminal segment of NSP proteins is of variable length and subject to alternative splicing in BCAR3 and NSP3.[78] Only the longer version of this segment in NSP3 has been shown to promote association with the plasma membrane,[79] suggesting that the amino-terminal segment confers distinctive signaling properties to the different isoforms. This region is followed by a SH2 domain that can bind to activated receptor tyrosine kinases, including members of the ERBB and EPH families,[80-83] thus recruiting the associated CAS proteins and their signaling partners to the activated receptors (Fig. 2). The proline/serine-rich region that follows the SH2 domain contains putative binding sites for SH3 domain–containing proteins. This region is poorly conserved and may therefore recruit different binding partners to each NSP family member. Although no definite binding partners have yet been characterized, predictions suggest binding of various SH3 domain–containing proteins, including the CDC42 exchange factor intersectin to NSP1 and the ABL nonreceptor tyrosine kinase to NSP3 (scansite.mit.edu). Additionally, cortactin, a SRC substrate and actin cytoskeleton regulator involved in cell invasion,[84] is predicted to interact with all 3 NSP proteins (scansite.mit.org).

Perhaps the most intriguing region of the NSP proteins is their large carboxy-terminal domain, which is crucial for interaction with members of the CAS family.[81,85,86] This domain has sequence similarity with the CDC25 homology domain of guanine nucleotide exchange factors, which promote the exchange of the GDP nucleotide bound to inactive RAS GTPases with GTP, leading to RAS activation.[80,81,85] Hence, nucleotide exchange functions have been proposed for the NSP family.[87] However, enzymatic activity could not be confirmed using purified NSP CDC25 homology domains,[29,80] which is in line with recent structural studies revealing an architecture incompatible with enzymatic activity but exquisitely suited for CAS binding[13] (see below).

In essence, NSP proteins act as sophisticated adaptor molecules that use their SH2 and CDC25 homology domains to connect receptor tyrosine kinases and other cell surface receptors with CAS family members and integrin signaling cascades (Fig. 2). Yet, based on the number and diversity of potential signaling motifs present in the family members, it is likely that other binding partners, mechanisms, and pathways involving the 3 NSP proteins remain to be discovered. For example, little is known about the role of NSP phosphorylation, which represents an additional putative regulatory aspect for the NSP family. Multiple phosphorylation sites have been identified, mostly in the amino-terminal half of all 3 NSP proteins, in normal and cancer cells[80,81,86,88-91] (phosposite.org) (Fig. 1). The tyrosine-phosphorylated motifs likely result from the activity of SRC, ABL, and receptor tyrosine kinases, and presumably some

of them serve as binding sites for proteins containing SH2 or PTB domains. For example, sequence-based predictions suggest that the ABL kinase SH2 domain may bind to NSP3 (scansite.mit.edu). Furthermore, the NSP amino-terminal segments and proline/serine-rich regions contain multiple serine/threonine-proline (S/TP) motifs that are likely phosphorylated by proline-directed kinases such as ERK[86,92] (scansite.mit.edu). Additionally, AMP kinase is predicted to phosphorylate several serines in NSP1 (scansite.mit.edu). A number of serine/threonine-phosphorylated motifs in all 3 NSP proteins are also predicted to bind 14-3-3 proteins.

Consistent with promoting CAS signaling and cancer malignancy, many studies have shown that NSP proteins can enhance SRC activity and CAS tyrosine and serine phosphorylation in a variety of cell culture and *in vivo* systems.[21,79,89,93-99] The amino-terminal half of the NSP proteins, including the SH2 and proline/serine-rich domains, seems to be required to enhance CAS phosphorylation.[21,94,96,98,99] CAS-dependent signaling involving CRK and PI3 kinase likely accounts for the ability of all 3 NSP proteins to activate RAC1 and the other RHO family GTPase, CDC42, as well as AKT[93,100-103] (Fig. 2). Furthermore, overexpression of NSP1 and NSP3 has been shown to activate the RAC1 downstream effector JNK1.[81,86,104]

All 3 NSP family members can also increase CAS protein levels, which likely further potentiates CAS signaling.[96,103] Although the underlying mechanism for NSP-dependent CAS stabilization is not known, an interesting possibility is that NSP binding might prevent the association with ubiquitin ligases that also interact with the CAS carboxy-terminal FAT domain,[14,15] thereby reducing CAS proteolytic degradation. Overall, we are only beginning to understand the signaling pathways and functions of NSP proteins and their CAS complexes in cancer development and progression. Current information on each family member is outlined in the next sections.

NSP1 (SH2D3A). NSP1 was first identified from a database of human-expressed sequence tags as a new SH2 domain–containing protein.[81] NSP1 is the shortest member of the family due to its shorter amino-terminal and proline/serine-rich regions (Fig. 1) and appears to be a pseudogene in the mouse.[78] Of the 3 family members, NSP1 has the most restricted expression, and in adult tissues, its transcripts are mainly found in the lung, pancreas, kidney, and liver.[78,81] However, NSP1 is present at substantial levels in a variety of cancer cell lines, including pancreatic and lung cancer cells (broadinstitute.org/ccle), where it likely functions downstream of integrins and activated receptor tyrosine kinases including members of the EGF and insulin receptor families.[81,82] For example, upon EGF stimulation of COS cells, NSP1 binds to the EGF receptor and becomes phosphorylated on 2 of its 3 tyrosines.[81] Both tyrosine and serine/threonine phosphorylation sites have also been detected for NSP1 by mass spectrometry in human tumors and cancer cell lines, most frequently in lung cancers (phosphosite.org) (Fig. 1). This suggests a role for NSP1 in lung cancer, although the functional consequences of NSP1 phosphorylation are not yet known. Interestingly, upregulation of NSP1 expression has been reported as part of the gene expression signature of "KRAS-addicted" lung and pancreatic cancers, suggesting that NSP1 could contribute to KRAS transformation and serve as a biomarker for KRAS-dependent tumors.[105] Furthermore, NSP1 overexpression in MCF7 breast cancer cells moderately increases BCAR1 tyrosine phosphorylation and the appearance of a serine-phosphorylated form of BCAR1 with reduced electrophoretic mobility.[94] Although NSP1 overexpression in breast cancer cells also activates RAC1, CDC42, and AKT, these signaling activities do not seem sufficient to confer resistance to antiestrogens.[103]

BCAR3. The BCAR3 gene encodes at least 2 protein isoforms that differ in the amino-terminal segment preceding the SH2 domain,[78] but only the longer isoform of 825 amino acids has been studied so far. BCAR3 mRNA is widely expressed in most human tissues[78,106] and in cell lines from most types of cancers, with lowest levels in leukemias and lymphomas (broadinstitute.org/ccle) despite the expression of BCAR3 in normal B cells.[100] In cell lines from breast, ovarian, and endometrial cancers, BCAR3 mRNA expression seems to be inversely correlated with estrogen receptor expression.[103,106] In addition, BCAR3 tyrosine-phosphorylated peptides have been detected by mass spectrometry in many cancers, with a preponderance in lung cancer (phosphosite.org). The widespread expression and phosphorylation of BCAR3 in cancer cells suggest a role in many cancer types. Although the involvement of BCAR3 in lung cancer has not yet been investigated, a number of studies have characterized its role in breast cancer.

BCAR3 exerts a profound influence on various aspects of breast cancer malignancy. It was first identified in the same screen for proteins conferring antiestrogen resistance that also identified the CAS protein BCAR1.[106] Later studies revealed that BCAR3-BCAR1 complexes are more evident in more aggressive and estrogen receptor–negative breast cancer cell lines, where BCAR1 signaling is known to promote survival, migration, and invasiveness.[39,94,99,103,107] Multiple pathways involved in cell proliferation and survival could contribute to BCAR3-induced estrogen independence in breast cancer cells.[108] The ability of BCAR3 to promote proliferation of estrogen-dependent breast cancer cells in the presence of antiestrogens requires both the SH2 and CDC25 homology domains, suggesting that this depends on its ability to link cell surface receptors with CAS signaling networks[102] (Fig. 2). A critical event for the antiestrogen resistance phenotype is RAC1 activation,

which occurs downstream of FAK–CAS–PI3 kinase as well as CAS-CRK-DOCK180 pathways, leading to increased cyclin D1 levels through the downstream kinase PAK1.[101,102] AKT activation downstream of PI3 kinase may also contribute to BCAR3-dependent antiestrogen resistance.[102,109]

Another key role of BCAR3 likely contributing to estrogen-independent growth involves increasing the activity of SRC recruited to BCAR1, thus leading to not only phosphorylation of the BCAR1 substrate domain and subsequent CRK-RAC1 signaling[21,37,89,99,101,102] but likely also other SRC-dependent activities.[108,110-112] Interestingly, endogenous BCAR3 has also been found to mediate some of the proliferative effects of the EGF receptor in the nontransformed MCF12A human breast cell line, suggesting that a similar cross-talk with the EGF receptor might also play a role in breast cancer cell proliferation and antiestrogen resistance.[83,107,110] Remarkably, although all 3 NSP family members can promote RAC1, CDC42, and AKT activation when overexpressed in breast cancer cells, only BCAR3 can increase cyclin D1 levels and promote robust antiestrogen resistance. BCAR3 is also the most effective of the NSP proteins in inducing BCAR1 and NEDD9 tyrosine and serine phosphorylation.[94,98,99,107] Hence, BCAR3 appears to have stronger signaling abilities and/or additional distinctive signaling functions that promote breast cancer cell malignancy.[99,103]

Estrogen independence is typically accompanied by a pronounced mesenchymal and invasive breast cancer cell phenotype.[111,113,114] Interestingly, besides enabling growth in the presence of antiestrogens, BCAR3 promotes mesenchymal attributes as well as cell spreading, migration, and invasiveness. These are also critical aspects of cancer malignancy that encompass the core features of NSP-CAS-CRK signaling (Fig. 2). For example, BCAR3 overexpression in the less aggressive, more epithelial-like MCF7 and T47D breast cancer cells decreases E-cadherin localization at cell-cell junctions with concomitant disruption of junctional integrity and increased fibronectin production.[98,103,107] BCAR3 also promotes the formation of membrane ruffles and cell protrusion, which are hallmarks of increased RAC1 signaling and a migratory phenotype.[98,103,107] Indeed, BCAR3 can cause BCAR1 relocalization from focal contacts to membrane ruffles and cell protrusions (where BCAR3 is also enriched), thus positioning BCAR1 for the promotion of cell migration and invasiveness.[89,99,107] Conversely, siRNA-mediated downregulation of BCAR3 in the more aggressive MDA-MB-231 and BT549 breast cancer cells leads to a less malignant phenotype, including a decrease in SRC activation, BCAR1 tyrosine/serine phosphorylation, and BCAR1 association with CRK accompanied by a transition from a mesenchymal to a more epithelial-like morphology as well as defects in cell spreading, migration, and invasiveness.[21,94,107]

NSP3 (SH2D3C). NSP3 was independently identified as an NSP1 family member,[81] as a protein that interacts with the EPHB2 receptor tyrosine kinase,[80] and as an antigen that localizes at cell-cell junctions.[86] Its 2 shorter isoforms of 702 to 703 amino acids are widely expressed,[78,81,86] whereas its longer isoform of 860 amino acids is prevalent in hematopoietic cells (Fig. 1). NSP3 is the only family member with a carboxy-terminal PDZ domain–binding motif, which mediates association with the adaptor protein CARD11/CARMA.[115] CARD11 is a positive regulator of antigen receptor signaling in B and T cells and forms a signalosome with the NFκB activators BCL10 and MALT1, whose deregulation has been linked to lymphoma development.[116]

NSP3 mRNA is most highly expressed in the brain, lung, blood vessels, and immune cells.[78,81,86] Its transcripts are also preferentially expressed in lymphoma and leukemia cell lines, and thus, NSP3 seems to have complementary expression with BCAR3 in cancer cell lines (broadinstitute.org/ccle). Increased NSP3 protein expression has also been reported in gastric cancers,[117] and NSP3-phosphorylated peptides have been detected by mass spectrometry in leukemias, lymphomas, and lung cancers (phosphosite.org), suggesting an involvement in these malignancies. Indeed, NSP3 has been shown to be tyrosine phosphorylated downstream of the BCR-ABL oncogene and may function in concert with NEDD9 in BCR-ABL–transformed cells.[16,88]

Although the role of NSP3 in chronic myelogenous leukemia and other hematological cancers has not yet been investigated, its activities in B and T cells suggest potential functions in tumorigenesis. The long NSP3 isoform has been implicated in B-cell development and function.[95,118] In fact, NSP3 knockout mice almost completely lack a population of B cells in the spleen known as marginal-zone B cells. Furthermore, the knockout B cells have defects in NEDD9 serine phosphorylation and B-cell migration in response to cytokines, although no major defects have been observed in NSP3 knockout T cells. Nevertheless, several observations point to a potential role of NSP3 in T-cell malignancies. One is the impairment of T-cell migration in culture and homing to peripheral tissues *in vivo* upon siRNA-mediated downregulation of NSP3.[77,79] Interestingly, NSP3 membrane localization driven by the unique amino-terminal segment of the long isoform induces the NEDD9 serine phosphorylation, RAP1 activation, and integrin-mediated adhesion underlying T-cell migration. An additional, albeit controversial, factor is the increased production of interleukin-2 (a hallmark of T-cell activation) upon overexpression of the long NSP3 isoform in the Jurkat T-cell leukemia cell line.[77,104,115] This effect of NSP3 on interleukin-2 was connected to JNK1 activation through NEDD9 and the FAK-related PYK2 kinase as well as association with the PDZ domain of CARD11.

Similar to the long isoform, a direct involvement of the shorter NSP3

isoforms in cancer malignancy has yet to be proven. However, NSP3 activities downstream of cell surface receptors may play a role in tumor angiogenesis as well as cell migration and invasiveness, which are key factors in cancer development and progression. A potential role in tumor angiogenesis is suggested by the expression and phosphorylation of NSP3 in cultured endothelial cells and in the vasculature of mouse mammary tumors and MDA-MB-231 breast cancer xenografts grown in nude mice[78] (phosphosite.org). However, NSP3 knockout mice do not exhibit obvious vascular defects, raising the possibility of a redundancy with BCAR3 or of residual activities of a truncated NSP3 form present in at least 1 of the 2 reported NSP3 knockout mouse lines.[78,96,97] NSP3 also interacts with the EPHA4 and EPHB2 receptor tyrosine kinases through its SH2 domain and can be phosphorylated on tyrosine residues downstream of EPHB2 and the EGF receptor.[80,90] Additionally, EGF and NGF stimulation in PC12 pheochromocytoma cells and T-cell receptor stimulation in primary mouse T cells cause an upward electrophoretic mobility shift in NSP3, whose appearance is prevented by the ERK pathway inhibitor PD98059, consistent with the presence of multiple potential ERK consensus phosphorylation sites.[86,92]

Furthermore, NSP3 localizes to membrane ruffles of COS cells stimulated with EGF and promotes cell migration towards EGF.[13,86,90] This ability is dependent on the interaction with BCAR1, further exemplifying the importance of NSP-CAS modules in cell migration. NSP3 can also increase RAP1 activity, integrin-mediated cell adhesion and spreading, and membrane ruffling in NIH3T3 cells through CAS-CRK-C3G.[92] Interestingly, more prominent effects were observed using engineered myristoylated forms of the protein, emphasizing the importance of membrane targeting, which also leads to SRC-dependent NSP3 phosphorylation.[90,92] Finally, NSP3 knockout mice show defects in the olfactory axons, which *in vivo* are unable to grow through the basal lamina surrounding the brain (as needed to form synapses in the olfactory bulb) and in explant culture have an impaired ability to penetrate the extracellular matrix.[97] These findings highlight a proinvasive role of NSP3 *in vivo*, suggesting a similar role in cancer cell invasiveness.

Structural Features of NSP-CAS Complexes

A recent study has provided surprising insight into the structure and function of the NSP carboxy-terminal domain. As mentioned above, in all NSP family members, this domain has a sequence similarity with the CDC25 homology fold found in nucleotide exchange factors for RAS family GTPases.[13] The crystal structure of the BCAR3 carboxy-terminal domain has indeed confirmed that a large portion of this domain closely resembles a prototypical CDC25 homology domain[13] (Fig. 3A). However, a segment termed the "helical hairpin," which in enzymatically active exchange factors inserts into the RAS GTPase nucleotide-binding cleft to elicit GDP displacement,[119] is grossly distorted in BCAR3 (Fig. 3A). This region folds towards the body of the BCAR3 domain, thus blocking the canonical RAS GTPase-binding site. This results in a novel "closed" form of the CDC25 homology domain. A second structure of the carboxy-terminal domain of NSP3 in complex with BCAR1 shows that NSP3 also shares the closed conformation of the helical hairpin (Fig. 3A). Importantly, the remodeled hairpin forms the majority of the binding site for BCAR1, with further contributions from a sequence insertion that is only found in the CDC25 homology domains of the NSP family. Overall, these findings and the conservation of the NSP- and CAS-interacting domains (Fig. 3B) suggest that NSP proteins have repurposed an enzymatic nucleotide exchange factor domain to serve as an adaptor domain that is highly specific for the recruitment of CAS family members. In addition, the conservation of residues within the binding interfaces of different NSP and CAS proteins suggests that multiple combinations of NSP-CAS pairs should be able to form tight signaling associations. Indeed, multiple NSP-CAS combinations have already been found to function in different signaling contexts[77,81,85,86] (Fig. 3B). Therefore, the carboxy-termini of all members of the 2 families (with the possible exception of the less conserved CASS4) enable a highly promiscuous interaction system, creating a spectrum of NSP-CAS complexes that combine the distinctive signaling features of each binding partner to differentially modulate cellular processes and cancer malignancy.

Concluding Remarks

The strong interaction between NSP and CAS family proteins suggests that the 2 families are able to form stable complexes in which NSP proteins are critical modulators of CAS function. Studies with BCAR1 and NEDD9 have demonstrated the paramount importance of NSP-CAS downstream signaling pathways in normal physiology and cancer malignancy, whereas the mechanisms of upstream NSP-CAS regulation are less well understood.

CAS and NSP family proteins can both be phosphorylated on tyrosine and serine/threonine residues in response to cell substrate adhesion as well as cell stimulation with growth factors and cytokines. NSP proteins can potentiate CAS phosphorylation in normal and cancer cells through mechanisms that likely involve both anchoring CAS proteins to receptor tyrosine kinases and recruiting them near plasma membrane–localized SRC. This highlights their dual role as both adaptor and scaffolding proteins that can act in a positive feedback loop to further increase cell adhesion (Fig. 2). The fact that BCAR3, the long NSP3 isoform, and myristoylated NSP3 more readily induce CAS tyrosine and serine phosphorylation as compared to NSP1 or

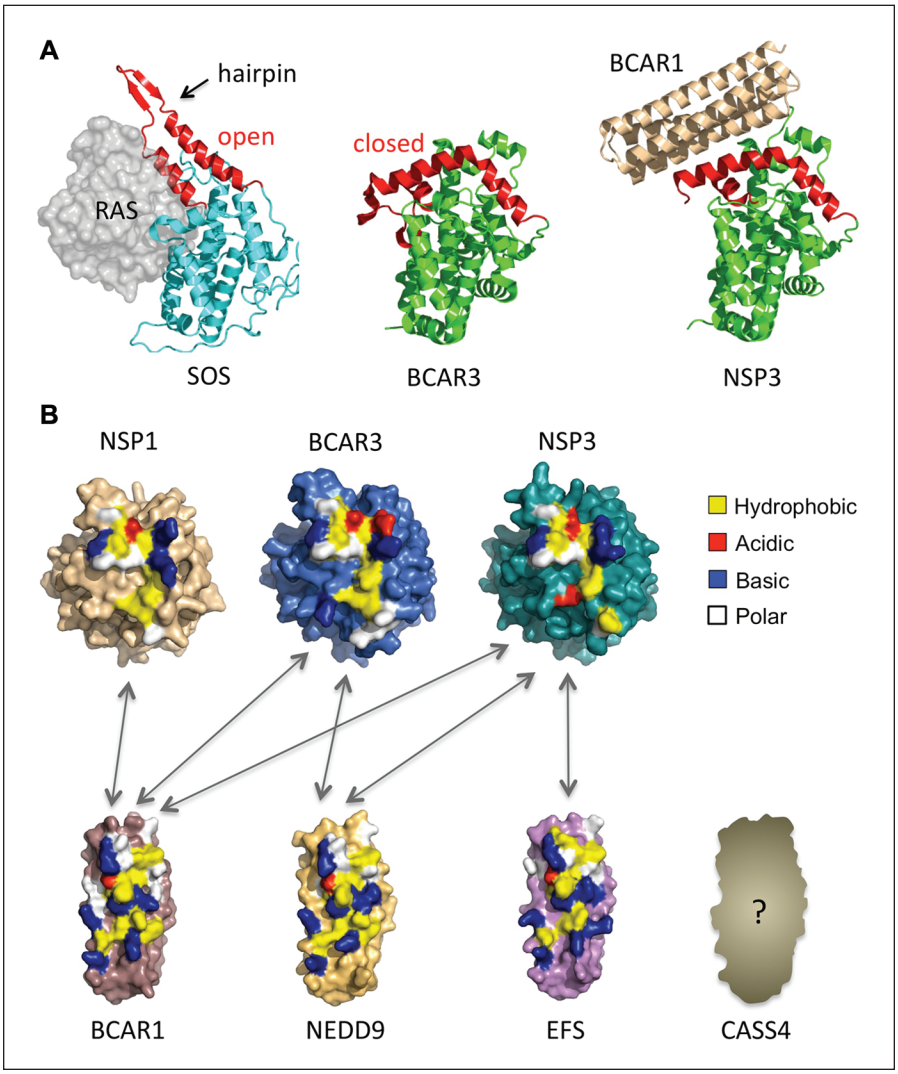

Figure 3. Conserved interaction domains of NSP and CAS family members enable promiscuous interactions. (**A**) The NSP CDC25 homology domain is in a "closed" conformation that cannot bind RAS proteins but can tightly interact with CAS proteins. (**Left**) Structure of the CDC25 homology domain of the active exchange factor SOS bound to its target GTPase, RAS.[119] (**Middle**) The structure of the carboxy-terminal domain of BCAR3 reveals that it also adopts a CDC25 homology domain fold, but in a new closed conformation incapable of RAS binding and exchange factor activity. (**Right**) The structure of the NSP3-BCAR1 complex reveals that the carboxy-terminal domain of NSP3 also adopts the closed conformation observed for BCAR3. The altered conformation enables strong interaction with the carboxy-terminal FAT domain of the CAS family protein BCAR1 to form an NSP-CAS complex, thus converting the exchange factor domain into an adaptor domain. (**B**) Surface representations of BCAR1, BCAR3, and NSP3 structures solved by X-ray crystallography,[13] and models of NSP1, NEDD9, and EFS. The carboxy-terminus of CASS4 was not modeled due to its greater degree of sequence divergency from the structurally characterized BCAR1. Colors indicate interface residue types identified in the NSP3-BCAR1 complex and the corresponding residues for the other family members. The color coding of interface residues highlights the similarities in the binding interfaces of NSP or CAS family members and thus the potential for promiscuous interactions between the 2 families (with the possible exception of the less conserved CASS4). Arrows indicate experimentally confirmed associations between NSP and CAS family members.

shorter NSP3 isoforms suggests that membrane targeting through the longer amino-terminal segment could act in concert with NSP SH2 domain interactions with cell surface receptors to more effectively promote CAS signaling. It will also be interesting to investigate if NSP proteins bound to the CAS carboxy-terminal FAT domain function together with proteins bound to the CAS SH3 domain as part of the mechanosensory machinery that stretches the central CAS substrate domain, leading to its phosphorylation by SRC.[4,5] The mechanisms and kinases responsible for NSP-induced CAS family serine phosphorylation, and whether this phosphorylation may be a consequence of increased substrate adhesion, also remain to be elucidated.

The functional effects of NSP phosphorylation are also unknown, except for phosphorylation of a tyrosine in the NSP3 CDC25 homology domain, which has been reported to prevent interaction with BCAR1.[90] A special connection between NSP3 and the ABL nonreceptor tyrosine kinase is suggested by the observed NSP3 phosphorylation downstream of the BCR-ABL oncogene[88] (phosphosite.org) and by the predicted binding of the ABL SH2 and SH3 domains to NSP3 but also remains to be explored.

Further characterizing the NSP-CAS association will also help to understand the physiological and pathological activities of the various family members. For example, it will be important to know whether the binding affinities (which are below 30 nM for the BCAR3-BCAR1 and NSP3-BCAR1 complexes[13]) differ depending on the NSP-CAS pair and if they can be physiologically regulated, for example, by posttranslational modifications.[90] It will also be useful to determine the proportion of each protein found in NSP-CAS complexes in the cellular environment and clarify the subcellular localization of the complexes. Structure-based mutations designed to affect NSP-CAS interaction without causing overall conformational changes will be instrumental for these investigations.[13] These types of studies have confirmed the importance of NSP-CAS complexes in processes such as the induction of CAS tyrosine phosphorylation and regulation of cell morphology and migration.[13,90,98,99] Additionally, the effects of BCAR3 carboxy-terminal

deletions support the importance of the CDC25 homology domain and the NSP-CAS association in antiestrogen resistance, SRC activation, CAS relocalization to membrane ruffles, and cell migration.[89,101]

According to some recent reports, however, substantial impairment of NSP-CAS association by single amino acid changes does not seem to impact NSP protein–dependent SRC and RAC1 activation and antiestrogen resistance induced by BCAR3 overexpression.[89,98] Further work will be needed to resolve these discrepancies. Furthermore, deletion of the CDC25 homology domain has demonstrated that at least some BCAR1 serine phosphorylation events do not seem to require interaction with NSP proteins.[94] On the other hand, gene transcription analyses and pathway activation mapping have revealed that overexpression of BCAR3 or BCAR1 activates signaling networks that have not only common elements but also distinctive features.[109,120] Taken together, these findings highlight the complexities in the activities of NSP and CAS proteins and their modules, which remain to be further unraveled in future studies.

In summary, the role of NSP and CAS proteins in cancer appears to depend on their protein abundance and phosphorylation state and possibly on the particular family member or isoform expressed. Although BCAR1, BCAR3, and SRC mRNA levels may not show a positive correlation with aggressiveness or poor responsiveness to tamoxifen therapy,[121] BCAR1 protein levels in breast cancer samples correlate with prognosis and could be useful to decide on treatment options.[53,54] Screening for BCAR1 phosphorylation levels could be even more powerful.[55,56] On the other hand, only a few mutations have been identified so far in each of the 3 NSP genes as well as in BCAR1 and NEDD9 in different types of cancers (sanger.ac.uk/cosmic), and no information is yet available on the functional effects of the mutations or their relevance to cancer development and malignancy. With regard to therapy, siRNA-based strategies will allow the reduction of NSP-CAS complexes and their malignant activities. Furthermore, better understanding of NSP-CAS signaling mechanisms will enable effective targeting of enzymatic activities associated with the complex or disruption of interactions with upstream regulators and downstream effectors. Developing agents that can disrupt NSP-CAS complexes will be more challenging due to the large interface and strong binding between the 2 classes of molecules.

An article published after submission of this review[122] reports that BCAR3 recruits BCAR1 to integrin-mediated focal adhesions by binding through its SH2 domain to a tyrosine phosphorylated sequence of the receptor-like protein tyrosine phosphatase a (PTPa). This leads to BCAR1 phosphorylation by SRC and downstream signals that promote cell migration

Declaration of Conflicting Interests

The author(s) declared no potential conflicts of interest with respect to the research, authorship, and/or publication of this article.

Funding

The author(s) received the following financial support for the research, authorship, and/or publication of this article: National Institutes of Health grants R01CA160457 and P01CA138390 to S.J.R. and E.B.P.; R01CA116099, R21NS067502, and P01HD025938 to E.B.P., and Department of Defense Breast Cancer Research Program postdoctoral fellowship BC100466 to P.D.M.

References

1. Pawson T. Dynamic control of signaling by modular adaptor proteins. Curr Opin Cell Biol. 2007;19:112-6.
2. Scott JD, Pawson T. Cell signaling in space and time: where proteins come together and when they're apart. Science. 2009;326:1220-4.
3. Harte MT, Hildebrand JD, Burnham MR, Bouton AH, Parsons JT. p130Cas, a substrate associated with v-Src and v-Crk, localizes to focal adhesions and binds to focal adhesion kinase. J Biol Chem. 1996;271:13649-55.
4. Sawada Y, Tamada M, Dubin-Thaler BJ, *et al*. Force sensing by mechanical extension of the Src family kinase substrate p130Cas. Cell. 2006; 127:1015-26.
5. Tamada M, Sheetz MP, Sawada Y. Activation of a signaling cascade by cytoskeleton stretch. Dev Cell. 2004;7:709-18.
6. Klemke RL, Leng J, Molander R, Brooks PC, Vuori K, Cheresh DA. CAS/Crk coupling serves as a "molecular switch" for induction of cell migration. J Cell Biol. 1998;140:961-72.
7. Feller SM. Crk family adaptors-signalling complex formation and biological roles. Oncogene. 2001;20:6348-71.
8. Chodniewicz D, Klemke RL. Regulation of integrin-mediated cellular responses through assembly of a CAS/Crk scaffold. Biochim Biophys Acta. 2004;1692:63-76.
9. Garcia-Guzman M, Dolfi F, Russello M, Vuori K. Cell adhesion regulates the interaction between the docking protein p130(Cas) and the 14-3-3 proteins. J Biol Chem. 1999;274: 5762-8.
10. Briknarova K, Nasertorabi F, Havert ML, *et al*. The serine-rich domain from Crk-associated substrate (p130cas) is a four-helix bundle. J Biol Chem. 2005;280:21908-14.
11. Cabodi S, del Pilar Camacho-Leal M, Di Stefano P, Defilippi P. Integrin signalling adaptors: not only figurants in the cancer story. Nat Rev Cancer. 2010;10:858-70.
12. Tikhmyanova N, Little JL, Golemis EA. CAS proteins in normal and pathological cell growth control. Cell Mol Life Sci. 2010;67:1025-48.
13. Mace PD, Wallez Y, Dobaczewska MK, *et al*. NSP-Cas protein structures reveal a promiscuous interaction module in cell signaling. Nat Struct Mol Biol. 2011;18:1381-7.
14. Feng L, Guedes S, Wang T. Atrophin-1-interacting protein 4/human Itch is a ubiquitin E3 ligase for human enhancer of filamentation 1 in transforming growth factor-beta signaling pathways. J Biol Chem. 2004;279:29681-90.
15. Nourry C, Maksumova L, Pang M, Liu X, Wang T. Direct interaction between Smad3, APC10, CDH1 and HEF1 in proteasomal degradation of HEF1. BMC Cell Biol. 2004;5:20.
16. Singh M, Cowell L, Seo S, O'Neill G, Golemis E. Molecular basis for HEF1/NEDD9/Cas-L action as a multifunctional co-ordinator of invasion, apoptosis and cell cycle. Cell Biochem Biophys. 2007;48:54-72.
17. O'Neill GM, Seo S, Serebriiskii IG, Lessin SR, Golemis EA. A new central scaffold for metastasis: parsing HEF1/Cas-L/NEDD9. Cancer Res. 2007;67:8975-9.
18. Alexandropoulos K, Baltimore D. Coordinate activation of c-Src by SH3- and SH2-binding sites on a novel p130Cas-related protein, Sin. Genes Dev. 1996;10:1341-55.
19. Burnham MR, Bruce-Staskal PJ, Harte MT, *et al*. Regulation of c-SRC activity and function by the adapter protein CAS. Mol Cell Biol. 2000;20:5865-78.
20. Nasertorabi F, Tars K, Becherer K, *et al*. Molecular basis for regulation of Src by the docking protein p130Cas. J Mol Recognit. 2006;19: 30-8.
21. Schuh NR, Guerrero MS, Schrecengost RS, Bouton AH. BCAR3 regulates Src/p130 Cas association, Src kinase activity, and breast cancer adhesion signaling. J Biol Chem. 2010;285: 2309-17.
22. Hamasaki K, Mimura T, Morino N, *et al*. Src kinase plays an essential role in integrin-mediated tyrosine phosphorylation of Crk-associated substrate p130Cas. Biochem Biophys Res Commun. 1996;222:338-43.

23. Ruest PJ, Shin NY, Polte TR, Zhang X, Hanks SK. Mechanisms of CAS substrate domain tyrosine phosphorylation by FAK and Src. Mol Cell Biol. 2001;21:7641-52.
24. Vuori K, Hirai H, Aizawa S, Ruoslahti E. Introduction of p130cas signaling complex formation upon integrin-mediated cell adhesion: a role for Src family kinases. Mol Cell Biol. 1996;16:2606-13.
25. Kiyokawa E, Hashimoto Y, Kurata T, Sugimura H, Matsuda M. Evidence that DOCK180 upregulates signals from the CrkII-p130(Cas) complex. J Biol Chem. 1998;273:24479-84.
26. Ohashi Y, Tachibana K, Kamiguchi K, Fujita H, Morimoto C. T cell receptor-mediated tyrosine phosphorylation of Cas-L, a 105-kDa Crk-associated substrate-related protein, and its association of Crk and C3G. J Biol Chem. 1998;273: 6446-51.
27. Guo W, Giancotti FG. Integrin signalling during tumour progression. Nat Rev Mol Cell Biol. 2004;5:816-26.
28. Kim C, Ye F, Ginsberg MH. Regulation of integrin activation. Annu Rev Cell Dev Biol. 2011;27:321-45.
29. Bos JL, de Rooij J, Reedquist KA. Rap1 signalling: adhering to new models. Nat Rev Mol Cell Biol. 2001;2:369-77.
30. Dolfi F, Garcia-Guzman M, Ojaniemi M, Nakamura H, Matsuda M, Vuori K. The adaptor protein Crk connects multiple cellular stimuli to the JNK signaling pathway. Proc Natl Acad Sci U S A. 1998;95:15394-9.
31. Radha V, Mitra A, Dayma K, Sasikumar K. Signalling to actin: role of C3G, a multitasking guanine-nucleotide-exchange factor. Biosci Rep. 2011;31:231-44.
32. Kiyokawa E, Hashimoto Y, Kobayashi S, Sugimura H, Kurata T, Matsuda M. Activation of Rac1 by a Crk SH3-binding protein, DOCK180. Genes Dev. 1998;12:3331-6.
33. Cote JF, Vuori K. Identification of an evolutionarily conserved superfamily of DOCK180-related proteins with guanine nucleotide exchange activity. J Cell Sci. 2002;115:4901-13.
34. Huang C, Rajfur Z, Borchers C, Schaller MD, Jacobson K. JNK phosphorylates paxillin and regulates cell migration. Nature. 2003;424: 219-23.
35. Shin NY, Dise RS, Schneider-Mergener J, Ritchie MD, Kilkenny DM, Hanks SK. Subsets of the major tyrosine phosphorylation sites in Crk-associated substrate (CAS) are sufficient to promote cell migration. J Biol Chem. 2004;279:38331-7.
36. Bos JL. Linking Rap to cell adhesion. Curr Opin Cell Biol. 2005;17:123-8.
37. Cabodi S, Tinnirello A, Di Stefano P, *et al*. p130Cas as a new regulator of mammary epithelial cell proliferation, survival, and HER2-neu oncogene-dependent breast tumorigenesis. Cancer Res. 2006;66:4672-80.
38. Almeida EA, Ilic D, Han Q, *et al*. Matrix survival signaling: from fibronectin via focal adhesion kinase to c-Jun NH(2)-terminal kinase. J Cell Biol. 2000;149:741-54.
39. Cunningham-Edmondson AC, Hanks SK. p130Cas substrate domain signaling promotes migration, invasion, and survival of estrogen receptor-negative breast cancer cells. Breast Cancer. 2009;2009:39-52.
40. Reynolds AB, Kanner SB, Wang HC, Parsons JT. Stable association of activated pp60src with two tyrosine-phosphorylated cellular proteins. Mol Cell Biol. 1989;9:3951-8.
41. Kanner SB, Reynolds AB, Wang HC, Vines RR, Parsons JT. The SH2 and SH3 domains of pp60src direct stable association with tyrosine phosphorylated proteins p130 and p110. EMBO J. 1991;10:1689-98.
42. Matsuda M, Mayer BJ, Fukui Y, Hanafusa H. Binding of transforming protein, P47gag-crk, to a broad range of phosphotyrosine-containing proteins. Science. 1990;248:1537-9.
43. Honda H, Oda H, Nakamoto T, *et al*. Cardiovascular anomaly, impaired actin bundling and resistance to Src-induced transformation in mice lacking p130Cas [see comments]. Nat Genet. 1998;19:361-5.
44. Brabek J, Constancio SS, Siesser PF, Shin NY, Pozzi A, Hanks SK. Crk-associated substrate tyrosine phosphorylation sites are critical for invasion and metastasis of SRC-transformed cells. Mol Cancer Res. 2005;3:307-15.
45. Cabodi S, Tinnirello A, Bisaro B, *et al*. p130Cas is an essential transducer element in ErbB2 transformation. FASEB J. 2010;24:3796-808.
46. Ambrogio C, Voena C, Manazza AD, *et al*. p130Cas mediates the transforming properties of the anaplastic lymphoma kinase. Blood. 2005;106:3907-16.
47. Pylayeva Y, Gillen KM, Gerald W, Beggs HE, Reichardt LF, Giancotti FG. Ras- and PI3K-dependent breast tumorigenesis in mice and humans requires focal adhesion kinase signaling. J Clin Invest. 2009;119:252-66.
48. Wendt MK, Smith JA, Schiemann WP. p130Cas is required for mammary tumor growth and transforming growth factor-beta-mediated metastasis through regulation of Smad2/3 activity. J Biol Chem. 2009;284:34145-56.
49. Dorssers LC, van Agthoven T, Dekker A, van Agthoven TL, Kok EM. Induction of antiestrogen resistance in human breast cancer cells by random insertional mutagenesis using defective retroviruses: identification of bcar-1, a common integration site. Mol Endocrinol. 1993;7: 870-8.
50. Brinkman A, van der Flier S, Kok EM, Dorssers LC. BCAR1, a human homologue of the adapter protein p130Cas, and antiestrogen resistance in breast cancer cells. J Natl Cancer Inst. 2000;92:112-20.
51. van Agthoven T, Veldscholte J, Smid M, *et al*. Functional identification of genes causing estrogen independence of human breast cancer cells. Breast Cancer Res Treat. 2009;114:23-30.
52. Ta HQ, Thomas KS, Schrecengost RS, Bouton AH. A novel association between p130Cas and resistance to the chemotherapeutic drug adriamycin in human breast cancer cells. Cancer Res. 2008;68:8796-804.
53. van der Flier S, Brinkman A, Look MP, *et al*. Bcar1/p130Cas protein and primary breast cancer: prognosis and response to tamoxifen treatment. J Natl Cancer Inst. 2000;92:120-7.
54. Dorssers LC, Grebenchtchikov N, Brinkman A, *et al*. The prognostic value of BCAR1 in patients with primary breast cancer. Clin Cancer Res. 2004;10:6194-202.
55. Brinkman A, de Jong D, Tuinman S, Azaouagh N, van Agthoven T, Dorssers LC. The substrate domain of BCAR1 is essential for anti-estrogen-resistant proliferation of human breast cancer cells. Breast Cancer Res Treat. 2010;120:401-8.
56. Soni S, Lin BT, August A, Nicholson RI, Kirsch KH. Expression of a phosphorylated p130(Cas) substrate domain attenuates the phosphatidylinositol 3-kinase/Akt survival pathway in tamoxifen resistant breast cancer cells. J Cell Biochem. 2009;107:364-75.
57. Salgia R, Pisick E, Sattler M, *et al*. p130CAS forms a signaling complex with the adapter protein CRKL in hematopoietic cells transformed by the BCR/ABL oncogene. J Biol Chem. 1996;271:25198-203.
58. Eisenmann KM, McCarthy JB, Simpson MA, *et al*. Melanoma chondroitin sulphate proteoglycan regulates cell spreading through Cdc42, Ack-1 and p130cas. Nat Cell Biol. 1999;1:507-13.
59. Frankel P, Pellet-Many C, Lehtolainen P, *et al*. Chondroitin sulphate-modified neuropilin 1 is expressed in human tumour cells and modulates 3D invasion in the U87MG human glioblastoma cell line through a p130Cas-mediated pathway. EMBO Rep. 2008;9:983-9.
60. Hamamura K, Furukawa K, Hayashi T, *et al*. Ganglioside GD3 promotes cell growth and invasion through p130Cas and paxillin in malignant melanoma cells. Proc Natl Acad Sci U S A. 2005;102:11041-6.
61. Feng H, Hu B, Liu KW, *et al*. Activation of Rac1 by Src-dependent phosphorylation of Dock180(Y1811) mediates PDGFRalpha-stimulated glioma tumorigenesis in mice and humans. J Clin Invest. 2011;121:4670-84.
62. Nick AM, Stone RL, Armaiz-Pena G, *et al*. Silencing of p130cas in ovarian carcinoma: a novel mechanism for tumor cell death. J Natl Cancer Inst. 2011;103:1596-612.
63. Fromont G, Cussenot O. The integrin signalling adaptor p130CAS is also a key player in prostate cancer. Nat Rev Cancer. 2011;11:227.
64. Kim M, Gans JD, Nogueira C, *et al*. Comparative oncogenomics identifies NEDD9 as a melanoma metastasis gene. Cell. 2006;125:1269-81.
65. Seo S, Ichikawa M, Kurokawa M. Structure and function of cas-L and integrin-mediated signaling. Crit Rev Immunol. 2006;26:391-406.
66. Ahn J, Sanz-Moreno V, Marshall CJ. The metastasis gene NEDD9 product acts through integrin beta3 and Src to promote mesenchymal motility and inhibit amoeboid motility. J Cell Sci. 2012;125:1814-26.
67. Natarajan M, Stewart JE, Golemis EA, *et al*. HEF1 is a necessary and specific downstream effector of FAK that promotes the migration of glioblastoma cells. Oncogene. 2006;25:1721-32.
68. Ji H, Ramsey MR, Hayes DN, *et al*. LKB1 modulates lung cancer differentiation and metastasis. Nature. 2007;448:807-10.
69. Giampieri S, Manning C, Hooper S, Jones L, Hill CS, Sahai E. Localized and reversible

TGFbeta signalling switches breast cancer cells from cohesive to single cell motility. Nat Cell Biol. 2009;11:1287-96.
70. Sanz-Moreno V, Gadea G, Ahn J, *et al*. Rac activation and inactivation control plasticity of tumor cell movement. Cell. 2008;135:510-23.
71. Lucas JT Jr., Salimath BP, Slomiany MG, Rosenzweig SA. Regulation of invasive behavior by vascular endothelial growth factor is HEF1-dependent. Oncogene. 2010;29:4449-59.
72. Kim SH, Xia D, Kim SW, Holla V, Menter DG, Dubois RN. Human enhancer of filamentation 1 Is a mediator of hypoxia-inducible factor-1alpha-mediated migration in colorectal carcinoma cells. Cancer Res. 2010;70:4054-63.
73. Yang WH, Lan HY, Huang CH, *et al*. RAC1 activation mediates Twist1-induced cancer cell migration. Nat Cell Biol. 2012;14:366-74.
74. Izumchenko E, Singh MK, Plotnikova OV, *et al*. NEDD9 promotes oncogenic signaling in mammary tumor development. Cancer Res. 2009;69:7198-206.
75. Singh MK, Izumchenko E, Klein-Szanto AJ, Egleston BL, Wolfson M, Golemis EA. Enhanced genetic instability and dasatinib sensitivity in mammary tumor cells lacking NEDD9. Cancer Res. 2010;70:8907-16.
76. Singh MK, Dadke D, Nicolas E, *et al*. A novel Cas family member, HEPL, regulates FAK and cell spreading. Mol Biol Cell. 2008;19:1627-36.
77. Alexandropoulos K, Regelmann AG. Regulation of T-lymphocyte physiology by the Chat-H/CasL adapter complex. Immunol Rev. 2009;232:160-74.
78. Vervoort VS, Roselli S, Oshima RG, Pasquale EB. Splice variants and expression patterns of SHEP1, BCAR3 and NSP1, a gene family involved in integrin and receptor tyrosine kinase signaling. Gene. 2007;391:161-70.
79. Regelmann AG, Danzl NM, Wanjalla C, Alexandropoulos K. The hematopoietic isoform of Cas-Hef1-associated signal transducer regulates chemokine-induced inside-out signaling and T cell trafficking. Immunity. 2006;25:907-18.
80. Dodelet VC, Pazzagli C, Zisch AH, Hauser CA, Pasquale EB. A novel signaling intermediate, SHEP1, directly couples Eph receptors to R-Ras and Rap1A. J Biol Chem. 1999;274:31941-6.
81. Lu Y, Brush J, Stewart TA. NSP1 defines a novel family of adaptor proteins linking integrin and tyrosine kinase receptors to the c-Jun N-terminal kinase/stress-activated protein kinase signaling pathway. J Biol Chem. 1999;274:10047-52.
82. Jones RB, Gordus A, Krall JA, MacBeath G. A quantitative protein interaction network for the ErbB receptors using protein microarrays. Nature. 2006;439:168-74.
83. Oh MJ, van Agthoven T, Choi JE, *et al*. BCAR3 regulates EGF-induced DNA synthesis in normal human breast MCF-12A cells. Biochem Biophys Res Commun. 2008;375:430-4.
84. Murphy DA, Courtneidge SA. The 'ins' and 'outs' of podosomes and invadopodia: characteristics, formation and function. Nat Rev Mol Cell Biol. 2011;12:413-26.
85. Cai D, Clayton LK, Smolyar A, Lerner A. AND-34, a novel p130Cas-binding thymic stromal cell protein regulated by adhesion and inflammatory cytokines. J Immunol. 1999;163:2104-12.
86. Sakakibara A, Hattori S. Chat, a Cas/HEF1-associated adaptor protein that integrates multiple signaling pathways. J Biol Chem. 2000;275:6404-10.
87. Gotoh T, Cai D, Tian X, Feig LA, Lerner A. p130Cas regulates the activity of AND-34, a novel Ral, Rap1, and R-Ras guanine nucleotide exchange factor. J Biol Chem. 2000;275:30118-23.
88. Salomon AR, Ficarro SB, Brill LM, *et al*. Profiling of tyrosine phosphorylation pathways in human cells using mass spectrometry. Proc Natl Acad Sci U S A. 2003;100:443-8.
89. Riggins RB, Quilliam LA, Bouton AH. Synergistic promotion of c-Src activation and cell migration by Cas and AND-34/BCAR3. J Biol Chem. 2003;278:28264-73.
90. Dail M, Kalo MS, Seddon JA, Cote JF, Vuori K, Pasquale EB. SHEP1 function in cell migration is impaired by a single amino acid mutation that disrupts association with the scaffolding protein cas but not with Ras GTPases. J Biol Chem. 2004;279:41892-902.
91. Heckel T, Czupalla C, Expirto Santo AI, *et al*. Src-dependent repression of ARF6 is required to maintain podosome-rich sealing zones in bone-digesting osteoclasts. Proc Natl Acad Sci U S A. 2009;106:1451-6.
92. Sakakibara A, Ohba Y, Kurokawa K, Matsuda M, Hattori S. Novel function of Chat in controlling cell adhesion via Cas-Crk-C3G-pathway-mediated Rap1 activation. J Cell Sci. 2002;115:4915-24.
93. Near RI, Smith RS, Toselli PA, *et al*. Loss of AND-34/BCAR3 expression in mice results in rupture of the adult lens. Mol Vis. 2009;15:685-99.
94. Makkinje A, Near RI, Infusini G, *et al*. AND-34/BCAR3 regulates adhesion-dependent p130Cas serine phosphorylation and breast cancer cell growth pattern. Cell Signal. 2009;21:1423-35.
95. Browne CD, Hoefer MM, Chintalapati SK, *et al*. SHEP1 partners with CasL to promote marginal zone B-cell maturation. Proc Natl Acad Sci U S A. 2010;107:18944-9.
96. Roselli S, Wallez Y, Wang L, Vervoort V, Pasquale EB. The SH2 domain protein Shep1 regulates the in vivo signaling function of the scaffolding protein Cas. Cell Signal. 2010;22:1745-52.
97. Wang L, Vervoort V, Wallez Y, Core N, Cremer H, Pasquale EB. The SRC homology 2 domain protein shep1 plays an important role in the penetration of olfactory sensory axons into the forebrain. J Neurosci. 2010;30:13201-10.
98. Vanden Borre P, Near RI, Makkinje A, Mostoslavsky G, Lerner A. BCAR3/AND-34 can signal independent of complex formation with CAS family members or the presence of p130Cas. Cell Signal. 2011;23:1030-40.
99. Makkinje A, Vanden Borre P, Near RI, Patel PS, Lerner A. Breast cancer anti-estrogen resistance 3 (BCAR3) augments binding of the c-Src kinase SH3 domain to Crk-associated substrate (p130Cas). J Biol Chem. 2012;287:27703-14.
100. Cai D, Felekkis KN, Near RI, *et al*. The GDP exchange factor AND-34 is expressed in B cells, associates with HEF1, and activates Cdc42. J Immunol. 2003;170:969-78.
101. Cai D, Iyer A, Felekkis KN, *et al*. AND-34/BCAR3, a GDP exchange factor whose overexpression confers antiestrogen resistance, activates Rac, PAK1, and the cyclin D1 promoter. Cancer Res. 2003;63:6802-8.
102. Felekkis KN, Narsimhan RP, Near R, *et al*. AND-34 activates phosphatidylinositol 3-kinase and induces anti-estrogen resistance in a SH2 and GDP exchange factor-like domain-dependent manner. Mol Cancer Res. 2005;3:32-41.
103. Near RI, Zhang Y, Makkinje A, Vanden Borre P, Lerner A. AND-34/BCAR3 differs from other NSP homologs in induction of anti-estrogen resistance, cyclin D1 promoter activation and altered breast cancer cell morphology. J Cell Physiol. 2007;212:655-65.
104. Sakakibara A, Hattori S, Nakamura S, Katagiri T. A novel hematopoietic adaptor protein, Chat-H, positively regulates T cell receptor-mediated interleukin-2 production by Jurkat cells. J Biol Chem. 2003;278:6012-7.
105. Singh A, Greninger P, Rhodes D, *et al*. A gene expression signature associated with "K-Ras addiction" reveals regulators of EMT and tumor cell survival. Cancer Cell. 2009;15:489-500.
106. van Agthoven T, van Agthoven TL, Dekker A, van der Spek PJ, Vreede L, Dorssers LC. Identification of BCAR3 by a random search for genes involved in antiestrogen resistance of human breast cancer cells. EMBO J. 1998;17:2799-808.
107. Schrecengost RS, Riggins RB, Thomas KS, Guerrero MS, Bouton AH. Breast cancer antiestrogen resistance-3 expression regulates breast cancer cell migration through promotion of p130Cas membrane localization and membrane ruffling. Cancer Res. 2007;67:6174-82.
108. Riggins RB, Schrecengost RS, Guerrero MS, Bouton AH. Pathways to tamoxifen resistance. Cancer Lett. 2007;256:1-24.
109. van Agthoven T, Godinho MF, Wulfkuhle JD, Petricoin EF 3rd, Dorssers LC. Protein pathway activation mapping reveals molecular networks associated with antiestrogen resistance in breast cancer cell lines. Int J Cancer. 2012;131:1998-2007.
110. Riggins RB, Thomas KS, Ta HQ, *et al*. Physical and functional interactions between Cas and c-Src induce tamoxifen resistance of breast cancer cells through pathways involving epidermal growth factor receptor and signal transducer and activator of transcription 5b. Cancer Res. 2006;66:7007-15.
111. Shah AN, Gallick GE. Src, chemoresistance and epithelial to mesenchymal transition: are they related? Anticancer Drugs. 2007;18:371-5.
112. Tikhmyanova N, Golemis EA. NEDD9 and BCAR1 negatively regulate E-cadherin membrane localization, and promote E-cadherin degradation. PLoS One. 2011;6:e22102.
113. Hiscox S, Morgan L, Barrow D, Dutkowskil C, Wakeling A, Nicholson RI. Tamoxifen resistance in breast cancer cells is accompanied by an enhanced motile and invasive phenotype:

inhibition by gefitinib ('Iressa', ZD1839). Clin Exp Metastasis. 2004;21:201-12.

114. Lacroix M, Leclercq G. Relevance of breast cancer cell lines as models for breast tumours: an update. Breast Cancer Res Treat. 2004;83:249-89.
115. Giallourakis C, Cao Z, Green T, *et al*. A molecular-properties-based approach to understanding PDZ domain proteins and PDZ ligands. Genome Res. 2006;16:1056-72.
116. Rosebeck S, Rehman AO, Lucas PC, McAllister-Lucas LM. From MALT lymphoma to the CBM signalosome: three decades of discovery. Cell Cycle. 2011;10:2485-96.
117. Ryu JW, Kim HJ, Lee YS, *et al*. The proteomics approach to find biomarkers in gastric cancer. J Korean Med Sci. 2003;18:505-9.
118. Al-Shami A, Wilkins C, Crisostomo J, *et al*. The adaptor protein Sh2d3c is critical for marginal zone B cell development and function. J Immunol. 2010;185:327-34.
119. Boriack-Sjodin PA, Margarit SM, Bar-Sagi D, Kuriyan J. The structural basis of the activation of Ras by Sos. Nature. 1998;394:337-43.
120. Dorssers LC, van Agthoven T, Brinkman A, Veldscholte J, Smid M, Dechering KJ. Breast cancer oestrogen independence mediated by BCAR1 or BCAR3 genes is transmitted through mechanisms distinct from the oestrogen receptor signalling pathway or the epidermal growth factor receptor signalling pathway. Breast Cancer Res. 2005;7:R82-92.
121. van Agthoven T, Sieuwerts AM, Meijer-van Gelder ME, *et al*. Relevance of breast cancer antiestrogen resistance genes in human breast cancer progression and tamoxifen resistance. J Clin Oncol. 2009;27:542-9.
122. Sun G, Cheng SY, Chen M, Lim CJ, Pallen CJ. Protein tyrosine phosphatase alpha phosphotyrosyl-789 binds BCAR3 to position Cas for activation at integrin-mediated focal adhesions. Mol Cell Biol 2012;32:3776-89.

NSP-Cas protein structures reveal a promiscuous interaction module in cell signaling

Peter D Mace[1], Yann Wallez[2], Małgorzata K Dobaczewska[1], JeongEun J Lee[1], Howard Robinson[3], Elena B Pasquale[2,4] & Stefan J Riedl[1]

Members of the novel SH2-containing protein (NSP) and Crk-associated substrate (Cas) protein families form multidomain signaling platforms that mediate cell migration and invasion through a collection of distinct signaling motifs. Members of each family interact via their respective C-terminal domains, but the mechanism of this association has remained enigmatic. Here we present the crystal structures of the C-terminal domain from the NSP protein BCAR3 and the complex of NSP3 with p130Cas. BCAR3 adopts the Cdc25-homology fold of Ras GTPase exchange factors, but it has a 'closed' conformation incapable of enzymatic activity. The structure of the NSP3–p130Cas complex reveals that this closed conformation is instrumental for interaction of NSP proteins with a focal adhesion-targeting domain present in Cas proteins. This enzyme-to-adaptor conversion enables high-affinity, yet promiscuous, interactions between NSP and Cas proteins and represents an unprecedented mechanistic paradigm linking cellular signaling networks.

The integration of signals triggered by diverse stimuli is essential for cell communication in higher organisms and is achieved primarily through the assembly of multiprotein signaling nodes. The Cas and NSP families form one such class of signaling nodes and correspondingly harbor multiple protein-protein interaction domains and motifs that mediate association with many cell signaling factors. This allows them to function as mediators that integrate signals emanating from cell adhesion and environmental stimuli to promote cell migration, adhesion and invasion. Dysregulation of signaling through Cas and NSP proteins is relevant to a spectrum of disease processes, particularly tumor progression and cancer metastasis.

The complexity of NSP-Cas functions is exemplified by two prominent family members, p130Cas and the NSP protein BCAR3, which also confer antiestrogen resistance in breast cancer[1,2]. Firmly embedded in the Src-Crk signaling axis, p130Cas interacts with more than a dozen signaling factors in addition to Src family kinases and Crk, including FAK, PYK2, FRNK, RapGEF1, Aurora kinase A, PI3K, NMP4, NCK1 and SHIP2 (reviewed in ref. 3). BCAR3 is associated with enhanced PI3K activity downstream of growth factor receptors and with subsequent activation of Rac, Cdc42, AKT and PAK1 (ref. 4). p130Cas and BCAR3 also bind directly to each other[5], thereby linking their respective signaling networks to form a platform that mediates migratory signaling. In addition to BCAR3, p130Cas can also interact with NSP family members NSP3 and NSP1 (refs. 6,7). BCAR3 also interacts with HEF1 (Cas-L) in addition to p130Cas[8]. Further combinations are created by association of NSP family members NSP3 and NSP1 with Cas proteins Cas-L and Efs, increasing the diversity of NSP-Cas signaling networks[9–11]. NSP and Cas family proteins can therefore propagate class-specific but promiscuous combinatorial networks, which are essential to their diverse functions in specialized cellular processes. The effect of aberrant NSP-Cas signaling is manifested in a range of disease processes. p130Cas and BCAR3 exert a concerted effect in cancer[12,13], whereas the NSP3 (SHEP1)–Cas-L signaling node is crucial for B-cell migration and maturation[9,11]. Additionally, the NSP3-p130Cas module is essential in neuronal cells for proper olfactory development, and its absence causes a phenotype reminiscent of the human developmental disorder Kallmann syndrome[14]. These examples underline the importance of distinct NSP-Cas modules in cellular processes that require integration of adhesion and chemotactic stimuli.

Although the respective C-terminal domains of Cas and NSP proteins are fundamental to their interaction (**Supplementary Fig. 1a**)[7], it is unclear at the molecular level how different family members can interact in this class-specific yet promiscuous manner. Moreover, the predicted nature of the C-terminal Cas and NSP domains suggests an interaction mechanism that has not previously been observed. The NSP-binding portion of Cas proteins has been proposed to assume a focal adhesion targeting (FAT) domain–like fold, whereas the C-terminal domain of NSP proteins shares weak homology with Cdc25-homology domains (Cdc25-hd) found in GTPase exchange factors[15,16]. However, the molecular mechanism of a direct Cdc25-hd–FAT interaction is currently without precedent, and the question of how this influences the putative activities of each domain while mechanically linking NSP and Cas signaling remains outstanding.

[1]Program of Apoptosis and Cell Death Research, Cancer Center, Sanford-Burnham Medical Research Institute, La Jolla, California, USA. [2]Program of Signal Transduction, Cancer Center, Sanford-Burnham Medical Research Institute, La Jolla, California, USA. [3]Department of Biology, Brookhaven National Laboratory, Upton, New York, USA. [4]Pathology Department, University of California San Diego, San Diego, California, USA. Correspondence should be addressed to S.J.R. (sriedl@sanfordburnham.org).

Received 10 May; accepted 30 August; published online 13 November 2011; doi:10.1038/nsmb.2152

To elucidate the molecular features enabling the formation of Cas-NSP signaling modules, we solved the crystal structures of the C-terminal region of unbound human BCAR3 and of the complex between human NSP3 and p130Cas. These structures, in combination with our biochemical and biological analyses, show that the Cdc25-homology domain present in NSP proteins has evolved as an adaptor domain based on an enzymatic fold used in RasGEFs. This NSP structure tightly binds the FAT domain of Cas proteins using an extended interface. Furthermore, the class-specific interaction patterns we observed in the NSP3 and p130Cas interfaces are conserved among the members of both families. As a result, NSP and Cas proteins can promiscuously interact with each other to form various combinations of signaling modules that regulate cellular processes.

RESULTS

BCAR3 has an unconventional Cdc25-homology domain

To shed light on NSP protein signaling, we carried out structural and mechanistic investigations of the C-terminal domain of the best-characterized family member, BCAR3. After testing various constructs, we generated a soluble BCAR3 C-terminal domain (residues 502–825) with properties suitable for biochemical and structural investigation. Extensive screening of crystallization conditions led to well-diffracting BCAR3 crystals, which allowed us to solve the structure of BCAR3 at a resolution of 2.4 Å (**Fig. 1a** and **Table 1**). The crystal structure contains four molecules of BCAR3 in the asymmetric unit, which overlay with high fidelity (r.m.s. deviation range 0.24–0.45 Å). The BCAR3 structure reveals a Ras-type GDP exchange factor architecture with unexpected modifications that clarify earlier contradictory findings about NSP proteins. BCAR3 adopts the overall fold of the Cdc25-homology domain structures solved so far with r.m.s. deviation values between the BCAR3 core and SOS, EPAC2 or RasGRF1 of 2.18 Å, 2.35 Å and 2.19 Å, respectively[17–19] (**Supplementary Fig. 1b**). However, BCAR3 shows marked deviations in two distinct regions that lead to an unusual closed arrangement of the Cdc25-homology domain (**Fig. 1** and **Supplementary Fig. 2**). In detail, helices α_h and α_i (nomenclature derived from SOS[17]) each bend ~60° in orthogonal directions relative to their known GEF counterparts (**Fig. 1c**,**d**). Helix α_h is also markedly shorter in BCAR3 than in other Cdc25-homology domains, and hydrophobic interactions by Leu713, Val714 and Leu716 cause the helix to be buried between α_b and α_i. Helix α_i is broken into two portions (α_i and α_{i*}, **Supplementary Fig. 2**), with α_i folding toward the C terminus of α_f in the Cdc25-homology domain core, achieving the closed BCAR3 conformation (**Fig. 1**). The second, markedly different region comprises residues 565–592. This 'NSP-specific region' adopts a conformation that includes helices α_{NSPa} and α_{NSPb} and is well conserved in all NSP proteins.

Comparison of the BCAR3 structure with complexes of catalytically competent Cdc25-homology domains bound to their target GTPases showed that BCAR3 assumes a conformation incompatible with classical GEF function because its GTPase-binding site is completely occluded (**Fig. 1e** and **Supplementary Fig. 3a**). This occlusion is mainly achieved by the closed conformation of helix α_i and its preceding linker comprising BCAR3 residues 718–736. In active 'open' Cdc25-homology domains, helices α_h and α_i form a hairpin structure (**Fig. 1**) that is crucial for activity because it displaces the switch 1 region of target GTPases[17,20]. In fact, even slight conformational adjustments in this hairpin have substantial effects on exchange activity[19,21]. Thus, the marked changes observed in BCAR3 suggest a considerable functional redirection of crucial GEF catalytic elements.

Closed BCAR3 lacks catalytic activity *in vitro*

To validate our structural observations and gain further insight into the functional properties of the BCAR3 C-terminal domain, we examined its ability to promote nucleotide exchange *in vitro*, which has been controversial in the literature[5,16,22–24]. Using $BCAR3_{502–825}$, we assessed the ability of BCAR3 to induce GDP release from its putative target GTPase, Rap1A[25]. In contrast to positive controls with either EDTA or C3G (a bona fide GEF for Rap1A[26]), which effectively promoted GDP release from Rap1A, we observed no activity for BCAR3 (**Fig. 1f**). Furthermore, we detected no interaction between the BCAR3 Cdc25-homology domain and Rap1A in *in vitro* pull-downs or isothermal titration calorimetry experiments (data not shown). We observed no catalytic activity for BCAR3, in accordance with the crystal structure, indicating that BCAR3 represents a noncatalytic adaption of the Cdc25-homology domain fold.

Structure of the NSP3–p130Cas complex

To further understand the function of the observed closed NSP conformation and clarify the molecular basis of NSP-Cas signaling modules, we next sought to obtain the structure of an NSP–Cas interaction complex.

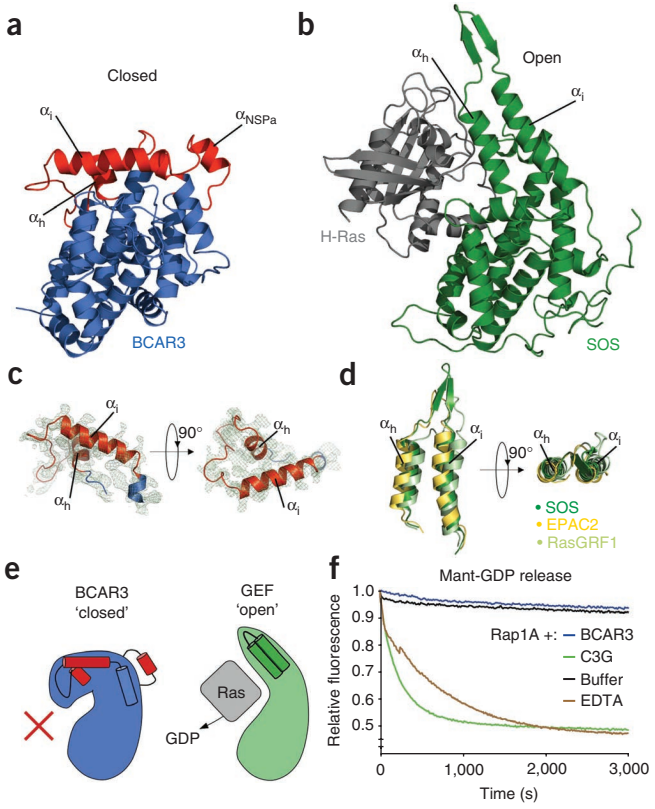

Figure 1 The BCAR3 C-terminal domain resembles a Cdc25-homology domain but adopts a closed conformation incapable of canonical GEF function. (**a**) Structure of BCAR3 Cas interaction domain. C-terminal domain of NSP BCAR3 (blue) with rearranged NSP-specific structural elements indicated (red). (**b**) SOS (green) in complex with H-Ras (gray; PDB 1BKD)[17]. (**c**) Structure of closed 'helical hairpin' in BCAR3 with $2F_o - F_c$ electron density map (contoured to 1 σ) shown from two orthogonal directions. (**d**) Helical hairpins of SOS, EPAC2 and RasGRF1. Orientations are as in **c**. (**e**) Schematic of conformations of closed BCAR3 compared with a canonical open GEF conformation. (**f**) GDP release assay. *In vitro* mantGDP release from Rap1A, a putative GTPase target for BCAR3, in the presence of BCAR3, C3G or EDTA.

To this end, we extended our investigations to the BCAR3 relative NSP3 (SHEP1) and the prototypical Cas family member p130Cas. We identified constructs encoding residues 382–703 of NSP3 and residues 645–870 of p130Cas, which allowed us to generate the individual protein domains and complexes of NSP3 or BCAR3 bound to p130Cas (**Supplementary Fig. 3b**,**c**). After extensive crystallization trials using both complexes, we solved the crystal structure of NSP3 bound to p130Cas at a resolution of 2.5 Å (**Fig. 2** and **Table 1**). The asymmetric unit of the crystal contains two NSP3–p130Cas complexes (**Supplementary Fig. 4**), one of which is more clearly defined by electron density and is described below. In agreement with our biochemical characterization (**Supplementary Figs. 3b**,**c** and **5a**–**c**), the crystal structure shows that the two proteins form a 1:1 arrangement characterized by an extensive binding interface that buries 1,192 Å^2. This substantial interface is in agreement with isothermal titration calorimetry results, which support a very tight (30 nM) interaction between p130Cas and the closely related NSP protein BCAR3 (**Supplementary Fig. 5d**).

Table 1 Data collection, phasing and refinement statistics

	BCAR3 native	NSP3–p130Cas native	NSP3–p130Cas SeMet	NSP3–p130Cas thimerosal
Data collection				
Space group	$P2_12_12_1$	$I4_1$	$I4_1$	$I4_1$
Cell dimensions				
a, *b*, *c* (Å)	50.23, 151.89, 196.50	171.88, 171.88, 78.27	172.04, 172.04, 79.16	171.72, 171.72, 77.76
			Peak	*Peak*
Wavelength	1.5418	1.075	0.9792	1.000
Resolution (Å)	19.85–2.4	29.5–2.5	29.6–2.9	50.0–2.6
R_{merge}	0.096 (0.532)	0.071 (0.844)	0.056 (0.697)	0.069 (0.552)
$I / \sigma I$	13.7 (3.0)	22.7 (3.7)	18.4 (2.3)	35.2 (3.6)
Completeness (%)	98.7 (96.3)	99.8 (100.0)	99.5 (98.0)	97.1 (83.1)
Redundancy	5.2 (4.6)	14.9 (14.9)	6.2 (6.1)	14.7 (12.0)
Refinement				
Resolution (Å)	19.75–2.4	29.5–2.5		
No. reflections	56,380	37,296		
R_{work} / R_{free}	17.4 / 24.4	19.6 / 26.6		
No. atoms				
Protein	9,883	6,532		
Ligand/ion	41	7		
Water	373	59		
B-factors				
Protein	42.4	100.4		
Ligand/ion	53.7	116		
Water	37.5	69.6		
R.m.s. deviations				
Bond lengths (Å)	0.008	0.008		
Bond angles (°)	1.053	1.064		

Values in parentheses are for highest-resolution shell.

In the final model of the NSP3–p130Cas complex (**Fig. 2a**), NSP3 residues 386–698 are well defined by electron density with the exception of the loop between residues 599 and 612, which was not included in the model. The C-terminal domain of p130Cas is defined by electron density from residues 739–872 and adopts the four-helix bundle fold characteristic of FAT domains. The structure of NSP3 closely resembles a Cdc25-homology domain fold but, notably, shares the closed conformation observed for unbound BCAR3. A comparative backbone r.m.s. deviation of 0.97 Å between p130Cas-bound NSP3 and unbound BCAR3 underscores their close structural similarity (**Supplementary Fig. 6a**).

Closed NSP conformation is instrumental for Cas binding

The structure of the NSP3–p130Cas complex reveals that the closed conformation observed for the NSP3 C-terminal domain is key in enabling a Cdc25-hd–FAT domain interaction to form a previously undescribed signaling tether. This binding interface used by NSP3 and p130Cas can be divided into two main binding motifs (**Fig. 3** and **Supplementary Fig. 7a**), which coincide with the two regions that deviate from the canonical Cdc25-homology domain fold of NSP3 (and BCAR3) and depend on the closed conformation of the domain. In the first motif, which we call site 1, a hydrophobic strip in helix α_i of NSP3 interacts with a highly complementary surface on p130Cas. Site 2 is generated by a distinct region between α_{NSPa} and α_b of NSP3 and synergizes with site 1 to generate a tight signaling interaction.

Specifically, in site 1, Val616, Leu620 and Leu623 on helix α_i pack into the hydrophobic groove between α_2 and α_3 of the p130Cas FAT domain (**Fig. 4a** and **Supplementary Fig. 7a**). These contacts are augmented by charged interactions mediated by Glu617, Glu624 and Arg627 of NSP3. In site 2, helix α_{NSPb} and subsequent residues Glu465 and Leu469-Pro470-His471 interact with a predominantly hydrophobic groove between α_1 and α_2 of the p130Cas FAT domain. Supplementing the two main interfaces is a peripheral association of residues 386–388 from the N terminus of the NSP3 Cdc25-homology domain and Leu596 from helix α_h of NSP3 (**Fig. 3c**), which contributes to a hydrophobic surface that links the site 1 and site 2 binding motifs.

As we discussed for BCAR3, the closed NSP3 conformation renders key elements of the Cdc25-homology domain incapable of participating

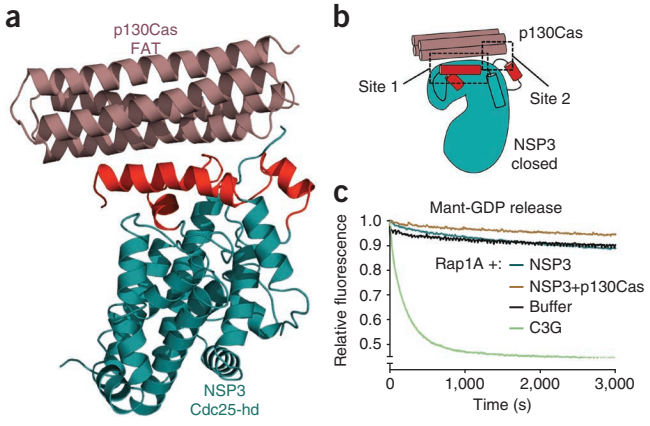

Figure 2 The NSP3–p130Cas complex. (**a**) Crystal structure of NSP3–p130Cas complex. NSP3 (cyan) and p130Cas (brown) are shown, with NSP-specific binding elements colored red. (**b**) Schematic of NSP3-p130Cas interaction. (**c**) NSP3 GEF activity assay with and without p130Cas C-terminal domain.

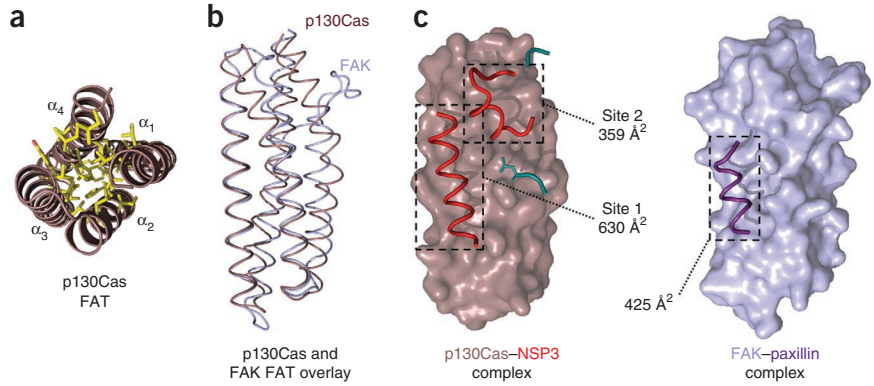

Figure 3 FAT domain of p130Cas is well defined and uses a previously unknown extended binding mode. (**a**) p130Cas FAT domain core. End-on view of four-helical bundle of p130Cas (brown) with hydrophobic core residues displayed in stick representation (yellow). (**b**) Backbone overlay of p130Cas (brown) with FAK (light blue, PDB 1OW7)[30]. (**c**) Interaction mode used by FAT domain of p130Cas and NSP3 compared with FAK binding to paxillin LD-4 peptide (purple). NSP3 elements contributing to site 1 and site 2 binding motifs are red. Buried surface areas for NSP3–p130Cas site 1, site 2 and FAK–paxillin are indicated. Additional NSP3 residues participating in Cas interaction are colored cyan.

in a canonical interaction with a Ras GTPase. Furthermore, the presence of Cas in the complex provides even greater steric hindrance to such a hypothetical GTPase interaction. To further validate this structural observation, we carried out *in vitro* nucleotide exchange assays with both unbound NSP3 and NSP3 in complex with the p130Cas FAT domain. In addition to Rap1A, we included Rap2A as a further putative target GTPase for NSP3 (ref. 27). We did not detect any *in vitro* exchange activity for either unbound or Cas-bound NSP3 (**Fig. 2c** and **Supplementary Fig. 6b**). This is in accordance with our structural observation that a closed conformation of the NSP3 Cdc25-homology domain is essential for Cas binding.

Cas extends the paradigm of FAT domain interactions

In addition to revealing a critical adaption in NSP proteins, the NSP3–p130Cas complex provides the first atomic-resolution evidence that the C-terminal domains of Cas family proteins adopt a well-defined FAT domain–type four-helix bundle. Extensive hydrophobic interactions in the core of the domain suggest a stable arrangement of these helices (**Fig. 3a**). Generally, FAT domains function as adaptor domains in focal adhesion signaling[28], interacting with binding partners by recruiting helical motifs to surface grooves between their constituent helices[29–31]. However, these interactions are characteristically weak[29,32], whereas we observed a K_d in the low nanomolar range for the binding of BCAR3 to the FAT domain of p130Cas, and tight binding between NSP3 and p130Cas (**Supplementary Fig. 5**). Although the tertiary structure of the C-terminal domain of p130Cas is nearly identical to that of other FAT domains (**Fig. 3b**), p130Cas achieves extremely tight binding to

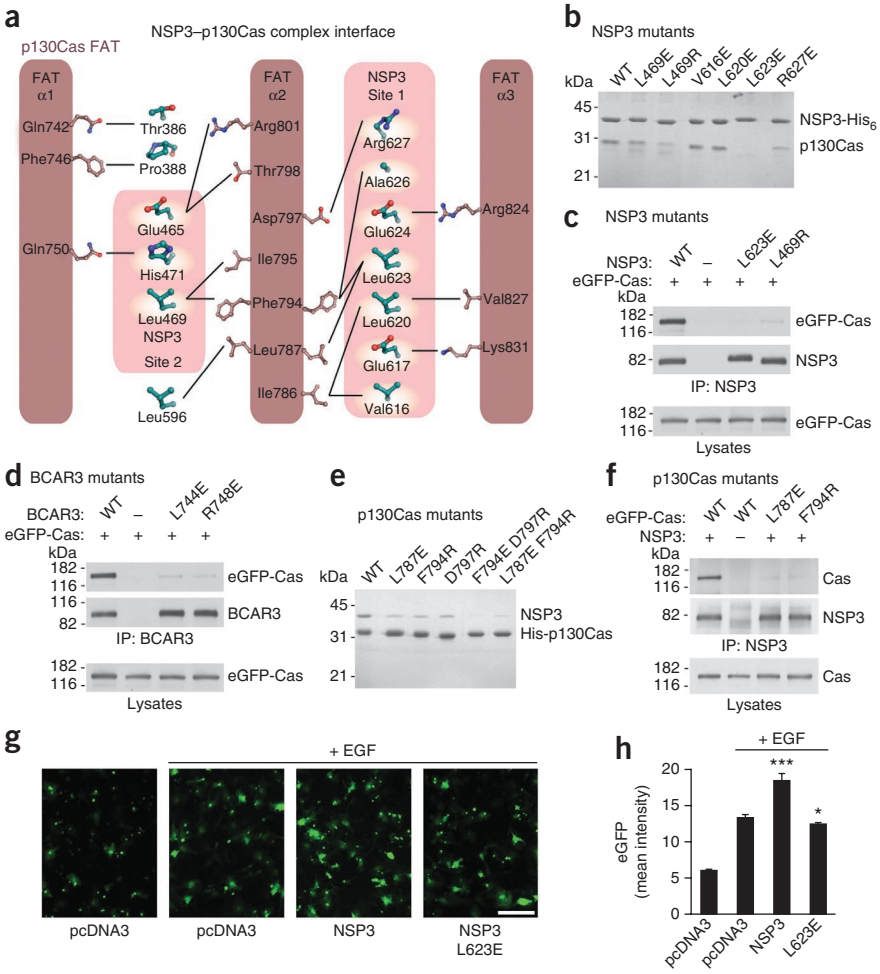

Figure 4 Analysis of NSP family–p130Cas interactions *in vitro* and *in vivo*. (**a**) Schematic of interfaces between NSP3 and p130Cas. (**b**) Subset of well-expressed NSP3 mutants (Cdc25-homology domain) were purified as His_6-tagged proteins and assayed for ability to selectively co-purify untagged wild-type (WT) p130Cas C-terminal domain from *Escherichia coli* lysates. (**c**) Coimmunoprecipitation of full-length p130Cas with full-length wild-type NSP3 compared to NSP3 interface mutants L623E and L469R. (**d**) L744E and R748E in BCAR3 (equivalent to NSP3 Leu623 and Arg627, respectively) were examined for interaction with Cas after immunoprecipitation with an antibody to BCAR3. (**e**) Co-purification of recombinant p130Cas mutants with NSP3, done as in **b**, but using p130Cas with a His_6 tag and untagged NSP3. (**f**) p130Cas mutants were examined for ability to bind NSP3 in COS cells by immunoprecipitation with antibody to NSP3. (**g**,**h**) Transwell migration assays measuring NSP3–Cas mediated chemotaxis toward an EGF chemoattractant. Representative images of cells that relocated from top to bottom side of Transwell filter are shown in **g** (scale bar, 100 μm). Histogram quantifying mean eGFP intensity from transfected cells on bottom side of filters is shown in **h**. Values are mean ± s.d. of six microscope field measurements. $^*P < 0.05$; $^{***}P < 0.001$.

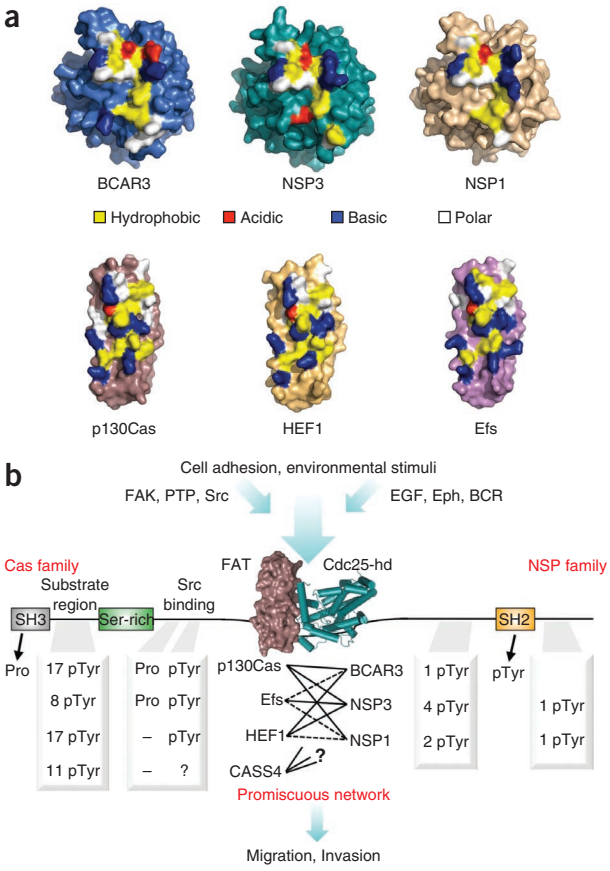

Figure 5 NSP-Cas modules form class-specific yet promiscuous signaling nodes. (**a**) Surface representations of BCAR3, NSP3 and p130Cas structures solved in this work, and models of NSP1, HEF1 and Efs. Color code indicates residue types. (**b**) Schematic of NSP-Cas signaling nodes. Phosphorylation sites (pTyr) are annotated using http://www.phosphosite.org/, except for Efs, which is based on reference 10. Proline motifs (Pro) for Src family kinase binding were identified manually based on the sequence of each Cas family protein. PTP, protein tyrosine phosphatases; EGF, epidermal growth factor; Eph, ephrin receptors; BCR, B-cell receptor.

NSP3 by a previously unknown adaptation of the FAT domain interaction mode (**Fig. 3c**) using the bipartite binding motifs described above. First, the NSP3-p130Cas interaction at site 1 is accomplished through a binding groove between helices α_2 and α_3 of the p130Cas FAT domain. This interaction is reminiscent of the α_2-α_3 binding site used by FAK and Pyk2 to bind paxillin[30,31], but p130Cas accommodates a distinctly longer helical stretch from NSP3 and buries a substantially greater surface area of 630 Å^2 (**Fig. 3c**). The interaction at site 2, in contrast, has not been observed for other FAT-type four-helical bundles. On p130Cas this interface is formed by helix α_1 and the C-terminal portion of helix α_2 of the FAT scaffold, and in concert with the extended site 1 interface, this achieves the tight binding of the p130Cas FAT domain to NSP proteins.

Biochemistry and biology of NSP–Cas complexes

To verify our structural findings, we carried out extensive biochemical and biological mutational studies. We designed structure-based mutations to disrupt binding elements while conserving the integrity of the protein domains (**Fig. 4a**). All NSP3, BCAR3 and p130Cas mutant domains showed expression and solubility suitable for binding assays. The NSP3 R627E site 1 mutation or L469R site 2 mutation reduced complex formation with the p130Cas FAT domain *in vitro*, indicating that they substantially weaken the tight interaction (**Fig. 4b** and **Supplementary Fig. 7b**). In addition, the NSP3 L623E site 1 mutation completely abrogated the interaction even at the substantial concentrations used in our *in vitro* association experiments (**Fig. 4b**). In COS cells the full-length NSP3 L623E and L469R mutants also efficiently disrupted the complex with full-length p130Cas when the two proteins were coexpressed (**Fig. 4c**). BCAR3 residues Leu744 and Arg748 correspond to Leu623 and Arg627 in NSP3, and when mutated also effectively disrupted the association with p130Cas in COS cells, confirming that different NSP proteins use a conserved p130Cas-binding mode (**Fig. 4d**). Mutation of Arg743 in mouse BCAR3, corresponding to Arg748 in human BCAR3, has also been independently confirmed to disrupt p130Cas binding in recent studies[16,33]. However, our *in vitro* results suggest that mutating Leu623 in NSP3 more effectively abrogates binding and therefore is a more potent probe for dissecting NSP3-Cas signaling modules. The potency of Leu623 is in agreement with its location in the hydrophobic core of the site 1 interaction, near the hydrophobic pair Phe794 and Leu787 of p130Cas (**Fig. 4a**). In contrast, the salt bridge that Arg627 forms with Asp797 of p130Cas is more peripheral to the interface.

We also examined interface mutations in p130Cas for their ability to counteract complex formation with NSP proteins. On the basis of our structural results, we chose Leu787, Phe794 and Asp797 as promising candidates for mutagenesis. Individual mutations of each of these residues (L787E, F794R and D797R) weakened the *in vitro* association of the p130Cas FAT domain with the NSP3 Cdc25-homology domain, whereas combinations of two mutations virtually abolished complex formation (**Fig. 4e** and **Supplementary Fig. 7c**). In addition, the single p130Cas L787E and F794R mutations markedly reduced association between full-length p130Cas and NSP3 coexpressed in COS cells, confirming features of the NSP3–p130Cas complex in the cellular context (**Fig. 4f**).

To examine the functional effects of targeted disruption of the NSP3-p130Cas module on cell migration, we tested the NSP3 L623E mutant in a Transwell migration assay. NSP3 promotes COS cell migration toward epidermal growth factor (EGF) as a chemoattractant in a Cas-dependent manner[27]. The specific interface mutant L623E abrogated the NSP3-dependent enhancement of COS cell migration toward EGF. Cells expressing this mutant showed migratory ability toward EGF similar to that of cells transfected with empty vector control (**Fig. 4g**,**h**). This emphasizes the role of NSP-Cas module formation in linking cell motility and growth factor signaling and demonstrates the use of structural interface mutations for investigation of these signaling nodes.

Promiscuous yet class-specific NSP-Cas interactions

The structures of BCAR3, NSP3 and p130Cas provide not only insight into the C-terminal regions of NSP and Cas proteins and their interactions, but also a basis for applying features depicted in the wider context of NSP and Cas family signaling. To this end, we created molecular models for the C-terminal domains of the remaining family members on the basis of sequence profile alignments and the crystal structures solved in this work. We mapped primary interface residues onto these models and found that residues involved in formation of NSP–Cas complex are conserved within each family (**Fig. 5a**). In agreement with this degree of conservation are residues that determine the core fold of NSP and Cas family C-terminal domains (**Supplementary Fig. 8**), whereas remaining surface features are considerably more divergent. This indicates that all three NSP family proteins have pervasively repurposed an enzymatic fold as a recruitment

module, whereas Cas family proteins share a C-terminal FAT domain that accommodates the extended and tight binding interface observed in the NSP3–p130Cas complex. This extended interface, built upon the site 1 and site 2 binding motifs, is specific to NSP-Cas interactions yet allows different combinations of high-affinity mechanical linkages that integrate heterogeneous signaling pathways between the two families of proteins.

DISCUSSION

NSP and Cas family proteins interact with each other to form multidomain signaling modules. Members of both families have been linked to pathological processes such as breast cancer antiestrogen resistance[2,34] and metastasis in melanoma and lung cancer[35,36]. Analysis of an NSP3 knockout mouse line also suggests that these proteins may be involved in developmental disorders such as Kallmann syndrome[14]. Here we provide the first crystal structures of the unbound BCAR3 Cdc25-homology domain and the complex of the NSP3 Cdc25-homology domain with the FAT domain of the scaffolding protein p130Cas along with comprehensive biochemical and cell-based analyses of these regions.

The Cdc25-homology domain is typically found in exchange factors for Ras-type small GTPases, which activate their target GTPases by catalyzing nucleotide exchange. Because the GTP-GDP-dependent cycling of Ras proteins is essential for many aspects of normal cellular physiology and has a critical role in diseases such as cancer, Cdc25-homology domains have been the focus of intense investigation. Several structural studies have revealed the molecular mechanisms underlying nucleotide exchange by Cdc25-homology domains[17,19,20], including their regulation by additional interacting domains[18,37] and other proteins including Ras itself[38]. In contrast to these catalytically active Cdc25-homology domains, the BCAR3 Cdc25-homology domain adopts an unexpected closed conformation with nearly all functional elements completely remodeled, rendering it incapable of carrying out canonical exchange factor function. Moreover, the structure of the NSP3–p130Cas complex shows that the same closed conformation is essential for a tight interaction with the FAT domain of p130Cas. Residues at the interface between NSP3 and p130Cas partially overlap with the interface suggested in a recent small-angle X-ray scattering (SAXS) study of the BCAR3–HEF1 complex[16]. However, this SAXS model assumes that the BCAR3 Cdc25-homology domain adopts a classical GEF-type fold similar to that of SOS, rather than the closed form we observed in the crystal structures of both isolated BCAR3 and NSP3 bound to p130Cas. The complete rearrangement of the helical hairpin in NSP proteins markedly modifies the Cdc25-homology domain and creates a new binding surface. Consequently, NSP proteins use an aberrant enzymatic domain as an adaptor to link two multidomain signaling proteins.

Alignments of NSP proteins and Cas proteins show that both families (except the more distantly related CASS4) have preserved the residues that are critical for their interaction (**Fig. 5a** and **Supplementary Fig. 8**). This analysis explains how NSP and Cas proteins can tightly associate in a promiscuous but class-specific manner[11,12,39]. As a consequence, different pairwise combinations of NSP and Cas proteins can exploit functional differences such as divergent phosphorylation sites characteristic of the particular NSP-Cas protein module[3,6,10,27] (**Fig. 5b**). In this manner, the signaling outcome can be fine-tuned by the particular NSP-Cas signaling nodes present in a cell type. This class-specific promiscuity is an effective structural mechanism for regulation of cellular signaling networks by NSP–Cas modules.

In summary, the previously unknown closed Cdc25-homology domain conformation of NSP proteins is an adaption enabling tight interaction with the C-terminal FAT domain of Cas proteins. This work reveals a structural paradigm used by the NSP class of adaptor complexes and provides a new basis for investigating the role of NSP-Cas signaling modules in cell migration, invasiveness and other key physiological and pathological processes.

METHODS

Methods and any associated references are available in the online version of the paper at http://www.nature.com/nsmb/.

Accession codes. Protein Data Bank: Coordinates of BCAR3 and the NSP3–p130Cas complex have been deposited with accession codes 3T6A and 3T6G, respectively.

Note: Supplementary information is available on the Nature Structural & Molecular Biology website.

ACKNOWLEDGMENTS

We thank S. Snipas for protein sequencing, A. Bobkov for analytical ultracentrifugation and isothermal titration calorimetry and G. Salvesen for critical discussion of the manuscript. We also thank the Hope for a Cure Foundation for donation of equipment, J. Badger (DeltaG Technologies) for assistance in model evaluation, and the NKI Protein Facility for providing expression vectors. This work was supported by US National Institutes of Health (NIH) grants P01CA102583 and R01CA160457 to S.J.R. and E.B.P., R01CA116099 and P01HD025938 to E.B.P. and DOD-BCRP Fellowship BC100466 to P.D.M. Data collection at beamline X29 of the National Synchrotron Light Source was also supported by Biological and Environmental Research Department of Energy and the NIH National Center for Research Resources.

AUTHOR CONTRIBUTIONS

P.D.M. grew crystals, solved the crystal structures, designed and carried out *in vitro* experiments and wrote the manuscript. Y.W. designed, carried out and analyzed *in vivo* experiments, M.K.D. and J.J.L. expressed and purified proteins and grew initial NSP3–p130Cas crystals. H.R. carried out crystallographic data collection. S.J.R. and E.B.P. designed experiments, analyzed data and wrote the manuscript.

COMPETING FINANCIAL INTERESTS

The authors declare no competing financial interests.

Published online at http://www.nature.com/nsmb/.
Reprints and permissions information is available online at http://www.nature.com/reprints/index.html.

1. Brinkman, A., van der Flier, S., Kok, E.M. & Dorssers, L.C. BCAR1, a human homologue of the adapter protein p130Cas, and antiestrogen resistance in breast cancer cells. *J. Natl. Cancer Inst.* **92**, 112–120 (2000).
2. van Agthoven, T. *et al.* Identification of BCAR3 by a random search for genes involved in antiestrogen resistance of human breast cancer cells. *EMBO J.* **17**, 2799–2808 (1998).
3. Cabodi, S., Del Pilar Camacho-Leal, M., Di Stefano, P. & Defilippi, P. Integrin signalling adaptors: not only figurants in the cancer story. *Nat. Rev. Cancer* **10**, 858–870 (2010).
4. Felekkis, K., Quilliam, L.A. & Lerner, A. Characterization of AND-34 function and signaling. *Methods Enzymol.* **407**, 55–63 (2006).
5. Gotoh, T., Cai, D., Tian, X., Feig, L.A. & Lerner, A. p130Cas regulates the activity of AND-34, a novel Ral, Rap1, and R-Ras guanine nucleotide exchange factor. *J. Biol. Chem.* **275**, 30118–30123 (2000).
6. Lu, Y., Brush, J. & Stewart, T.A. NSP1 defines a novel family of adaptor proteins linking integrin and tyrosine kinase receptors to the c-Jun N-terminal kinase/stress-activated protein kinase signaling pathway. *J. Biol. Chem.* **274**, 10047–10052 (1999).
7. Sakakibara, A. & Hattori, S. Chat, a Cas/HEF1-associated adaptor protein that integrates multiple signaling pathways. *J. Biol. Chem.* **275**, 6404–6410 (2000).
8. Cai, D. *et al.* The GDP exchange factor AND-34 is expressed in B cells, associates with HEF1, and activates Cdc42. *J. Immunol.* **170**, 969–978 (2003).
9. Al-Shami, A. *et al.* The adaptor protein Sh2d3c is critical for marginal zone B cell development and function. *J. Immunol.* **185**, 327–334 (2010).
10. Alexandropoulos, K. & Regelmann, A.G. Regulation of T-lymphocyte physiology by the Chat-H/CasL adapter complex. *Immunol. Rev.* **232**, 160–174 (2009).
11. Browne, C.D. *et al.* SHEP1 partners with CasL to promote marginal zone B-cell maturation. *Proc. Natl. Acad. Sci. USA* **107**, 18944–18949 (2010).

12. Schrecengost, R.S., Riggins, R.B., Thomas, K.S., Guerrero, M.S. & Bouton, A.H. Breast cancer antiestrogen resistance-3 expression regulates breast cancer cell migration through promotion of p130Cas membrane localization and membrane ruffling. *Cancer Res.* **67**, 6174–6182 (2007).
13. Schuh, N.R., Guerrero, M.S., Schrecengost, R.S. & Bouton, A.H. BCAR3 regulates Src/p130 Cas association, Src kinase activity, and breast cancer adhesion signaling. *J. Biol. Chem.* **285**, 2309–2317 (2010).
14. Wang, L. *et al.* The SRC homology 2 domain protein Shep1 plays an important role in the penetration of olfactory sensory axons into the forebrain. *J. Neurosci.* **30**, 13201–13210 (2010).
15. Cai, D., Clayton, L.K., Smolyar, A. & Lerner, A. AND-34, a novel p130Cas-binding thymic stromal cell protein regulated by adhesion and inflammatory cytokines. *J. Immunol.* **163**, 2104–2112 (1999).
16. Garron, M.-L. *et al.* Structural insights into the association between BCAR3 and Cas family members, an atypical complex implicated in anti-oestrogen resistance. *J. Mol. Biol.* **386**, 190–203 (2009).
17. Boriack-Sjodin, P.A., Margarit, S.M., Bar-Sagi, D. & Kuriyan, J. The structural basis of the activation of Ras by Sos. *Nature* **394**, 337–343 (1998).
18. Rehmann, H., Das, J., Knipscheer, P., Wittinghofer, A. & Bos, J.L. Structure of the cyclic-AMP-responsive exchange factor Epac2 in its auto-inhibited state. *Nature* **439**, 625–628 (2006).
19. Freedman, T.S. *et al.* A Ras-induced conformational switch in the Ras activator Son of sevenless. *Proc. Natl. Acad. Sci. USA* **103**, 16692–16697 (2006).
20. Rehmann, H. *et al.* Structure of Epac2 in complex with a cyclic AMP analogue and RAP1B. *Nature* **455**, 124–127 (2008).
21. Freedman, T.S. *et al.* Differences in flexibility underlie functional differences in the Ras activators son of sevenless and Ras guanine nucleotide releasing factor 1. *Structure* **17**, 41–53 (2009).
22. Bos, J.L., de Rooij, J. & Reedquist, K.A. Rap1 signalling: adhering to new models. *Nat. Rev. Mol. Cell Biol.* **2**, 369–377 (2001).
23. Dodelet, V.C., Pazzagli, C., Zisch, A.H., Hauser, C.A. & Pasquale, E.B. A novel signaling intermediate, SHEP1, directly couples Eph receptors to R-Ras and Rap1A. *J. Biol. Chem.* **274**, 31941–31946 (1999).
24. Sakakibara, A., Ohba, Y., Kurokawa, K., Matsuda, M. & Hattori, S. Novel function of Chat in controlling cell adhesion via Cas-Crk-C3G-pathway-mediated Rap1 activation. *J. Cell Sci.* **115**, 4915–4924 (2002).
25. Riggins, R.B., Quilliam, L.A. & Bouton, A.H. Synergistic promotion of c-Src activation and cell migration by Cas and AND-34/BCAR3. *J. Biol. Chem.* **278**, 28264–28273 (2003).
26. van den Berghe, N., Cool, R.H., Horn, G. & Wittinghofer, A. Biochemical characterization of C3G: an exchange factor that discriminates between Rap1 and Rap2 and is not inhibited by Rap1A(S17N). *Oncogene* **15**, 845–850 (1997).
27. Dail, M. *et al.* SHEP1 function in cell migration is impaired by a single amino acid mutation that disrupts association with the scaffolding protein cas but not with Ras GTPases. *J. Biol. Chem.* **279**, 41892–41902 (2004).
28. Deakin, N.O. & Turner, C.E. Paxillin comes of age. *J. Cell Sci.* **121**, 2435–2444 (2008).
29. Bertolucci, C.M., Guibao, C.D. & Zheng, J. Structural features of the focal adhesion kinase-paxillin complex give insight into the dynamics of focal adhesion assembly. *Protein Sci.* **14**, 644–652 (2005).
30. Hoellerer, M.K. *et al.* Molecular recognition of paxillin LD motifs by the focal adhesion targeting domain. *Structure* **11**, 1207–1217 (2003).
31. Lulo, J., Yuzawa, S. & Schlessinger, J. Crystal structures of free and ligand-bound focal adhesion targeting domain of Pyk2. *Biochem. Biophys. Res. Commun.* **383**, 347–352 (2009).
32. Thomas, J.W. *et al.* The role of focal adhesion kinase binding in the regulation of tyrosine phosphorylation of paxillin. *J. Biol. Chem.* **274**, 36684–36692 (1999).
33. Vanden Borre, P., Near, R.I., Makkinje, A., Mostoslavsky, G. & Lerner, A. BCAR3/AND-34 can signal independent of complex formation with CAS family members or the presence of p130Cas. *Cell. Signal.* **23**, 1030–1040 (2011).
34. van Agthoven, T. *et al.* Functional identification of genes causing estrogen independence of human breast cancer cells. *Breast Cancer Res. Treat.* **114**, 23–30 (2009).
35. Ji, H. *et al.* LKB1 modulates lung cancer differentiation and metastasis. *Nature* **448**, 807–810 (2007).
36. Kim, M. *et al.* Comparative oncogenomics identifies NEDD9 as a melanoma metastasis gene. *Cell* **125**, 1269–1281 (2006).
37. Sondermann, H. *et al.* Structural analysis of autoinhibition in the Ras activator Son of sevenless. *Cell* **119**, 393–405 (2004).
38. Margarit, S.M. *et al.* Structural evidence for feedback activation by Ras.GTP of the Ras-specific nucleotide exchange factor SOS. *Cell* **112**, 685–695 (2003).
39. Roselli, S., Wallez, Y., Wang, L., Vervoort, V. & Pasquale, E.B. The SH2 domain protein Shep1 regulates the in vivo signaling function of the scaffolding protein Cas. *Cell. Signal.* **22**, 1745–1752 (2010).

ONLINE METHODS

Protein purification and crystallization. Expression constructs for crystallization were cloned into pET29b using standard PCR-based methods, and mutants were generated using QuikChange site-directed mutagenesis. $BCAR3_{502–825}$ (Uniprot: O75815) was expressed with a C-terminal His_6 tag in *E. coli* BL21(DE3) and was purified by Ni^{2+} affinity chromatography followed by anion exchange (Source Q 10/10), leading to typical final protein concentrations of 10–12 mg ml^{-1} BCAR3 in 10 mM HEPES, pH 7.9, 100 mM NaCl and 2 mM DTT. Initial crystals of wild-type protein grew by vapor diffusion from 15–20% (w/v) PEG3350, 0.04 M citric acid and 0.06 M Bis-Tris propane, pH 6.4, at room temperature. A contaminant lower-molecular-mass species was avoided by creating a $BCAR3_{502–825}$ M536L construct, and crystals for data collection were grown after mixing 3 µl of BCAR3 with 1.5 µl of the original mother liquor incorporating 4% (w/v) polypropylene glycol 400 additive.

The complex between NSP3 (Uniprot: Q8N5H7 isoform 2) and p130Cas (Uniprot: P56945) was prepared by mixing cell lysates after expression of C-terminally His-tagged $NSP3_{382–703}$ and untagged $p130Cas_{645–870}$. The complex was purified by both affinity and anion-exchange chromatography in a final buffer consisting of 10 mM Tris, pH 8.0, ~150 mM NaCl and 2 mM DTT. Initial crystals were obtained using wild-type NSP3–p130Cas proteins, whereas a construct incorporating C497S and C598S mutations in NSP3 (referred to as NSP3) crystallized in an identical manner and was used for data collection. Final crystals were prepared by mixing complex with mother liquor containing PEG3350 and sodium citrate, pH 7.8, in a 2:1 ratio. Diffraction was markedly improved by exchange of sodium citrate for sodium acetate in mother liquor after crystal growth. Both BCAR3 and NSP3–p130Cas crystals were prepared for data collection by introducing glycerol up to 20% and 15% (w/v), respectively, before flash freezing.

Structure determination and refinement. Diffraction data from BCAR3 crystals was collected using a Rigaku Superbright rotating-anode source. Data was integrated and scaled with XDS[40] and SCALA[41] and the structure of BCAR3 was solved by molecular replacement in Phaser[42] using the structure of NSP3 solved below as search model. The model was refined using Phenix[43] and rebuilt using COOT[44]. Phases of the NSP3–p130Cas complex were obtained from crystals containing SeMet-derivatized NSP3 and by soaking native complex crystals in 10 mM thimerosal for 1 h before flash freezing. Derivative data were collected at wavelengths corresponding to the peak of anomalous dispersion for selenium and mercury at National Synchrotron Light Source beamline X29. Data were integrated, reduced and scaled with HKL2000 (ref. 45), or XDS and SCALA. Phasing by MIRAS and density modification were carried out using AutoSharp[46] and partially built using Buccaneer[41]. The model was completed in COOT and refined against native diffraction data using Phenix. Data collection and final refinement statistics of both structures are in **Table 1**. Molecular models were created using FFAS[47] and Modeller[48], and all figures were created using PyMOL (http://pymol.org/).

Protein biochemistry. Expression constructs for target GTPases $Rap1a_{1–167}$ (Uniprot P62834)[49], $rRas_{27–196}$ (Uniprot P10301), $Rap2_{1–167}$ (Uniprot P10114)[50] and $C3G_{830–1077}$ (Uniprot Q13905)[26] were created by ligation-independent cloning into a modified pET vector incorporating an N-terminal His tag. Proteins were purified by affinity chromatography and size-exclusion chromatography on a Superdex 200 column.

Isothermal titration calorimetry was carried out using a MicroCal iTC_{200} calorimeter, and proteins at stated concentrations were prepared in a matched buffer containing 10 mM Tris, 100 mM NaCl and 0.5 mM Tris-(2-carboxyethyl)phosphine (TCEP). Analytical ultracentrifugation sedimentation equilibrium experiments were done in ProteomeLab XL-I (BeckmanCoulter) analytical ultracentrifuge with protein in 20 mM Tris, pH 8.0, 150 mM NaCl and 1 mM DTT. Analysis was done using HeteroAnalysis software (by J.L. Cole and J.W. Lary, University of Connecticut; http://www.biotech.uconn.edu/auf/).

Nucleotide exchange assays. For GDP exchange assays, GTPases were loaded with mant-GDP using standard protocols[51], and exchange of mantGDP in an excess of unlabeled GDP was measured by tracking fluorescence at 460 nm after excitation at 355 nm in a Molecular Devices fMax fluorescent plate reader at 25 °C. Exchange assays were carried out with ~0.3 µM GTPase in a buffer containing 10 mM HEPES, pH 7.8, 100 mM NaCl, 0.5 mM TCEP and 2 mM $MgCl_2$, and ~0.1 mg ml^{-1} BSA was included to stabilize GTPases in solution.

Antibodies. A rabbit polyclonal antibody to the 11 C-terminal residues of NSP3 was used for immunoprecipitations (10 µg) and a Shep1 SH2 antibody[23] was used for immunoblotting (0.5 µg ml^{-1}). The following primary antibodies were also used: p130Cas (BD Transduction laboratories; 1:600 dilution of a 0.25 mg ml^{-1} stock for immunoblotting), BCAR3 (Santa Cruz, 1 µg ml^{-1} for immunoblotting and 2 µg for immunoprecipitation) and GFP (GeneTex; 1 µl serum for immunoprecipitation).

Transwell migration assays. Cells co-transfected with NSP3 constructs in pcDNA3 and the peGFP-N3 plasmid (Clontech) were seeded on Transwell filters coated on both sides with 10 mg ml^{-1} fibronectin (Millipore). EGF (20 ng ml^{-1}) was added in the lower chamber as a chemoattractant, in comparison to no EGF as a control. The cells were allowed to migrate for 4 h, and the mean eGFP intensity from transfected cells on the bottom side of the filters was measured from microscope images. Comparisons between wells with EGF were made by one-way ANOVA and Dunnett's post-hoc test. Similar results were obtained in four different experiments.

Probing NSP-Cas interactions in cells. COS cells were cultured in DMEM supplemented with 10% (w/v) FBS and were transiently transfected with the indicated plasmids using Lipofectamine 2000 (Invitrogen). At 24 h after transfection, cells were lysed in RIPA buffer and centrifuged at 16,000*g* for 15 min at 4 °C. For immunoprecipitations, cell lysates were incubated at 4 °C with antibody for 2 h, followed by incubation with Gamma-bind beads (GE Health Care Health Sciences) for 1 h. Beads were washed with RIPA buffer and immunocomplexes were eluted by boiling for 5 min in SDS sample buffer. Extracts were separated by SDS-PAGE and transferred to a PVDF membrane (Millipore). After primary antibody incubation, membranes were probed with HRP-conjugated anti-mouse or anti-rabbit antibodies (Millipore; 1:5,000 dilution).

40. Kabsch, W. XDS. *Acta Crystallogr. D Biol. Crystallogr.* **66**, 125–132 (2010).
41. CCP4. The CCP4 suite: programs for protein crystallography. *Acta Crystallogr. D Biol. Crystallogr.* **50**, 760–763 (1994).
42. Storoni, L., McCoy, A. & Read, R. Likelihood-enhanced fast rotation functions. *Acta Crystallogr. D Biol. Crystallogr.* **60**, 432–438 (2004).
43. Adams, P.D. *et al.* PHENIX: a comprehensive Python-based system for macromolecular structure solution. *Acta Crystallogr. D Biol. Crystallogr.* **66**, 213–221 (2010).
44. Emsley, P. & Cowtan, K. Coot: model-building tools for molecular graphics. *Acta Crystallogr. D Biol. Crystallogr.* **60**, 2126–2132 (2004).
45. Otwinowski, Z. & Minor, W. Processing of X-ray diffraction data collected in oscillation mode. *Methods Enzymol.* **276**, 307–326 (1997).
46. Vonrhein, C., Blanc, E., Roversi, P. & Bricogne, G. Automated structure solution with autoSHARP. *Methods Mol. Biol.* **364**, 215–230 (2006).
47. Rychlewski, L., Jaroszewski, L., Li, W. & Godzik, A. Comparison of sequence profiles. Strategies for structural predictions using sequence information. *Protein Sci.* **9**, 232–241 (2000).
48. Eswar, N., Eramian, D., Webb, B., Shen, M.Y. & Sali, A. Protein structure modeling with MODELLER. *Methods Mol. Biol.* **426**, 145–159 (2008).
49. Nassar, N. *et al.* The 2.2 A crystal structure of the Ras-binding domain of the serine/threonine kinase c-Raf1 in complex with Rap1A and a GTP analogue. *Nature* **375**, 554–560 (1995).
50. Cherfils, J. *et al.* Crystal structures of the small G protein Rap2A in complex with its substrate GTP, with GDP and with GTPgammaS. *EMBO J.* **16**, 5582–5591 (1997).
51. Lenzen, C.U., Cool, R.H. & Wittinghofer, A. Analysis of intrinsic and CDC25-stimulated guanine nucleotide exchange of p21ras-nucleotide complexes by fluorescence measurements. *Methods Enzymol.* **255**, 95–109 (1995).

doi:10.1038/nsmb.2152